



HAL
open science

Exact theory of dense amorphous hard spheres in high dimension. III. The full RSB solution

Patrick Charbonneau, Jorge Kurchan, Giorgio Parisi, Pierfrancesco Urbani,
Francesco Zamponi

► **To cite this version:**

Patrick Charbonneau, Jorge Kurchan, Giorgio Parisi, Pierfrancesco Urbani, Francesco Zamponi.
Exact theory of dense amorphous hard spheres in high dimension. III. The full RSB solution.
Journal of Statistical Mechanics: Theory and Experiment, 2014, 2014, pp.10009. 10.1088/1742-5468/2014/10/P10009 . cea-01464503

HAL Id: cea-01464503

<https://cea.hal.science/cea-01464503>

Submitted on 10 Feb 2017

HAL is a multi-disciplinary open access archive for the deposit and dissemination of scientific research documents, whether they are published or not. The documents may come from teaching and research institutions in France or abroad, or from public or private research centers.

L'archive ouverte pluridisciplinaire **HAL**, est destinée au dépôt et à la diffusion de documents scientifiques de niveau recherche, publiés ou non, émanant des établissements d'enseignement et de recherche français ou étrangers, des laboratoires publics ou privés.

Exact theory of dense amorphous hard spheres in high dimension

III. The full replica symmetry breaking solution

Patrick Charbonneau,^{1,2} Jorge Kurchan,³ Giorgio Parisi,^{4,5} Pierfrancesco Urbani,⁶ and Francesco Zamponi⁷

¹*Department of Chemistry, Duke University, Durham, North Carolina 27708, USA*

²*Department of Physics, Duke University, Durham, North Carolina 27708, USA*

³*LPS, École Normale Supérieure, UMR 8550 CNRS, 24 Rue Lhomond, 75005 Paris, France*

⁴*Dipartimento di Fisica, Sapienza Università di Roma, P.le A. Moro 2, I-00185 Roma, Italy*

⁵*INFN, Sezione di Roma I, IPFC – CNR, P.le A. Moro 2, I-00185 Roma, Italy*

⁶*IPhT, CEA/DSM-CNRS/URA 2306, CEA Saclay, F-91191 Gif-sur-Yvette Cedex, France*

⁷*LPT, École Normale Supérieure, UMR 8549 CNRS, 24 Rue Lhomond, 75005 Paris, France*

In the first part of this paper, we derive the general replica equations that describe infinite-dimensional hard spheres at any level of replica symmetry breaking (RSB) and in particular in the fullRSB scheme. We show that these equations are formally very similar to the ones that have been derived for spin glass models, thus showing that the analogy between spin glasses and structural glasses conjectured by Kirkpatrick, Thirumalai, and Wolynes is realized in a strong sense in the mean field limit. We also suggest how the computation could be generalized in an approximate way to finite dimensional hard spheres. In the second part of the paper, we discuss the solution of these equations and we derive from it a number of physical predictions. We show that, below the Gardner transition where the 1RSB solution becomes unstable, a fullRSB phase exists and we locate the boundary of the fullRSB phase. Most importantly, we show that the fullRSB solution predicts correctly that jammed packings are isostatic, and allows one to compute analytically the critical exponents associated with the jamming transition, which are missed by the 1RSB solution. We show that these predictions compare very well with numerical results.

Contents

I. Introduction	3
I General equations	
II. Generic expression of the entropy	5
III. The replicated entropy for hierarchical RSB matrices	7
A. Parametrization of hierarchical matrices	8
B. The algebra of hierarchical matrices and the entropic term	9
1. General expression of the entropic term	9
2. 1RSB and 2RSB	10
3. k RSB	11
C. The interaction term	11
1. k RSB derivation	11
2. 1RSB and 2RSB	12
3. Continuum limit	13
D. 1RSB, 2RSB, k RSB, fullRSB expressions of the replicated entropy	13
IV. Variational equations	14
A. Variational equations for the k RSB solution	14
B. Variational equations for the fullRSB solution	16
1. Lagrange multipliers	17
2. Continuum limit of the k RSB variational equations	18
V. Derivation within the Gaussian ansatz	18
A. Gaussian parametrization and the entropic term	19
B. k RSB Gaussian parametrization and the interaction term	19
1. Finite dimensions	19

II Extraction of the results from the equations

VI. Summary of the equations, and a numerically convenient formulation	24
A. Scaled variables and the jamming limit	24
B. The continuum limit	26
VII. Perturbative 2RSB solution around the Gardner line	26
A. Development around the 1RSB solution	27
B. Asymptotic expression for $\lambda(m)$ at large densities on the Gardner line	29
VIII. The jamming limit of the 2RSB solution	30
A. The 2RSB equations at $m = 0$	31
B. The high density limit of the 2RSB solution at $m = 0$	32
C. Numerical solution of the 2RSB equations at $m = 0$: the 2RSB threshold	34
D. The 2RSB phase diagram	35
1. Phase diagram in the $(m, \hat{\varphi})$ plane	35
2. Phase diagram in the $(1/p, \hat{\varphi})$ plane: isocomplexity assumption	36
IX. Critical scaling of the fullRSB solution at jamming ($m = 0$)	37
A. Scaling of $\Delta(y)$, and asymptotic scaling of $\hat{P}(y, h)$ for $h \rightarrow -\infty$	37
B. Complete scaling of $\hat{P}(y, h)$	38
C. A toy model	39
1. Scaling in the matching region	39
2. Computation of $p_0(z)$	40
3. Summary	41
D. Scaling of the functions $\hat{j}(y, h)$ and $\hat{P}(y, h)$ in the matching region	42
E. Determination of the critical exponents	42
1. Some exact relations	43
2. Scaling regime	43
X. Numerical test of the critical scaling of the fullRSB solution	44
A. Dependence on the cutoffs k and y_{\max}	44
B. Test of the critical exponents	44
XI. Critical scaling of physical observables	45
A. Scaling of the cage radius with pressure	46
B. Pair correlation function	47
1. Finite k RSB	47
2. FullRSB	47
C. Force distribution	48
D. Isostaticity	49
XII. Marginal stability	49
XIII. Comparison with results of molecular dynamics simulations in finite dimensions	51
XIV. Conclusions	52
Acknowledgments	53
A. Extension to soft spheres	53
1. The zero temperature limit	53
2. The jamming limit and the force distribution	56
References	57

I. INTRODUCTION

In the two previous papers of this series [1, 2] (on which the present work relies heavily), we have considered a system of identical hard spheres in spatial dimension $d \rightarrow \infty$, and we have obtained an exact expression of its replicated partition function. Within the Random First Order Transition (RFOT) general scenario for the glass transition [3–6], which relies on the conjecture that structural glasses behave in the same way as a certain class of mean field spin glass models, the replicated partition function describes the amorphous arrested states of the system, i.e. its glasses [7, 8].

Previous work on structural glasses in the RFOT context always focused on the simplest replica scheme, the one-step replica symmetry breaking (1RSB). The 1RSB scheme indeed already predicts the most important phase transitions that happen upon approaching the glass phase, namely the dynamical and Kauzmann transitions. An approximate 1RSB treatment of finite-dimensional glasses was developed in [9, 10], and applied to hard spheres in [11]; these works have shown that the 1RSB approach gives quite accurate predictions of thermodynamic and structural quantities in three-dimensional glasses. Moreover, within the 1RSB scheme, the exact expression obtained in [1, 2] coincides with the infinite-dimensional limit of the finite-dimensional approach of [11] while a series of numerical works [12, 13] in $d = 3, \dots, 12$ have shown that the main qualitative properties of the system evolve smoothly with dimensions (although the investigated dimensions are quite far from the asymptotic $d \rightarrow \infty$ regime [12]). One could therefore think that the 1RSB scheme is sufficient to describe the properties of glasses within RFOT theory in all the range of physical parameters.

However, when one tries to apply the 1RSB scheme to study the properties of hard or soft-sphere glasses at very high pressures and low temperatures, close to the jamming transition that marks the transition from a mechanically loose to a mechanically rigid glass state, one finds contradictory results. On the one hand, the behavior of the main thermodynamic quantities (pressure, energy, ...) is quite well reproduced [11, 14]. On the other hand, the scaling properties of other observables are not. It is therefore natural to search for the origin of this discrepancy.

A first step in this direction was made through the investigation of nearly jammed sphere packings. It was shown that hard sphere glasses at high pressures are close to a mechanical instability, the so-called “isostatic” point where the number of mechanical constraints exactly equals the number of degrees of freedom [15–17]. Due to this proximity, anomalous low-frequency modes appear in the vibrational spectrum [18–22]. Based on this observation, in a series of papers Wyart and coworkers [20, 23–25] assumed that hard sphere glasses at high pressure are *marginally stable*, and under this assumption they derived a scaling theory of the jamming transition that is able to describe most of its basic phenomenology. In particular, it was shown both analytically and numerically [20, 23, 26] that marginality is associated with a particular scaling of the mean square displacement Δ in the hard sphere glass, which vanishes when the pressure $p \rightarrow \infty$ as $\Delta \sim p^{-\kappa}$ with $\kappa \sim 3/2$ (naive free-volume considerations would suggest $\Delta \sim p^{-2}$). It was confirmed in [26] that the exponent κ plays an important role, and in fact controls all the criticality of the jamming transition.

This analysis suggests that a 1RSB description is incorrect in this regime, because 1RSB states are perfectly stable and do not show any sign of marginality. In fact, the 1RSB solution further wrongly¹ predicts $\Delta \sim p^{-1}$ [11], and furthermore misses other critical exponents associated to the structure and the force distribution [25, 27, 28]. In the context of spin glasses, it is well known that fullRSB phases are always associated with marginal stability and anomalous low-frequency modes [29, 30], which affect the low-temperature scaling of physical quantities [30]. It appears therefore that a fullRSB phase is a natural candidate for explaining the marginal stability of low-temperature glasses.

Additional insights came from analyzing the out-of-equilibrium dynamical behavior of one of the simplest spin glass models that are at the basis of the RFOT scenario, the Ising p -spin model [31–34]. It was shown that, although the 1RSB solution correctly describes the approach to the glass phase at equilibrium, when the system is instantaneously quenched out-of-equilibrium it evolves towards a region of phase space where the 1RSB solution is unstable, the so-called Gardner phase² [35, 36], in which a fullRSB solution is present [33]. The behavior of the Ising p -spin model is not yet fully understood, but this model nonetheless strongly suggests that fullRSB effects may be observable in low-temperature glasses.

Many other observations hint to the presence of a fullRSB phase in low temperature or high pressure glasses (see e.g. [37]), which we reviewed in [2]. Based on these observations, in the previous paper of this series [2] we used our exact expression for the replicated partition function of infinite-dimensional hard spheres to investigate the stability

¹ Still, as noted in [26], the 1RSB prediction shows a sign of an anomalous behavior of the mean square displacement with respect to the naive expectation.

² The existence of a transition at low temperature from a 1RSB to a fullRSB solution was discovered independently in [35, 36] and its precise location was found in [35].

of the 1RSB phase, a computation that could not be done previously because the finite-dimensional approximations of [9–11] have been formulated only at the 1RSB level. Our analysis showed that the 1RSB phase is stable around the dynamical glass transition, but becomes unstable at high pressures close to the jamming transition. This result gives additional indications in favor of the presence of a different phase that could better describe the properties of high pressure (or low temperature) glasses.

The aim of this work is to write explicitly the replica equations in the k RSB scheme and send $k \rightarrow \infty$ to describe the fullRSB solution, in order to check if this solution predicts correctly the scaling properties of the jamming transition. In the first part of this work we derive the set of equations that give the replicated entropy at the level of k RSB. Interestingly, the equations we obtain are remarkably similar to those describing the Ising p -spin model with, however, some crucial differences. The proof of this formal similarity between the equations that describe a disordered mean field spin glass model and a system of interacting particles without any quenched disorder somehow completes the program initiated by Kirkpatrick, Thirumalai and Wolynes, who constructed the RFOT scenario by assuming that such a similarity existed and proved some arguments supporting it, see e.g. [7, 38].

In the second part of the paper, we extract physical quantities from the equations. Our main results are that (i) a fullRSB phase always exists at high pressures, hence the jamming transition always lies in the fullRSB region; (ii) as in the SK model [39–42], the fullRSB phase is *marginally stable*, because one of the eigenvalues of the stability matrix of the replicated entropy is identically vanishing; (iii) jammed packings are *predicted* to be isostatic at all densities; (iv) the fullRSB solution predicts a different scaling of the mean square displacement in the glass, namely $\Delta \sim p^{-\kappa}$ with an exponent κ very close to $3/2$; (v) the fullRSB solution predicts a power-law divergence of the pair correlation function of jammed packings at contact, $g(r) \sim (D - r)^{-\alpha}$; (vi) the force distribution vanishes at small forces as $P(f) \sim f^\theta$; (vii) we obtain analytical predictions for the exponents κ, α, θ .

In [25, 28, 43], the exponents θ and α were argued to control the stability of packings and the presence of avalanches, and a scaling relation between them was derived assuming marginal stability. The value of one exponent was lacking however to have a complete scaling picture. Our predicted values of κ, α, θ are perfectly compatible with the scaling relations derived in [25, 28, 43] and with previous numerical investigations [25, 27, 28, 44–46] (except for θ , where the situation remains somehow unclear). By means of additional numerical simulations, we show that the prediction for κ is correct in all spatial dimensions.

These results open the way to many different studies. For example, one could now hope to compute the shear modulus [21, 47–49], the distribution of avalanche sizes [50], the complete scaling on both sides of the jamming transition [14, 26], and so on. Moreover, the results could be extended to finite dimensional systems within the effective potential approximation scheme of [11, 14], which would allow one to directly compare the predictions with numerical simulations and experiments. We discuss briefly these possible developments in the conclusions. An important open question is how the fullRSB structure affects the off-equilibrium dynamics [31–33].

Because the paper is quite long, we do not present a detailed plan here. At the beginning of each section, we explain what is the aim of the section and detail the structure of subsections. Reading the technical part of the paper requires familiarity with the general concepts of spin glass theory (see e.g. [30, 51] for reviews), with its application to structural glasses [10] and jamming [11], and with the previous papers of this series [1, 2]. A short account of this work, where the main physical ideas behind it and the main results are presented in a more accessible way for the reader not interested in technical details, has been presented in [52].

Part I

General equations

II. GENERIC EXPRESSION OF THE ENTROPY

In the following, we consider a system of N identical spheres of diameter D in a d -dimensional volume V , in the thermodynamic limit $N = \rho V$ and $V \rightarrow \infty$. At sufficiently high density, this system exhibits a glass phase, i.e., its dynamics arrests and an amorphous solid phase forms due to self-induced frustration. A strategy to obtain a thermodynamic description of the glass states has been derived in [4, 8, 38]. The idea behind these works is the following. In the dense supercooled regime the liquid phase splits in a collection of glass basins that can be defined as amorphous minima of an appropriate density functional [4]. Hence if one extracts one liquid configuration in equilibrium, this configuration falls into one of the multiple glass basins. To describe this glass basin thermodynamically, one has to consider a second configuration that is coupled to the first one. Its partition function gives the properties of the glass. The coupling to the first configuration acts as an external quenched disorder, and that disorder can be treated using replicas, in analogy with spin glasses [53]. This construction was made precise through the introduction of the so-called Franz-Parisi potential [54–56]. In this way one can easily follow the *adiabatic evolution* with density and temperature of glassy states that originate from an equilibrium liquid configuration (also known as the “state following” procedure [57]). Dynamically, this corresponds to preparing glassy states through a slow annealing.

A slightly different (and computationally simpler) strategy was proposed by Monasson [8]. Here m replicas are coupled to an external random field that selects glassy states. After averaging out the external field one is left with m coupled replicas. Because one uses here a completely random field, this procedure gives the properties of the “typical” states that exist at a given temperature or density [8, 11]. In this way one can compute the dynamical glass transition density, the Kauzmann density (when it exists), and the so-called dynamical line (or threshold line) that delimits the region of existence of glassy states. Dynamically, it is expected that after a *fast quench* the system becomes arrested in the glassy states that lie on this dynamical/threshold line [51, 58]. This strategy is very efficient and was used in many previous studies, see e.g. [59, 60] for pedagogical introductions and [10, 11] for reviews of previous results. In this paper, as in the previous papers of this series [1, 2], we follow this simpler approach and consider an m -times replicated system in order to describe glassy states. We will see that this treatment is sufficient to describe the marginal stability of jammed packings and to obtain the critical properties around the jamming transition. The state-following (or Franz-Parisi) computation is also possible, but is left for a future publication. In the second part of this paper, we will explain more precisely what kind of information on the phase diagram can be obtained from this procedure.

We consider m identical copies of the original hard sphere system, assuming that the spheres are arranged in molecules, each molecule containing an atom of each replica. A molecule is thus described by m vectors $\vec{x} = \{x_1 \cdots x_m\}$, each x_a being d -dimensional. The molecular liquid is translationally invariant, so each atom in a molecule fluctuates around the center of mass of the molecule $X = m^{-1} \sum_a x_a$. We call the displacement of one atom $u_a = x_a - X$. In the following, $m \times m$ matrices in replica spaces are indicated by a hat, e.g. the matrix $\hat{\alpha}$ has elements α_{ab} , and we denote by $\hat{\alpha}^{a,b}$ the $(m-1) \times (m-1)$ matrix obtained from $\hat{\alpha}$ by removing line a and column b . Wide hats are used to denote quantities that have been properly scaled to be finite in the limit $d \rightarrow \infty$; for example, $\hat{\varphi} = 2^d \varphi / d$ is the scaled packing fraction, with the usual packing fraction $\varphi = \rho V_d$, where V_d is the volume of a sphere of unit radius [1].

The aim of this section is to write the entropy of the replicated system in a convenient way. With the notations introduced above, we consider the general form of the replicated entropy that has been derived in paper II of this series [2]:

$$s[\hat{\alpha}] = 1 - \log \rho + d \log m + \frac{d}{2}(m-1) \log(2\pi e D^2 / d^2) + \frac{d}{2} \log \det(\hat{\alpha}^{m,m}) - \frac{d}{2} \hat{\varphi} \mathcal{F}(2\hat{\alpha}) , \quad (1)$$

where the matrix $\hat{\alpha}$ with elements $\alpha_{ab} = d \langle u_a \cdot u_b \rangle / D^2$ encodes the fluctuations of the replica displacement vectors u_a . The term proportional to $\hat{\varphi}$ comes from the density-density interaction and we refer to it below as the “interaction term”. The other terms encode the entropic contributions and we refer to them all as the “entropic term”. It is useful to define the scaled mean square displacement between two replicas

$$\Delta_{ab} = \frac{d}{D^2} \langle (u_a - u_b)^2 \rangle = \alpha_{aa} + \alpha_{bb} - 2\alpha_{ab} . \quad (2)$$

It has been shown in [1, 2] that the elements of the matrices $\hat{\Delta}$ and $\hat{\alpha}$ are finite in the limit $d \rightarrow \infty$. Because the vector u_a has d components, Eq. (2) implies that the variance of the norm of the vector $u_a - u_b$ is of order $1/d$, while the

variance of each one of its components is of order $1/d^2$. In order to find the thermodynamic entropy of the replicated liquid, the replicated entropy (1) must be optimized³ with respect to the matrices $\hat{\alpha}$ or $\hat{\Delta}$.

In [2] a generic expression for the interaction term $\mathcal{F}(2\hat{\alpha})$ has been derived, but we now want to write it in a more convenient form. It reads:

$$\mathcal{F}(2\hat{\alpha}) = \lim_{n \rightarrow 0} \sum_{n_1, \dots, n_m: \sum_a n_a = n} \frac{n!}{n_1! \dots n_m!} \exp \left[- \sum_{a=1}^m \alpha_{aa} \frac{n_a}{n} + \sum_{a,b}^m \alpha_{ab} \frac{n_a n_b}{n^2} \right]. \quad (3)$$

We will now suppose that the diagonal part of the matrix α is constant and $\alpha_{aa} = \alpha_d$ for all a , because this is true for matrices with a general k RSB structure. This implies that

$$2\alpha_{ab} = 2\alpha_d - \Delta_{ab}, \quad (4)$$

and therefore the function \mathcal{F} can be rewritten in terms of the matrix $\hat{\Delta}$ as

$$\begin{aligned} \mathcal{F}(\hat{\Delta}) &= \lim_{n \rightarrow 0} \sum_{n_1, \dots, n_m: \sum_a n_a = n} \frac{n!}{n_1! \dots n_m!} \exp \left[-\alpha_d + \frac{1}{2} \sum_{a,b}^m (2\alpha_d - \Delta_{ab}) \frac{n_a n_b}{n^2} \right] \\ &= \lim_{n \rightarrow 0} \sum_{n_1, \dots, n_m: \sum_a n_a = n} \frac{n!}{n_1! \dots n_m!} \exp \left[-\frac{1}{2} \sum_{a,b}^m \Delta_{ab} \frac{n_a n_b}{n^2} \right]. \end{aligned} \quad (5)$$

Note that the diagonal elements of the displacement matrix $\hat{\Delta}$ are all zero. Moreover, we temporarily define a matrix

$$\Delta_{ab}^* = \Delta_{ab} + \Lambda \delta_{ab} \quad (6)$$

and we write the interaction term as

$$\mathcal{F}(\hat{\Delta}) = \lim_{n \rightarrow 0} \sum_{n_1, \dots, n_m: \sum_a n_a = n} \frac{n!}{n_1! \dots n_m!} \exp \left[-\frac{1}{2} \sum_{a,b}^m \Delta_{ab}^* \frac{n_a n_b}{n^2} + \frac{\Lambda}{2} \sum_{a=1}^m \frac{n_a^2}{n^2} \right]. \quad (7)$$

We assume that the parameter Λ is positive. Using the identity

$$e^{-\frac{1}{2} \sum_{a,b}^m \Delta_{ab}^* \frac{n_a n_b}{n^2}} = e^{-\frac{1}{2} \sum_{a,b=1}^m \Delta_{ab}^* \frac{\partial^2}{\partial h_a \partial h_b}} e^{-\sum_{a=1}^m h_a \frac{n_a}{n}} \Bigg|_{\{h_a=0\}}, \quad (8)$$

and introducing $\mathcal{D}\lambda_a = d\lambda_a e^{-\lambda_a^2/2}/\sqrt{2\pi}$ as a Gaussian measure with zero mean and unit variance, $\mathcal{F}(\hat{\Delta})$ can be rewritten as

$$\begin{aligned} \mathcal{F}(\hat{\Delta}) &= \lim_{n \rightarrow 0} \sum_{n_1, \dots, n_m: \sum_a n_a = n} \frac{n!}{n_1! \dots n_m!} \exp \left[-\frac{1}{2} \sum_{a,b=1}^m \Delta_{ab}^* \frac{\partial^2}{\partial h_a \partial h_b} \right] \exp \left[\frac{\Lambda}{2} \sum_{a=1}^m \frac{n_a^2}{n^2} - \sum_{a=1}^m h_a \frac{n_a}{n} \right] \Bigg|_{\{h_a=0\}} \\ &= \lim_{n \rightarrow 0} \sum_{n_1, \dots, n_m: \sum_a n_a = n} \frac{n!}{n_1! \dots n_m!} \exp \left[-\frac{1}{2} \sum_{a,b=1}^m \Delta_{ab}^* \frac{\partial^2}{\partial h_a \partial h_b} \right] \times \\ &\quad \times \int \left(\prod_{a=1}^m \mathcal{D}\lambda_a \right) \exp \left[-\sqrt{\Lambda} \sum_{a=1}^m \frac{n_a}{n} \lambda_a - \sum_{a=1}^m \frac{n_a}{n} h_a \right] \Bigg|_{\{h_a=0\}} \\ &= \exp \left[-\frac{1}{2} \sum_{a,b=1}^m \Delta_{ab}^* \frac{\partial^2}{\partial h_a \partial h_b} \right] \int \left(\prod_{a=1}^m \mathcal{D}\lambda_a \right) \exp \left[-\min_a \left(\sqrt{\Lambda} \lambda_a + h_a \right) \right] \Bigg|_{\{h_a=0\}}. \end{aligned} \quad (9)$$

³ For integer $m > 1$, the optimum is a maximum, but for real $m < 1$ analytic continuation changes the sign of some eigenvalues and the optimum becomes a saddle point [30].

In the above expression, the integration measure of the λ_a corresponds to independent random variables with a Gaussian probability distribution. Then, the probability distribution of the random variable $h = -\min_a (\sqrt{\Lambda}\lambda_a + h_a) = \max_a (-\sqrt{\Lambda}\lambda_a - h_a)$ is given by

$$\mu_{\min}(h) = \frac{d}{dh} \prod_{a=1}^m \int_{-(h+h_a)/\sqrt{\Lambda}}^{\infty} \mathcal{D}\lambda_a = \frac{d}{dh} \prod_{a=1}^m \Theta\left(\frac{h+h_a}{\sqrt{2\Lambda}}\right), \quad (10)$$

because the product of integrals is the probability that $h \geq -\sqrt{\Lambda}\lambda_a - h_a$, $\forall a$, hence it is the probability that $h \geq \max_a (-\sqrt{\Lambda}\lambda_a - h_a)$, which is nothing but the cumulative distribution of h . Here we introduced the function $\Theta(z) = (1 + \text{erf}(z))/2$ and $\int_{-h}^{\infty} \mathcal{D}\lambda = \Theta(h/\sqrt{2})$. Therefore

$$\int \left(\prod_{a=1}^m \mathcal{D}\lambda_a \right) \exp\left[-\min_a (\sqrt{\Lambda}\lambda_a + h_a)\right] = \int_{-\infty}^{\infty} dh e^h \mu_{\min}(h) = \int_{-\infty}^{\infty} dh e^h \frac{d}{dh} \prod_{a=1}^m \Theta\left(\frac{h+h_a}{\sqrt{2\Lambda}}\right) \quad (11)$$

and collecting these results we obtain

$$\begin{aligned} \mathcal{F}(\hat{\Delta}) &= \exp\left[-\frac{1}{2} \sum_{a,b=1}^m \Delta_{ab}^* \frac{\partial^2}{\partial h_a \partial h_b}\right] \int_{-\infty}^{\infty} dh e^h \frac{d}{dh} \prod_{a=1}^m \Theta\left(\frac{h+h_a}{\sqrt{2\Lambda}}\right) \Big|_{\{h_a=0\}} \\ &= \int_{-\infty}^{\infty} dh e^h \frac{d}{dh} \left\{ \exp\left[-\frac{1}{2} \sum_{a,b=1}^m \Delta_{ab}^* \frac{\partial^2}{\partial h_a \partial h_b}\right] \prod_{a=1}^m \Theta\left(\frac{h_a}{\sqrt{2\Lambda}}\right) \right\} \Big|_{\{h_a=h\}}. \end{aligned} \quad (12)$$

By defining the Gaussian kernel $\gamma_a(z) = e^{-z^2/(2a)}/\sqrt{2\pi a}$, one obtains the relation

$$\exp\left[\frac{a}{2} \frac{d^2}{dh^2}\right] f(h) = \int_{-\infty}^{\infty} \frac{dz}{\sqrt{2\pi a}} e^{-\frac{z^2}{2a}} f(h-z) = \gamma_a \star f(h), \quad (13)$$

where we defined the $\gamma_a \star f$ operation as the convolution of the Gaussian kernel with the function $f(h)$. Then

$$\Theta(h/\sqrt{2a}) = \int_{-\infty}^{\infty} \frac{dz}{\sqrt{2\pi a}} e^{-\frac{z^2}{2a}} \theta(h-z) = \exp\left[\frac{a}{2} \frac{d^2}{dh^2}\right] \theta(h) = \gamma_a \star \theta(h). \quad (14)$$

Using this relation we obtain the compact result

$$\begin{aligned} \mathcal{F}(\hat{\Delta}) &= \int_{-\infty}^{\infty} dh e^h \frac{d}{dh} \left\{ \exp\left[-\frac{1}{2} \sum_{a,b=1}^m \Delta_{ab}^* \frac{\partial^2}{\partial h_a \partial h_b}\right] \prod_{a=1}^m e^{\frac{1}{2}\Lambda \frac{\partial^2}{\partial h_a^2}} \theta(h_a) \right\} \Big|_{\{h_a=h\}} \\ &= \int_{-\infty}^{\infty} dh e^h \frac{d}{dh} \left\{ \exp\left[-\frac{1}{2} \sum_{a,b=1}^m \Delta_{ab}^* \frac{\partial^2}{\partial h_a \partial h_b}\right] \prod_{a=1}^m \theta(h_a) \right\} \Big|_{\{h_a=h\}}. \end{aligned} \quad (15)$$

The replicated entropy is therefore given by Eq. (1), with the function \mathcal{F} given in Eq. (15). This expression is quite general and will be used to study k -step replica symmetry breaking schemes in the following. Note that it has been derived under the only assumption that the diagonal elements of α_{ab} are all equal.

III. THE REPLICATED ENTROPY FOR HIERARCHICAL RSB MATRICES

In spin glasses, it has been shown that a correct description of the system can be achieved by considering a special class of matrices, known as hierarchical k RSB matrices [30]. Therefore, we want to specialize the general expression of the replicated entropy given by Eqs. (1) and (15) to these matrices. In Sec. III A, we introduce hierarchical k RSB matrices and discuss some of their properties. In Sec. III B, we compute the entropic term of the replicated entropy for a k RSB matrix, and in Sec. III C we compute the interaction term. In Sec. III D, we present the final explicit expressions for the 1RSB, 2RSB, k RSB and fullRSB case.

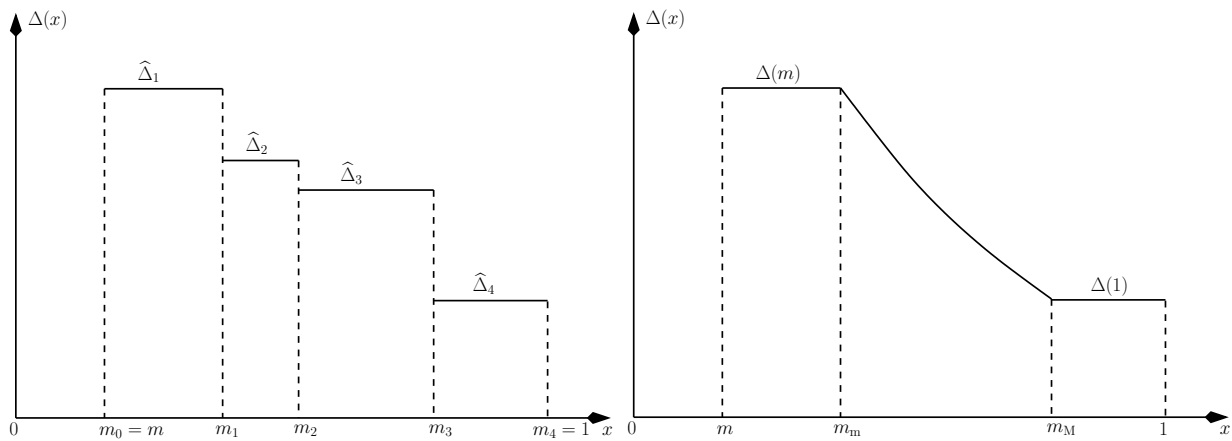


FIG. 1: (Left) An example of the parametrization of the matrix Δ_{ab} for a 4RSB case. When needed for notational purposes, we use the convention $\widehat{\Delta}_0 \equiv 0$. (Right) The expected form of the function $\Delta(x)$ in the fullRSB limit.

A. Parametrization of hierarchical matrices

The structure of hierarchical k RSB matrices is well-known and here we just summarize it briefly. Remember that with respect to the formalism of [30] we have an important difference, in that the diagonal elements of the matrices we consider are determined by the condition that $\sum_b \alpha_{ab} = 0, \forall b$. The simplest class is that of 1RSB matrices⁴, that has been studied in the first [1] and second [2] paper of this series. It corresponds to $\alpha_{ab} = -\widehat{\alpha}_1, \forall a \neq b$:

$$\alpha_{ab}^{1\text{RSB}} = \widehat{\alpha}_1 (m\delta_{ab} - 1) . \quad (16)$$

Here we used a slightly different but equivalent notation with respect to previous papers [1, 2, 11], to be consistent with the general k RSB notation⁵. A 2RSB matrix is parametrized as follows. Replicas are arranged in m/m_1 groups, and the matrix elements $\alpha_{ab} = -\widehat{\alpha}_2$ if they belong to the same group, or $\alpha_{ab} = -\widehat{\alpha}_1$ if they do not. If we say that $b \sim a$ when b is in the same subgroup of a , and $b \not\sim a$ otherwise, and we define a function $\text{I}(e) = 1$ if the event “e” is true and $\text{I}(e) = 0$ otherwise, a 2RSB matrix has the form:

$$\alpha_{ab}^{2\text{RSB}} = \delta_{ab} [(m_1 - 1)\widehat{\alpha}_2 + (m - m_1)\widehat{\alpha}_1] - (1 - \delta_{ab}) [\widehat{\alpha}_2 \text{I}(b \sim a) + \widehat{\alpha}_1 \text{I}(b \not\sim a)] . \quad (17)$$

At the 3RSB level, the blocks of m_1 replicas are each divided in m_1/m_2 sub-blocks of m_2 replicas, and the construction can be iterated to any desired level of RSB (which we denote k RSB). Note that diagonal elements of hierarchical matrices are all equal.

For each k , these “hierarchical” matrices form a closed algebra. Moreover, in the interesting case where one performs an analytic continuation to $m < 1$, a generic hierarchical matrix \widehat{Q} can be parametrized by its diagonal element q_d and a single function $q(x)$. This is done as follows. If we formally define $m_0 = m$ and $m_k = 1$, we can observe that for integer $m > 1$, one has $m_k \equiv 1 < m_{k-1} < m_{k-2} < \dots < m_1 < m_0 \equiv m$. When $m < 1$, these inequalities are reversed [30] and one has $1 > m_{k-1} > m_{k-2} > \dots > m_1 > m > 0$. Then we can define $q(x)$ to be a piecewise constant function for $x \in [0, 1]$, which in the interval $x \in [m_{i-1}, m_i]$ takes the value of the elements q_i in the corresponding sub-block (with $i = 1 \dots k$), and $q(x) = 0$ for $x \in [0, m_0]$. We write this parametrization as $\widehat{Q} \leftrightarrow \{q_d, q(x)\}$.

The matrices $\widehat{\alpha}$ are therefore defined by $\widehat{\alpha} \leftrightarrow \{\alpha_d, -\alpha(x)\}$ where $\alpha(x)$ is a piecewise constant function given by the $\widehat{\alpha}_i$ in each block, while α_d is fixed by the condition $\sum_b \alpha_{ab} = 0$ and is given by

$$\alpha_d = (m_{k-1} - 1)\widehat{\alpha}_k + (m_{k-2} - m_{k-1})\widehat{\alpha}_{k-1} + \dots + (m - m_1)\widehat{\alpha}_1 = - \int_m^1 dx \alpha(x) . \quad (18)$$

⁴ In the standard notation of [30] this would be called a replica-symmetric matrix, but remember that here we are using the Monasson’s real replica scheme [8] where we consider m coupled replicas and treat m as a parameter to select different metastable states. It is a standard convention to denote a RS matrix in the Monasson’s scheme as a “1RSB matrix”: the reason is that in models with quenched disorder the two schemes are indeed equivalent.

⁵ Note that in previous papers [1, 2, 11] we dropped the subscript, $\widehat{\alpha}_1 = \widehat{\alpha}$ because we only considered the 1RSB case, and we used $\widehat{A} = m\widehat{\alpha}$.

For a given matrix α_{ab} , one has a corresponding matrix $\Delta_{ab} = 2\alpha_{aa} - 2\alpha_{ab}$, which is therefore parametrized as $\hat{\Delta} \leftrightarrow \{0, \Delta(x)\}$ with

$$\Delta(x) = 2\alpha_d + 2\alpha(x) = -2 \int_m^1 dy \alpha(y) + 2\alpha(x) . \quad (19)$$

By integrating this relation we obtain $\int_m^1 dx \alpha(x) = \frac{1}{2m} \int_m^1 dx \Delta(x)$, therefore we can invert the relation to obtain

$$\alpha(x) = \frac{1}{2} \Delta(x) + \frac{1}{2m} \int_m^1 dy \Delta(y) . \quad (20)$$

The seemingly strange conventions that we adopted for the signs of the above parametrization are justified by the fact that with this choice both $\alpha(x)$ and $\Delta(x)$ are positive functions. Clearly this is the case by definition for $\Delta(x)$, and from Eq. (20) we deduce that the same must be true for $\alpha(x)$. Moreover, $\Delta(x)$ must be a *decreasing* function of x (contrary to the usual overlap function [30]). This is because larger values of x correspond to inner blocks of the matrix Δ_{ab} , hence to replicas that are “closer” to each other in the usual interpretation, and therefore must have a smaller value of Δ . An example is given in Fig. 1. Of course, the above construction can be generalized to the case where the function $\Delta(x)$ is allowed to have a continuous part: this can be thought as an appropriate limit of the k RSB construction when $k \rightarrow \infty$ and is therefore called “fullRSB” or “ ∞ RSB”.

B. The algebra of hierarchical matrices and the entropic term

1. General expression of the entropic term

In order to compute the entropic term, we need to compute $\log \det \hat{\alpha}^{m,m}$. For this we need to recall some standard results for the algebra of hierarchical matrices. Let us consider a generic hierarchical matrix q_{ab} , parametrized by the corresponding function $q(x)$ and with diagonal element q_d . Although our matrices \hat{Q}_m are $m \times m$ matrices with fixed $m < 1$, we can think to embed them in a $n \times n$ dimensional matrix \hat{Q}_n with $n \rightarrow 0$, and just set to zero the element of the outermost block. This is consistent with the fact that $q(x)$ is defined in $x \in [0, 1]$, and it corresponds to the special choice that $q(x)$ vanishes for $0 \leq x < m$. We can therefore use standard results for the algebra of $n \times n$ hierarchical matrices, in the limit $n \rightarrow 0$, see e.g. [61]. The important result of [61] that we need is that, introducing the notations

$$[q](x) = xq(x) - \int_0^x dy q(y) , \quad \langle q \rangle = \int_0^1 dx q(x) , \quad (21)$$

we have for the determinant [61, Eq.(AII.11)]

$$\lim_{n \rightarrow 0} \frac{1}{n} \log \det \hat{Q}_n = \log(q_d - \langle q \rangle) + \frac{q(0)}{q_d - \langle q \rangle} - \int_0^1 \frac{dy}{y^2} \log \left(\frac{q_d - \langle q \rangle - [q](y)}{q_d - \langle q \rangle} \right) , \quad (22)$$

and the inverse matrix is parametrized by [61, Eq.(AII.7)]

$$\begin{aligned} (q^{-1})_d &= \frac{1}{q_d - \langle q \rangle} \left(1 - \int_0^1 \frac{dy}{y^2} \frac{[q](y)}{q_d - \langle q \rangle - [q](y)} - \frac{q(0)}{q_d - \langle q \rangle} \right) , \\ (q^{-1})(x) &= -\frac{1}{q_d - \langle q \rangle} \left[\frac{q(0)}{q_d - \langle q \rangle} + \frac{[q](x)}{x(q_d - \langle q \rangle - [q](x))} + \int_0^x \frac{dy}{y^2} \frac{[q](y)}{q_d - \langle q \rangle - [q](y)} \right] . \end{aligned} \quad (23)$$

To adapt these results to our case, we note that if the outermost blocks vanish, we have $q(0) = 0$. Furthermore, $q(x) = [q](x) = 0$ for $x < m$. Finally, $\det \hat{Q}_n = (\det \hat{Q}_m)^{n/m}$, hence $\log \det \hat{Q}_n = (m/n) \log \det \hat{Q}_m$, and the diagonal

element of the inverse of \hat{Q}_n and \hat{Q}_m are identical. We conclude that in the $m \times m$ space

$$\begin{aligned}
\log \det \hat{Q}_m &= m \log(q_d - \langle q \rangle) - m \int_m^1 \frac{dy}{y^2} \log \left(\frac{q_d - \langle q \rangle - [q](y)}{q_d - \langle q \rangle} \right) \\
&= \log(q_d - \langle q \rangle) - m \int_m^1 \frac{dy}{y^2} \log(q_d - \langle q \rangle - [q](y)) , \\
(q^{-1})_d &= \frac{1}{q_d - \langle q \rangle} \left(1 - \int_m^1 \frac{dy}{y^2} \frac{[q](y)}{q_d - \langle q \rangle - [q](y)} \right) , \\
(q^{-1})(x) &= -\frac{1}{q_d - \langle q \rangle} \left[\frac{[q](x)}{x(q_d - \langle q \rangle - [q](x))} + \int_m^x \frac{dy}{y^2} \frac{[q](y)}{q_d - \langle q \rangle - [q](y)} \right] , \\
[q](x) &= xq(x) - \int_m^x dy q(y) , \\
\langle q \rangle &= \int_m^1 dx q(x) .
\end{aligned} \tag{24}$$

In order to compute $\log \det \hat{\alpha}^{m,m}$, we introduce a matrix $\hat{\beta}$ which is “regularized” in such a way that $\sum_b \beta_{ab} = \varepsilon$, and $\hat{\alpha} = \lim_{\varepsilon \rightarrow 0} \hat{\beta}$. For instance we can choose

$$\hat{\beta} \leftrightarrow \{\beta_d, \beta(x)\} = \{\alpha_d, -\alpha(x) + \varepsilon \delta(x - x_0)\} , \tag{25}$$

for any $x_0 \in [m, 1]$. The matrix $\hat{\beta}$ is invertible, hence we can use the relation $\det \hat{\beta}^{m,m} = (\hat{\beta}^{-1})_{mm} \det \hat{\beta}$. Using Eq. (24) we get

$$\begin{aligned}
\log \det \hat{\alpha}^{m,m} &= \lim_{\varepsilon \rightarrow 0} \left\{ \log \det \hat{\beta} + \log (\hat{\beta}^{-1})_{mm} \right\} = \lim_{\varepsilon \rightarrow 0} \left\{ \log \det \hat{\beta} + \log \beta_d^{-1} \right\} \\
&= \lim_{\varepsilon \rightarrow 0} \left\{ -m \int_m^1 \frac{dy}{y^2} \log(\beta_d - \langle \beta \rangle - [\beta](y)) + \log \left(1 - \int_m^1 \frac{dy}{y^2} \frac{[\beta](y)}{\beta_d - \langle \beta \rangle - [\beta](y)} \right) \right\} .
\end{aligned} \tag{26}$$

Note that for $\varepsilon \rightarrow 0$ we have $\langle \beta \rangle = -\int_m^1 dx \alpha(x) = \alpha_d = \beta_d$. However, the singular terms $\log(\beta_d - \langle \beta \rangle)$ cancel and we obtain a finite result

$$\log \det \hat{\alpha}^{m,m} = -m \int_m^1 \frac{dy}{y^2} \log([\alpha](y)) + \log \left(1 + \int_m^1 \frac{dy}{y^2} \right) = -\log m - m \int_m^1 \frac{dy}{y^2} \log([\alpha](y)) . \tag{27}$$

Expressed in terms of the function $\Delta(x)$ by means of Eq. (20), we have that

$$-m \int_m^1 \frac{dy}{y^2} \log([\alpha](y)) = -(m-1) \log 2 - m \int_m^1 \frac{dy}{y^2} \log \left[y \Delta(y) + \int_y^1 dz \Delta(z) \right] , \tag{28}$$

therefore

$$\log \det \hat{\alpha}^{m,m} = -\log m - (m-1) \log 2 - m \int_m^1 \frac{dy}{y^2} \log \left[y \Delta(y) + \int_y^1 dz \Delta(z) \right] . \tag{29}$$

2. 1RSB and 2RSB

When specialized to the 1RSB case Eq. (16), which corresponds to $\alpha(x) = \hat{\alpha}_1$ and $\Delta(x) = \hat{\Delta}_1 = 2m\hat{\alpha}_1$, we get

$$\log \det \hat{\alpha}_{1\text{RSB}}^{m,m} = -\log m + (m-1) \log(m\hat{\alpha}_1) = -\log m + (m-1) \log(\hat{\Delta}_1/2) , \tag{30}$$

which reproduces the results of [1, 2]. The 2RSB solution is parametrized by a step function

$$\alpha(x) = \begin{cases} \hat{\alpha}_1 & m \leq x < m_1 \\ \hat{\alpha}_2 & m_1 \leq x \leq 1 \end{cases} \quad [\alpha](x) = \begin{cases} m\hat{\alpha}_1 & m \leq x < m_1 \\ m_1\hat{\alpha}_2 + (m-m_1)\hat{\alpha}_1 & m_1 \leq x \leq 1 \end{cases} \tag{31}$$

and therefore

$$\log \det \hat{\alpha}_{2\text{RSB}}^{m,m} = -\log m + \left(\frac{m}{m_1} - 1\right) \log(m\hat{\alpha}_1) + \left(m - \frac{m}{m_1}\right) \log(m_1\hat{\alpha}_2 + (m - m_1)\hat{\alpha}_1) . \quad (32)$$

Using the relations

$$\begin{aligned} \hat{\Delta}_2 &= 2m_1\hat{\alpha}_2 + 2(m - m_1)\hat{\alpha}_1 , \\ \hat{\Delta}_1 &= \hat{\Delta}_2 + 2(\hat{\alpha}_1 - \hat{\alpha}_2) , \end{aligned} \quad (33)$$

or directly Eq. (29), we have

$$\log \det \hat{\alpha}_{2\text{RSB}}^{m,m} = -\log m - (m - 1) \log 2 + \left(\frac{m}{m_1} - 1\right) \log[m_1\hat{\Delta}_1 + (1 - m_1)\hat{\Delta}_2] + \left(m - \frac{m}{m_1}\right) \log \hat{\Delta}_2 . \quad (34)$$

3. *k*RSB

Writing explicitly the *k*RSB expression requires the introduction of a function

$$G(x) = x\Delta(x) + \int_x^1 dz \Delta(z) . \quad (35)$$

In fact, if $\Delta(x)$ is a *k*RSB piecewise constant function and using the notations of Fig. 1, it is easy to check that $G(x)$ is also a piecewise constant function parametrized by \hat{G}_i , with

$$\hat{G}_i = m_i \hat{\Delta}_i + \sum_{j=i+1}^k (m_j - m_{j-1}) \hat{\Delta}_j . \quad (36)$$

Note that $\frac{dG(x)}{dx} = x \frac{d\Delta(x)}{dx}$, and $G(1) = \Delta(1)$, therefore from $G(x)$ one can reconstruct $\Delta(x)$ as

$$\Delta(x) = G(1) - \int_x^1 \frac{dz}{z} \frac{dG(z)}{dz} = \frac{G(x)}{x} - \int_x^1 \frac{dz}{z^2} G(z) , \quad (37)$$

or for a *k*RSB function

$$\hat{\Delta}_i = \frac{\hat{G}_i}{m_i} + \sum_{j=i+1}^k \left(\frac{1}{m_j} - \frac{1}{m_{j-1}}\right) \hat{G}_j . \quad (38)$$

Then, from Eq. (29), we have

$$\begin{aligned} \log \det \hat{\alpha}_{k\text{RSB}}^{m,m} &= -\log m - m \int_m^1 \frac{dy}{y^2} \log[G(y)/2] \\ &= -\log m + \sum_{i=1}^k \left(\frac{m}{m_i} - \frac{m}{m_{i-1}}\right) \log(\hat{G}_i/2) \end{aligned} \quad (39)$$

Note that from this result we can recover the 1RSB and 2RSB results obtained above.

C. The interaction term

1. *k*RSB derivation

We now compute the interaction term of the replicated entropy for a generic hierarchical matrix Δ_{ab} parametrized by $\Delta(x)$. We start from Eq. (15), and we need to compute the function

$$g(m, h) = \left\{ \exp \left[-\frac{1}{2} \sum_{a,b=1}^m \Delta_{ab} \frac{\partial^2}{\partial h_a \partial h_b} \right] \prod_{a=1}^m \theta(h_a) \right\}_{\{h_a=h\}} . \quad (40)$$

Because Δ_{ab} is a hierarchical matrix, this computation can be done by taking the derivative with respect to the external fields in a hierarchical way [62]. Let us define the matrix $I_{ab}^{m_i}$, which has elements equal to 1 in blocks of size m_i around the diagonal, and zero otherwise. In other words, the matrix $I_{ab}^{m_i}$ is parametrized by a function $I^{m_i}(x) = 1$ for $m_i \leq x \leq 1$ and zero otherwise. Then, recalling the notations of Fig. 1, and noting that $I_{ab}^{m_k=1} = \delta_{ab}$, one can easily check that

$$\Delta_{ab} = \sum_{i=1}^k \widehat{\Delta}_i (I_{ab}^{m_{i-1}} - I_{ab}^{m_i}) = \sum_{i=0}^{k-1} (\widehat{\Delta}_{i+1} - \widehat{\Delta}_i) I_{ab}^{m_i} - \widehat{\Delta}_k \delta_{ab} . \quad (41)$$

Inserting this form in Eq. (40), one obtains a sequence of differential operators acting on the product of theta functions, each of them being the sum of partial derivatives inside a block. This sequence of operations can be written as a recursion; since the procedure is very well explained in [62], we only report the main results here. When acting with the term containing $\widehat{\Delta}_k$ we obtain, recalling Eq. (13):

$$g(1, h) = \exp \left[\frac{\widehat{\Delta}_k}{2} \frac{d^2}{dh^2} \right] \theta(h) = \gamma_{\widehat{\Delta}_k} \star \theta(h) = \Theta \left(\frac{h}{\sqrt{2\widehat{\Delta}_k}} \right) . \quad (42)$$

Then, the action of each of the terms $i = k-1, \dots, 0$ induces a recursion of the form

$$g(m_i, h) = \exp \left[\frac{\widehat{\Delta}_i - \widehat{\Delta}_{i+1}}{2} \frac{d^2}{dh^2} \right] g(m_{i+1}, h)^{\frac{m_i}{m_{i+1}}} = \gamma_{\widehat{\Delta}_i - \widehat{\Delta}_{i+1}} \star g(m_{i+1}, h)^{\frac{m_i}{m_{i+1}}} . \quad (43)$$

Note that the last of these iterations can be written explicitly as

$$g(m, h) = \gamma_{-\widehat{\Delta}_1} \star g(m_1, h)^{\frac{m}{m_1}} . \quad (44)$$

This recursive procedure allows us to compute easily $g(m, h)$ for any k , and, according to Eq. (15), the function $\mathcal{F}(\Delta)$.

The last iteration might seem problematic, because the kernel γ_a has a negative parameter $a = -\widehat{\Delta}_1$ and therefore cannot be represented as in Eq. (13). Luckily enough, this last iteration can be eliminated. In fact, we have

$$\begin{aligned} \mathcal{F}(\Delta) &= \int_{-\infty}^{\infty} dh e^h \frac{d}{dh} g(m, h) = \int_{-\infty}^{\infty} dh e^h e^{-\frac{\widehat{\Delta}_1}{2} \frac{d^2}{dh^2}} \frac{d}{dh} g(m_1, h)^{\frac{m}{m_1}} \\ &= \int_{-\infty}^{\infty} dh \left[e^{-\frac{\widehat{\Delta}_1}{2} \frac{d^2}{dh^2}} e^h \right] \frac{d}{dh} g(m_1, h)^{\frac{m}{m_1}} = e^{-\frac{\widehat{\Delta}_1}{2}} \int_{-\infty}^{\infty} dh e^h \frac{d}{dh} g(m_1, h)^{\frac{m}{m_1}} , \end{aligned} \quad (45)$$

where we performed an integration by parts and assumed that all the boundary terms vanish because all the derivatives of the function $\frac{d}{dh} g(m_1, h)^{\frac{m}{m_1}}$ vanish for $h \rightarrow \infty$. This is justified by the fact that $g(m_i, h)$ behaves, for large h , similarly to a $\Theta(h)$ function, as it can be seen from the recurrence equations (42) and (43). Assuming, for the same reason, that $1 - g(m_1, h)^{\frac{m}{m_1}}$ decays at $h \rightarrow -\infty$ faster than a simple exponential, in order to perform another integration by parts, we have

$$\mathcal{F}(\Delta) = e^{-\frac{\widehat{\Delta}_1}{2}} \int_{-\infty}^{\infty} dh e^h \frac{d}{dh} g(m_1, h)^{\frac{m}{m_1}} = e^{-\frac{\widehat{\Delta}_1}{2}} \int_{-\infty}^{\infty} dh e^h \left\{ 1 - g(m_1, h)^{\frac{m}{m_1}} \right\} . \quad (46)$$

2. 1RSB and 2RSB

Using Eq. (42) we obtain, at the 1RSB level,

$$\mathcal{F}_{1\text{RSB}}(\Delta) = e^{-\frac{\widehat{\Delta}_1}{2}} \int_{-\infty}^{\infty} dh e^h \left\{ 1 - [\gamma_{\widehat{\Delta}_1} \star \theta(h)]^m \right\} , \quad (47)$$

at the 2RSB level

$$\begin{aligned} g(m_1, h)^{\frac{m}{m_1}} &= \left[\gamma_{\widehat{\Delta}_1 - \widehat{\Delta}_2} \star g(1, h)^{m_1} \right]^{\frac{m}{m_1}} = \left[\gamma_{\widehat{\Delta}_1 - \widehat{\Delta}_2} \star \left(\gamma_{\widehat{\Delta}_2} \star \theta(h) \right)^{m_1} \right]^{\frac{m}{m_1}} , \\ \mathcal{F}_{2\text{RSB}}(\Delta) &= e^{-\frac{\widehat{\Delta}_1}{2}} \int_{-\infty}^{\infty} dh e^h \left\{ 1 - \left[\gamma_{\widehat{\Delta}_1 - \widehat{\Delta}_2} \star \left(\gamma_{\widehat{\Delta}_2} \star \theta(h) \right)^{m_1} \right]^{\frac{m}{m_1}} \right\} , \end{aligned} \quad (48)$$

and so on. At the 1RSB level, we reproduce the result of [1, 2].

3. Continuum limit

The above strategy is not very practical when $\Delta(x)$ is a continuous function. In this case, to take the continuum limit it is convenient to follow again [62]. We have $m_i = x - dx$, $m_{i+1} = x$, and $\hat{\Delta}_i - \hat{\Delta}_{i+1} = -\dot{\Delta}(x)dx$, where a dot denotes derivative with respect to x . Hence Eq. (43) becomes in the region where $\Delta(x)$ is a continuous function

$$g(x - dx, h) = \exp \left[-dx \frac{\dot{\Delta}(x)}{2} \frac{d^2}{dh^2} \right] g(x, h)^{\frac{x-dx}{x}} \quad (49)$$

and then expanding in powers of dx , at linear order we get the Parisi equation

$$\frac{\partial g(x, h)}{\partial x} = \frac{1}{2} \dot{\Delta}(x) \frac{\partial^2 g(x, h)}{\partial h^2} + \frac{1}{x} g(x, h) \log g(x, h) \quad (50)$$

that has to be solved with the initial condition (42). Note that the partial differential equation is well defined because $\dot{\Delta}(x) \leq 0$. This equation has to be integrated from $x = 1$ down to $x = m_1$. The resulting $g(m_1, h)$ can be inserted in Eq. (46) to obtain $\mathcal{F}(\Delta)$.

The partial differential equation written above can be also put in a more convenient form by introducing the function

$$f(x, h) = \frac{1}{x} \log g(x, h) \quad (51)$$

which obeys the equation

$$\frac{\partial f(x, h)}{\partial x} = \frac{1}{2} \dot{\Delta}(x) \left[\frac{\partial^2 f(x, h)}{\partial h^2} + x \left(\frac{\partial f(x, h)}{\partial h} \right)^2 \right] \quad (52)$$

with initial condition

$$f(1, h) = \log \Theta \left[\frac{h}{\sqrt{2\Delta(1)}} \right]. \quad (53)$$

Remarkably enough, the equations written above are identical to those of the SK model [30, 62]. The only difference is in the initial condition for the Parisi equation.

D. 1RSB, 2RSB, k RSB, fullRSB expressions of the replicated entropy

We therefore obtained the expression of the replicated entropy, under the assumption that the matrices $\hat{\alpha}$ and $\hat{\Delta}$ are hierarchical k RSB matrices, and we now summarize the results that we obtained at different levels of RSB for the replicated entropy (1). At any level of k RSB, the replicated entropy has the form

$$s[\hat{\alpha}_{k\text{RSB}}] = 1 - \log \rho + \frac{d}{2} m \log m + \frac{d}{2} (m-1) \log(\pi e D^2 / d^2) + \frac{d}{2} \mathcal{S}_{k\text{RSB}}, \quad (54)$$

$$\mathcal{S}_{k\text{RSB}} = (2-m) \log m + (m-1) \log 2 + \log \det(\hat{\alpha}_{k\text{RSB}}^{m,m}) - \hat{\varphi} \mathcal{F}(2\hat{\alpha}_{k\text{RSB}})$$

where $\mathcal{S}_{k\text{RSB}}$ has been defined in such a way that it contains the non-trivial dependence on $\hat{\alpha}$ and it has a good limit for $m \rightarrow 0$ (as we will discuss later).

At the 1RSB level, using Eqs. (30), (47) and (46), we obtain

$$\mathcal{S}_{1\text{RSB}} = (m-1) \log(\hat{\Delta}_1/m) - \hat{\varphi} e^{-\hat{\Delta}_1/2} \int_{-\infty}^{\infty} dh e^h \{1 - [\gamma_{\hat{\Delta}_1} \star \theta(h)]^m\} \quad (55)$$

which coincides with the previously derived results [1, 2, 11]. At the 2RSB level, we have, using Eqs. (34), (48) and (46),

$$\begin{aligned} \mathcal{S}_{2\text{RSB}} = & \left(\frac{m}{m_1} - 1 \right) \log[(m_1 \hat{\Delta}_1 + (1-m_1) \hat{\Delta}_2)/m] + \left(m - \frac{m}{m_1} \right) \log(\hat{\Delta}_2/m) \\ & - \hat{\varphi} e^{-\frac{\hat{\Delta}_1}{2}} \int_{-\infty}^{\infty} dh e^h \left[1 - \left[\gamma_{\hat{\Delta}_1 - \hat{\Delta}_2} \star \left(\gamma_{\hat{\Delta}_2} \star \theta(h) \right)^{m_1} \right]^{m/m_1} \right] \end{aligned} \quad (56)$$

At the generic k RSB level we obtain from Eq. (39), (46), (42), (43), (44):

$$\begin{aligned}
\mathcal{S}_{k\text{RSB}} &= \sum_{i=1}^k \left(\frac{m}{m_i} - \frac{m}{m_{i-1}} \right) \log(\widehat{G}_i/m) - \widehat{\varphi} e^{-\widehat{\Delta}_1/2} \int_{-\infty}^{\infty} dh e^h \left\{ 1 - g(m_1, h)^{\frac{m}{m_1}} \right\}, \\
\widehat{G}_i &= m_i \widehat{\Delta}_i + \sum_{j=i+1}^k (m_j - m_{j-1}) \widehat{\Delta}_j, \\
g(1, h) &= \gamma_{\widehat{\Delta}_k} \star \theta(h), \\
g(m_i, h) &= \gamma_{\widehat{\Delta}_i - \widehat{\Delta}_{i+1}} \star g(m_{i+1}, h)^{\frac{m_i}{m_{i+1}}}, \quad i = 1 \cdots k-1.
\end{aligned} \tag{57}$$

Finally, the fullRSB expression is, from Eqs. (29), (46), (51), (52), (53):

$$\begin{aligned}
\mathcal{S}_{\infty\text{RSB}} &= -m \int_m^1 \frac{dy}{y^2} \log \left[\frac{y\Delta(y)}{m} + \int_y^1 dz \frac{\Delta(z)}{m} \right] - \widehat{\varphi} e^{-\Delta(m)/2} \int_{-\infty}^{\infty} dh e^h [1 - e^{mf(m,h)}], \\
\frac{\partial f(x, h)}{\partial x} &= \frac{1}{2} \dot{\Delta}(x) \left[\frac{\partial^2 f(x, h)}{\partial h^2} + x \left(\frac{\partial f(x, h)}{\partial h} \right)^2 \right], \\
f(1, h) &= \log \Theta \left[\frac{h}{\sqrt{2\Delta(1)}} \right].
\end{aligned} \tag{58}$$

IV. VARIATIONAL EQUATIONS

The replicated entropy depends on the function $\Delta(x)$ that parametrizes the hierarchical matrix $\widehat{\Delta}$. This function is determined by optimization of the replicated entropy through a variational principle [30]. In this section we derive the variational equations for the function $\Delta(x)$ that are obtained by optimization of the free energy, i.e. by imposing the equation $\frac{\partial s[\widehat{\Delta}]}{\partial \Delta_{ab}} = 0$. It is well known in the context of spin glasses [30] and structural glasses [10, 11] that, for integer $m > 1$, this corresponds to the usual maximization of the entropy or minimization of the free energy with respect to the variational parameters α_{ab} , but when the problem is analytically continued to real $m < 1$, the solution of these equations does not correspond to a maximum of the entropy, but to a saddle point. This not very important because to really characterize the stability of the saddle point one has first to compute the matrix of second derivatives $\frac{\partial^2 s[\widehat{\Delta}]}{\partial \Delta_{ab} \partial \Delta_{cd}}$, and then perform the analytic continuation of its eigenvalues to $m < 1$. The continued eigenvalues are required to be positive.

In this section we derive the variational equations for $\Delta(x)$, and we postpone a partial analysis of the stability matrix to the following sections. In Sec. IV A we derive the equation for $\widehat{\Delta}_i$ in the case of a k RSB structure. In Sec. IV B we derive the fullRSB equations in two equivalent ways: first by using Lagrange multipliers, and then by taking the $k \rightarrow \infty$ limit of the k RSB equations.

A. Variational equations for the k RSB solution

We consider first the k RSB solution for fixed k . We start from Eq. (57) and we want to impose the condition $\frac{\partial \mathcal{S}_{k\text{RSB}}}{\partial \Delta_i} = 0$. To do this, we consider Eq. (40) and (46). We have, without taking into account that the matrix Δ_{ab} is symmetric and for $a \neq b$:

$$\begin{aligned}
\frac{\partial g(m, h)}{\partial \Delta_{ab}} &= \left\{ \exp \left[-\frac{1}{2} \sum_{c,d=1}^m \Delta_{cd} \frac{\partial^2}{\partial h_c \partial h_d} \right] \left(-\frac{1}{2} \frac{\partial^2}{\partial h_a \partial h_b} \right) \prod_{f=1}^m \theta(h_f) \right\}_{\{h_a=h\}} \\
&= -\frac{1}{2} \left\{ \exp \left[-\frac{1}{2} \sum_{c,d=1}^m \Delta_{cd} \frac{\partial^2}{\partial h_c \partial h_d} \right] \delta(h_a) \delta(h_b) \prod_{f \neq a,b}^{1,m} \theta(h_f) \right\}_{\{h_a=h\}}
\end{aligned} \tag{59}$$

Note that there are $m(m_{\ell-1} - m_\ell)$ elements in the block $\ell = 1 \cdots k$ and they all give the same contribution, therefore

$$\frac{\partial g(m, h)}{\partial \widehat{\Delta}_\ell} = -\frac{m(m_{\ell-1} - m_\ell)}{2} \left\{ \exp \left[-\frac{1}{2} \sum_{c,d=1}^m \Delta_{cd} \frac{\partial^2}{\partial h_c \partial h_d} \right] \delta(h_a) \delta(h_b) \prod_{f \neq a,b}^{1,m} \theta(h_f) \right\}_{\{h_a=h\}} . \quad (60)$$

For a hierarchical matrix, we can use again the strategy of [62]. The difference is that at the beginning of the iteration, there is a special block that contains the delta instead of the theta function. At some level, the two blocks that contain the delta are merged. If the two replicas ab are in the ℓ -th block, then we have the following iteration equations:

$$\begin{aligned} N_\ell(1, h) &= \gamma_{\widehat{\Delta}_k} \star \delta(h) = \frac{e^{-h^2/(2\widehat{\Delta}_k)}}{\sqrt{2\pi\widehat{\Delta}_k}} \\ N_\ell(m_i, h) &= \gamma_{\widehat{\Delta}_i - \widehat{\Delta}_{i+1}} \star [N_\ell(m_{i+1}, h) g(m_{i+1}, h)^{m_i/m_{i+1}-1}] \quad i = k-1, \dots, \ell \\ N_\ell(m_{\ell-1}, h) &= \gamma_{\widehat{\Delta}_{\ell-1} - \widehat{\Delta}_\ell} \star [N_\ell(m_\ell, h)^2 g(m_\ell, h)^{m_{\ell-1}/m_\ell-2}] \\ N_\ell(m_i, h) &= \gamma_{\widehat{\Delta}_i - \widehat{\Delta}_{i+1}} \star [N_\ell(m_{i+1}, h) g(m_{i+1}, h)^{m_i/m_{i+1}-1}] \quad i = \ell-2, \dots, 0 \\ \frac{\partial g(m, h)}{\partial \widehat{\Delta}_\ell} &= -\frac{m(m_{\ell-1} - m_\ell)}{2} N_\ell(m, h) \end{aligned} \quad (61)$$

Note that these equations hold for all $\ell = k, \dots, 1$. In the discrete k RSB case, Eq. (51) reads

$$f(m_i, h) = \frac{1}{m_i} \log g(m_i, h) , \quad (62)$$

and we note that for $i > \ell$, namely before the two blocks are merged, we can show by recurrence that (denoting with primes the derivatives with respect to h)

$$g'(m_i, h) = m_i N_\ell(m_i, h) \quad \Leftrightarrow \quad f'(m_i, h) = N_\ell(m_i, h) / g(m_i, h) . \quad (63)$$

This allows for an important simplification because we do not need N_ℓ for $i \geq \ell$ anymore. We can rewrite Eqs. (61) equivalently as

$$\begin{aligned} N_\ell(m_{\ell-1}, h) &= \gamma_{\widehat{\Delta}_{\ell-1} - \widehat{\Delta}_\ell} \star [f'(m_\ell, h)^2 g(m_\ell, h)^{m_{\ell-1}/m_\ell}] \\ N_\ell(m_i, h) &= \gamma_{\widehat{\Delta}_i - \widehat{\Delta}_{i+1}} \star [N_\ell(m_{i+1}, h) g(m_{i+1}, h)^{m_i/m_{i+1}-1}] \quad i = \ell-2, \dots, 0 \\ \frac{\partial g(m, h)}{\partial \widehat{\Delta}_\ell} &= -\frac{m(m_{\ell-1} - m_\ell)}{2} N_\ell(m, h) \end{aligned} \quad (64)$$

Now, let us introduce a series of operators Γ_ℓ that are defined by the following equations for an arbitrary test function $t(h)$:

$$\begin{aligned} \Gamma_1 \star t(h) &= g(m_1, h)^{\frac{m}{m_1}} t(h) , \\ \Gamma_i \star t(h) &= \Gamma_{i-1} \star \left[\frac{1}{g(m_{i-1}, h)} \gamma_{\widehat{\Delta}_{i-1} - \widehat{\Delta}_i} \star g(m_i, h)^{\frac{m_{i-1}}{m_i}} t(h) \right] \quad i = 2, \dots, k . \end{aligned} \quad (65)$$

Then we have

$$N_\ell(m, h) = \gamma_{-\widehat{\Delta}_1} \star \Gamma_\ell \star f'(m_\ell, h)^2 . \quad (66)$$

The next step is to take the derivative with respect to \widehat{G}_i of the k RSB free energy, which we write in the form

$$\mathcal{S}_{k\text{RSB}} = \sum_{i=1}^k \left(\frac{m}{m_i} - \frac{m}{m_{i-1}} \right) \log(\widehat{G}_i/m) - \widehat{\varphi} \int_{-\infty}^{\infty} dh e^h \frac{d}{dh} g(m, h) , \quad (67)$$

and make use of the relation (38). We get

$$\begin{aligned}
\left(\frac{1}{m_i} - \frac{1}{m_{i-1}}\right) \frac{m}{\widehat{G}_i} &= \widehat{\varphi} \int_{-\infty}^{\infty} dh e^h \frac{d}{dh} \sum_{j=1}^k \frac{\partial g(m, h)}{\partial \widehat{\Delta}_j} \frac{\partial \widehat{\Delta}_j}{\partial \widehat{G}_i} \\
&= \widehat{\varphi} \int_{-\infty}^{\infty} dh e^h \frac{d}{dh} \left\{ \frac{1}{m_i} \frac{\partial g(m, h)}{\partial \widehat{\Delta}_i} + \sum_{j=1}^{i-1} \frac{\partial g(m, h)}{\partial \widehat{\Delta}_j} \left(\frac{1}{m_i} - \frac{1}{m_{i-1}}\right) \right\} \\
&= \frac{m \widehat{\varphi}}{2} \int_{-\infty}^{\infty} dh e^h \frac{d}{dh} \left\{ \frac{1}{m_i} (m_i - m_{i-1}) N_i(m, h) + \sum_{j=1}^{i-1} (m_j - m_{j-1}) N_j(m, h) \left(\frac{1}{m_i} - \frac{1}{m_{i-1}}\right) \right\}.
\end{aligned} \tag{68}$$

We observe from Eq. (61) that $N_i(m, h)$ behaves like a Gaussian for $h \rightarrow \pm\infty$, therefore we can safely integrate by parts, and the last expression can be written as

$$\begin{aligned}
\frac{1}{\widehat{G}_i} &= -\frac{\widehat{\varphi}}{2} \int_{-\infty}^{\infty} dh e^h \frac{d}{dh} \left\{ m_{i-1} N_i(m, h) - \sum_{j=1}^{i-1} (m_j - m_{j-1}) N_j(m, h) \right\} \\
&= -\frac{\widehat{\varphi}}{2} \int_{-\infty}^{\infty} dh e^h \gamma_{-\widehat{\Delta}_1} \star \frac{d}{dh} \left\{ m_{i-1} \Gamma_i \star f'(m_i, h)^2 - \sum_{j=1}^{i-1} (m_j - m_{j-1}) \Gamma_j \star f'(m_j, h)^2 \right\} \\
&= -\frac{\widehat{\varphi}}{2} e^{-\widehat{\Delta}_1/2} \int_{-\infty}^{\infty} dh e^h \frac{d}{dh} \left\{ m_{i-1} \Gamma_i \star f'(m_i, h)^2 - \sum_{j=1}^{i-1} (m_j - m_{j-1}) \Gamma_j \star f'(m_j, h)^2 \right\} \\
&= \frac{\widehat{\varphi}}{2} e^{-\widehat{\Delta}_1/2} \int_{-\infty}^{\infty} dh e^h \left\{ m_{i-1} \Gamma_i \star f'(m_i, h)^2 - \sum_{j=1}^{i-1} (m_j - m_{j-1}) \Gamma_j \star f'(m_j, h)^2 \right\},
\end{aligned} \tag{69}$$

using the same trick as in Eq. (45). Finally, we can show that

$$\int_{-\infty}^{\infty} dh e^h \Gamma_i \star f'(m_i, h)^2 = \int_{-\infty}^{\infty} dh P(m_i, h) f'(m_i, h)^2, \tag{70}$$

provided $P(m_i, h)$ satisfies the following recurrence equations:

$$P(m_1, h) = e^h g(m_1, h)^{\frac{m}{m_1}}, \tag{71}$$

$$P(m_i, h) = \int dz \frac{P(m_{i-1}, z)}{g(m_{i-1}, z)} \gamma_{\widehat{\Delta}_{i-1} - \widehat{\Delta}_i} (h - z) g(m_i, h)^{\frac{m_{i-1}}{m_i}} \quad i = 2, \dots, k. \tag{72}$$

We obtain therefore the final result

$$\frac{1}{\widehat{G}_i} = \frac{\widehat{\varphi}}{2} e^{-\widehat{\Delta}_1/2} \int_{-\infty}^{\infty} dh \left\{ m_{i-1} P(m_i, h) f'(m_i, h)^2 - \sum_{j=1}^{i-1} (m_j - m_{j-1}) P(m_j, h) f'(m_j, h)^2 \right\}. \tag{73}$$

Eqs. (73), (71)-(72), (42)-(43), (38) constitute a set of closed equations for the \widehat{G}_i , or equivalently the $\widehat{\Delta}_i$. They can be solved by the following iteration: starting from a guess for $\widehat{\Delta}_i$, one can solve first the recurrence (42)-(43) and then the recurrence (71)-(72). From the solutions one can compute the new \widehat{G}_i using Eq. (73) and from these the new $\widehat{\Delta}_i$ using Eq. (38).

B. Variational equations for the fullRSB solution

In this section we will derive the saddle point equations for this function $\Delta(x)$ in the continuum limit of fullRSB. We will do this in two different ways. The first derivation starts from Eq. (58), and it imposes the variational condition $\frac{d\mathcal{S}_{\text{fullRSB}}}{d\Delta(x)} = 0$ making use of Lagrange multipliers to enforce the Parisi equation [63]. The second derivation simply consists of taking the continuum limit of the variational equations obtained in the previous section. We obtain equivalent results which confirms that the calculation is correct. Given the complexity of the computation, this is a very useful check.

1. Lagrange multipliers

We need to introduce Lagrange multipliers because the entropy is written in terms of the function $g(x, h)$ or, equivalently, of the function $f(x, h)$, and this function must satisfy the Parisi equation (52). In order to do properly the optimization, one can introduce two Lagrange multipliers: $P(x, h)$ is the one needed to enforce the partial differential equation and $P(1, h)$ is the one needed to enforce the initial condition. Let us start from the complete fullRSB expression of the entropy, Eq. (58) (where terms that are not important to derive the saddle point equations are omitted), to which we add these Lagrange multipliers. As a reminder, we indicate the derivative with respect to x with a dot and the derivative with respect to h with a prime. With these notations, and using Eqs. (37), (35) with $\Delta(m) = \frac{G(m)}{m} - \int_m^1 \frac{dz}{z^2} G(z)$, we have to impose stationarity of the function

$$\begin{aligned} \mathcal{S}_{\infty\text{RSB}} = & -m \int_m^1 \frac{dx}{x^2} \log[G(x)/m] - \widehat{\varphi} e^{-\frac{\Delta(m)}{2}} \int_{-\infty}^{\infty} dh e^h [1 - e^{mf(m,h)}] \\ & + m\widehat{\varphi} e^{-\frac{\Delta(m)}{2}} \int_{-\infty}^{\infty} dh \int_m^1 dx P(x, h) \left\{ \dot{f}(x, h) - \frac{1}{2} \frac{\dot{G}(x)}{x} [f''(x, h) + xf'(x, h)^2] \right\} \\ & - m\widehat{\varphi} e^{-\frac{\Delta(m)}{2}} \int_{-\infty}^{\infty} dh P(1, h) \left\{ f(1, h) - \log \Theta \left(\frac{h}{\sqrt{2G(1)}} \right) \right\} \end{aligned} \quad (74)$$

over $\Delta(x)$, $f(x, h)$, $P(x, h)$, $f(m, h)$ and $P(1, h)$. The first two equations can be obtained by taking the variation with respect to $P(x, h)$ and $f(x, h)$

$$\dot{f}(x, h) = \frac{1}{2} \frac{\dot{G}(x)}{x} [f''(x, h) + xf'(x, h)^2] , \quad (75)$$

$$\dot{P}(x, h) = -\frac{1}{2} \frac{\dot{G}(x)}{x} [P''(x, h) - 2x(P(x, h)f'(x, h))'] . \quad (76)$$

Taking the variation over $P(1, h)$ and $f(m, h)$ we obtain

$$f(1, h) = \log \Theta \left(\frac{h}{\sqrt{2G(1)}} \right) , \quad (77)$$

$$P(m, h) = e^{mf(m,h)+h} . \quad (78)$$

Finally, taking the variation of $G(x)$ (for $x \neq 1$ and $x \neq m$) we obtain the following equation

$$\begin{aligned} \frac{m}{G(x)} = & -\frac{m\widehat{\varphi}}{2} e^{-\frac{\Delta(m)}{2}} \int_{-\infty}^{\infty} dh P(x, h) f''(x, h) - \frac{\widehat{\varphi}}{2} e^{-\frac{\Delta(m)}{2}} \int_{-\infty}^{\infty} dh e^h [1 - e^{mf(m,h)}] \\ = & -\frac{m\widehat{\varphi}}{2} e^{-\frac{\Delta(m)}{2}} \int_{-\infty}^{\infty} dh P(x, h) f''(x, h) - \frac{\widehat{\varphi}}{2} e^{-\frac{\Delta(m)}{2}} \int_{-\infty}^{\infty} dh e^h e^{mf(m,h)} m f'(m, h) \\ = & -\frac{m\widehat{\varphi}}{2} e^{-\frac{\Delta(m)}{2}} \left\{ \int_{-\infty}^{\infty} dh P(x, h) f''(x, h) + \int_{-\infty}^{\infty} dh P(m, h) f'(m, h) \right\} , \end{aligned}$$

which is more conveniently rewritten as

$$\frac{1}{G(x)} = -\frac{\widehat{\varphi}}{2} e^{-\frac{\Delta(m)}{2}} \int_{-\infty}^{\infty} dh [P(x, h) f''(x, h) + P(m, h) f'(m, h)] . \quad (79)$$

The system of Eqs. (75)-(79) can be in principle solved numerically, with the following procedure:

- one starts with a guess for $G(x)$;
- from this one solves Eq. (75) with boundary condition (77) to get $f(x, h)$;
- then one can solve Eq. (76) with boundary condition (78) to obtain $P(x, h)$;
- from Eq. (79) one obtains the new $G(x)$

2. Continuum limit of the k RSB variational equations

We now take the continuum limit of the discrete k RSB equations following the strategy of section III C 3. It was already shown in that section that in this limit the recurrence equations for $g(x, h)$, Eqs. (42) and (43), become the Parisi equation (75) with boundary condition (77). The boundary condition for $P(x, h)$ in the discrete, Eq. (71), is clearly equivalent to the one in the continuum, Eq. (78). It is quite simple, following the lines as in section III C 3, to show that Eq. (72) becomes, in the continuum limit, Eq. (76), so we do not report the derivation.

It remains to derive Eq. (79). We start from Eq. (73) which becomes in the continuum limit

$$\frac{1}{G(x)} = \frac{\hat{\varphi}}{2} e^{-\frac{\Delta(m)}{2}} \int_{-\infty}^{\infty} dh \left\{ xP(x, h)f'(x, h)^2 - \int_m^x dz P(z, h)f'(z, h)^2 \right\}. \quad (80)$$

We now show that Eq. (79) and Eq. (80) are equivalent. This amounts to showing that

$$\int_{-\infty}^{\infty} dh [P(x, h)f''(x, h) + P(m, h)f'(m, h)] = - \int_{-\infty}^{\infty} dh \left\{ xP(x, h)f'(x, h)^2 - \int_m^x dz P(z, h)f'(z, h)^2 \right\}. \quad (81)$$

The strategy to prove the equality (81) is the following. We first see that the two sides are the same at $x = m$ and then we prove that their derivatives with respect to x are the same. In the following, we say that $a(x, h) \sim b(x, h)$ if $\int_{-\infty}^{\infty} dh a(x, h) = \int_{-\infty}^{\infty} dh b(x, h)$ to simplify the notations. Doing integration by parts, and noting that from the initial condition (78) it follows that $P'(m, h) = [1 + mf'(m, h)]P(m, h)$, we find

$$P(m, h)f''(m, h) + P(m, h)f'(m, h) \sim f'(m, h)[P(m, h) - P'(m, h)] \sim -mP(m, h)f'(m, h)^2 \quad (82)$$

which shows that Eq. (81) holds at $x = m$. Next, we compute the derivative with respect to x of the arguments of the integrals that appear in Eq. (81). We have, using Eqs. (75) and (76), that

$$\dot{P}f'' + P\dot{f}'' \sim \dot{P}f'' + P''\dot{f} \sim \frac{1}{2} \frac{\dot{G}}{x} [(2x(Pf')' - P'')f'' + P''(f'' + xf'^2)] \sim \dot{G}P(f'')^2, \quad (83)$$

and

$$x\dot{P}f'^2 + 2xP\dot{f}'\dot{f}' \sim \frac{1}{2} \dot{G} [(2x(Pf')' - P'')f'^2 + 2Pf'(f''' + 2xf'f'')] \sim -\dot{G}P(f'')^2. \quad (84)$$

This proves that the derivatives of the two sides of Eq. (81) with respect to x coincide and therefore completes the proof of Eq. (81), and of the equivalence of Eq. (79) and Eq. (80). We have therefore derived the set of fullRSB equations Eqs. (75)-(79) in two independent ways.

V. DERIVATION WITHIN THE GAUSSIAN ANSATZ

Although the above results have been derived from an exact evaluation of the replicated entropy following [1, 2], they could be equivalently obtained from a suitable Gaussian ansatz in replica space [1]. Here we discuss the appropriate form of this ansatz. This approach is interesting for two reasons: it sheds some light on the physical interpretation of both the k RSB ansatz and the function $P(m_i, h)$ introduced in Sec. IV, and it opens the way to extend the result (in an approximate way) to finite dimensions, following the approach of [11, 14].

In general, the replicated entropy is a functional of the single molecule density $\rho(\bar{x})$, where $\bar{x} = \{x_1, \dots, x_m\}$ and x_a are the d -dimensional vectors corresponding to the positions of particles in the molecule. In terms of this object, the replicated entropy for $d \rightarrow \infty$ is given in [1, Eqs.(2)]:

$$\begin{aligned} \mathcal{S}[\rho(\bar{x})] &= \int d\bar{x} \rho(\bar{x}) [1 - \log \rho(\bar{x})] + \frac{1}{2} \int d\bar{x} d\bar{y} \rho(\bar{x}) \rho(\bar{y}) f(\bar{x} - \bar{y}), \\ f(\bar{x} - \bar{y}) &= \prod_{a=1}^m e^{-\beta v(x_a - y_a)} - 1. \end{aligned} \quad (85)$$

In Eq. (85), we introduced a generic interparticle potential $v(r)$ at inverse temperature β . In this paper we restrict ourselves to the hard sphere potential, where

$$e^{-\beta v(x-y)} = \theta(|x-y| - D), \quad (86)$$

but since the Gaussian derivation allows one to consider a generic potential, it will be useful to write the expressions for a generic $v(r)$ because this will be surely useful for future applications, e.g. to the soft sphere case following [14]. Note that in finite dimensions, the replicated entropy can be expressed as an infinite sum of diagrams [11], but for $d \rightarrow \infty$, and for potentials that have a hard core or a properly scaled soft core, one can truncate the series at the lowest order [11, 64], hence obtaining Eq. (85).

The Gaussian ansatz consists in making an appropriate Gaussian assumption on the function $\rho(\bar{x})$, thus introducing a set of variational parameters that are related to the matrix $\hat{\alpha}$ considered above. In Sec. V A we discuss the proper Gaussian parametrization of the density function, we compute the entropic term and we show that it has the same form as the one we found before. Finally, in Sec. V B we compute the interaction term, we discuss the connection with the correlation function, and we show that in the limit $d \rightarrow \infty$ we recover the results obtained above.

A. Gaussian parametrization and the entropic term

For the entropic term, we just need to recall some results already discussed in [1, 2], to which we refer for details. Thanks to translational invariance, we can choose a parametrization of $\rho(\bar{x})$ in terms of vectors $\bar{u} = \{u_1, \dots, u_m\}$ such that $\sum_{a=1}^m u_a = 0$, and in terms of a $m \times m$ symmetric matrix \hat{A} such that $\sum_{a=1}^m A_{ab} = 0$ for all b . Calling $\hat{A}^{m,m}$ the $(m-1) \times (m-1)$ matrix obtained from \hat{A} by removing the last line and column, the most general Gaussian form of $\rho(\bar{u})$ is

$$\rho(\bar{u}) = \frac{\rho m^{-d}}{(2\pi)^{(m-1)d/2} \det(\hat{A}^{m,m})^{d/2}} e^{-\frac{1}{2} \sum_{ab}^{1,m-1} (\hat{A}^{m,m})_{ab}^{-1} u_a \cdot u_b} \quad (87)$$

which is normalized according to $\rho = \int \mathcal{D}\bar{u} \rho(\bar{u})$ and $\mathcal{D}\bar{u} = m^d \delta(\sum_a u_a) du_1 \cdots du_m$. The parameters A_{ab} give the average of the squared replica displacements

$$\langle u_a \cdot u_b \rangle = \frac{1}{\rho} \int \mathcal{D}\bar{u} \rho(\bar{u}) u_a \cdot u_b = d A_{ab} , \quad (88)$$

for $a, b \in [1, m-1]$, while $\langle u_a \cdot u_m \rangle = -\sum_{b=1}^{m-1} \langle u_a \cdot u_b \rangle = A_{am}$ and $\langle u_m \cdot u_m \rangle = \sum_{ab}^{1,m-1} \langle u_a \cdot u_b \rangle = A_{mm}$. Hence, the relative replica displacements D_{ab} are given by

$$\langle (u_a - u_b)^2 \rangle = d D_{ab} = d(A_{aa} + A_{bb} - 2A_{ab}) . \quad (89)$$

These corresponds to the physical ‘‘overlaps’’, i.e. the mean square displacements between different states. By comparison with Eq. (2), we see that $\Delta_{ab} = d^2 D_{ab}/D^2$ and $\alpha_{ab} = d^2 A_{ab}/D^2$.

The entropic term is better computed by using Eq. (87). Using the fact that $d\bar{x} = dX \mathcal{D}\bar{u}$ with X a vector in the physical volume V [1], and using Eq. (88) and Eq. (87), the entropy per particle is

$$\begin{aligned} \frac{1}{N} \int d\bar{x} \rho(\bar{x}) [1 - \log \rho(\bar{x})] &= \frac{1}{\rho} \int \mathcal{D}\bar{u} \rho(\bar{u}) [1 - \log \rho(\bar{u})] = 1 - \langle \log \rho(\bar{u}) \rangle \\ &= 1 - \log \rho + d \log m + (m-1) \frac{d}{2} \log(2\pi e) + \frac{d}{2} \log \det \hat{A}^{m,m} , \end{aligned} \quad (90)$$

which corresponds indeed to the entropic term in Eq. (1), with the rescaling $\alpha_{ab} = d^2 A_{ab}/D^2$. Apart from this rescaling, all the derivation of section III B can therefore be repeated within the Gaussian ansatz and we arrive to exactly the same results for the entropic term, which therefore has the same form both in infinite dimensions and in finite dimensions within the Gaussian ansatz.

B. k RSB Gaussian parametrization and the interaction term

1. Finite dimensions

To compute the interaction term, we need to find a simpler parametrization of the k RSB form of the Gaussian single molecule density. Recall first that in the 1RSB case one has $A_{ab} = A_1(\delta_{ab} - 1/m)$, hence $D_{aa} = 0$ and for $a \neq b$, $D_{ab} = D_1 = 2A_1$. In that case Eq. (87) can be written as [9–11]:

$$\rho(\bar{x}) = \rho \int dX^1 \prod_{a=1}^m \gamma_{D_1/2}^d(X^1 - x_a) , \quad (91)$$

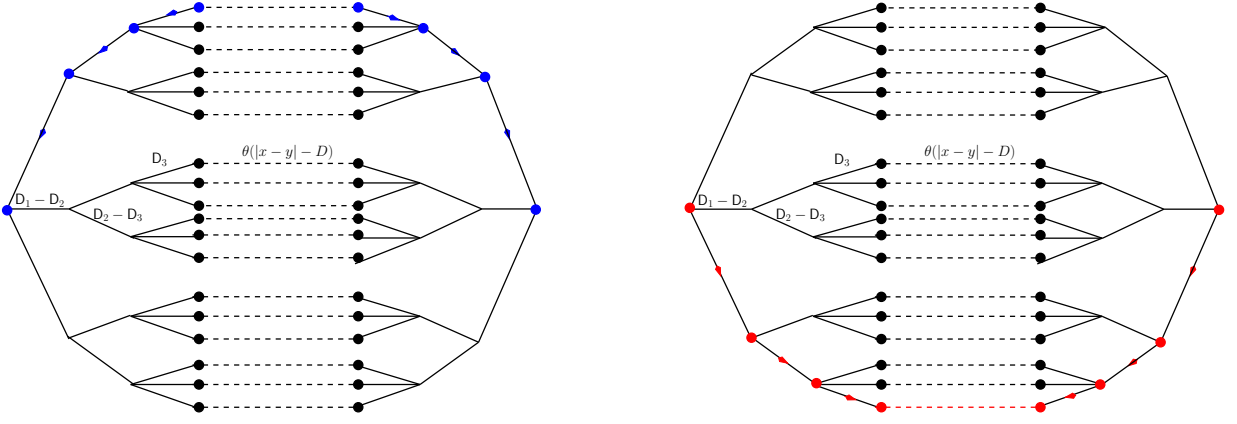


FIG. 2: Illustration of the relevant part of the interaction term, $\int d\bar{x}d\bar{y}\rho(\bar{x})\rho(\bar{y})\prod_{a=1}^m e^{-\beta v(x_a-y_a)}$. Each of the two k RSB molecule densities is represented by a tree graph made by full lines. The hard sphere interaction between the atoms of the two molecules is represented by dashed lines.

where the superscript on X^1 is here added for the purpose of later generalization, and

$$\gamma_A^d(x) = \frac{e^{-\frac{x^2}{2A}}}{(2\pi A)^{d/2}} \quad (92)$$

is a d -dimensional centered Gaussian. The simplest proof of the equivalence of Eq. (87) and Eq. (91) for 1RSB matrices is obtained by computing for $a \neq b$

$$\begin{aligned} \langle (u_a - u_b)^2 \rangle &= \langle (x_a - x_b)^2 \rangle = \frac{1}{\rho V} \int d\bar{x} \rho(\bar{x}) (x_a - x_b)^2 \\ &= \frac{1}{V} \int dX^1 dx_a dx_b (x_a - x_b)^2 \gamma_{D_1/2}^d(X^1 - x_a) \gamma_{D_1/2}^d(X^1 - x_b) \\ &= \int du_a du_b (u_a - u_b)^2 \gamma_{D_1/2}^d(u_a) \gamma_{D_1/2}^d(u_b) = d D_1. \end{aligned} \quad (93)$$

This shows that Eqs. (87) and (91) have the same (vanishing) first and (finite) second moments, and therefore they coincide because a Gaussian is only specified by its first two moments.

Let us consider next a matrix A_{ab} with a 2RSB structure. In this case we have two physical overlaps, the Edwards-Anderson D_2 and the inter-state $D_1 > D_2$. Let us call $B_i = \{1 + (i-1)m_1, \dots, im_1\}$, with $i = 1 \dots m/m_1$ the i -th block of the 2RSB matrix. Then we can write

$$\rho(\bar{x}) = \rho \int dX^1 \prod_{i=1}^{m/m_1} \left[\int dX_i^2 \gamma_{(D_1-D_2)/2}^d(X^1 - X_i^2) \left(\prod_{a \in B_i} \gamma_{D_2/2}^d(X_i^2 - x_a) \right) \right] \quad (94)$$

It is easy to check, through a computation very similar to Eq. (93), that $\langle (u_a - u_b)^2 \rangle = \langle (x_a - x_b)^2 \rangle$ is equal to D_2 if a, b belong to the same block B_i , and D_1 otherwise (and of course zero if $a = b$), hence we conclude that Eq. (94) is identical to Eq. (87) for a 2RSB matrix.

Generalizing this construction we easily obtain the structure of the k RSB Gaussian parametrization. We do not write it explicitly because this would require introducing a heavy notation for block indices, however it is clear that one should couple each group of replicas in the innermost blocks to reference points X_i^k , then group these reference points in blocks, each block being coupled to a reference X_i^{k-1} , and so on until the most external reference points are coupled to a single X^1 . This tree structure, and how it enters in the computation of the interaction term, is illustrated in Fig. 2.

We now show how the computation of the interaction term is performed recursively. We note that the term -1 in the Mayer function is obviously independent of the integration variables and we neglect it for the moment. The procedure is illustrated in the left panel of Fig. 2. Consider the innermost blue dots, which represent the coordinates of two atoms. They interact through the “bare” interaction $e^{-\beta v(x-y)}$. When we integrate over x, y , we generate a

“bare” interaction between the reference points X^k, Y^k , also marked by blue dots. This interaction is

$$\begin{aligned} \mathcal{G}(1, X^k - Y^k) &= \int dx dy \gamma_{\mathbb{D}_k/2}^d(X^k - x) \gamma_{\mathbb{D}_k/2}^d(Y^k - y) e^{-\beta v(x-y)} = \int dx \gamma_{\mathbb{D}_k}^d(x) e^{-\beta v(X^k - Y^k - x)} \\ &= (\gamma_{\mathbb{D}_k}^d \otimes e^{-\beta v})(X^k - Y^k), \end{aligned} \quad (95)$$

where we denoted by \otimes the d -dimensional convolution. Now, each of the k -level reference positions are coupled to m_{k-1}/m_k atoms, therefore the total bare interaction between each pair X^k, Y^k is $\mathcal{G}(1, X^k - Y^k)^{m_{k-1}/m_k}$. Now we can integrate over these variables to obtain the bare interaction between $(k-1)$ -level reference positions, and so on. It is easy to see that at each step of the iteration we have (we now use a similar notations as that of the previous sections):

$$\mathcal{G}(m_i, r) = \gamma_{\mathbb{D}_i - \mathbb{D}_{i+1}}^d \otimes \mathcal{G}(m_{i+1}, r)^{m_i/m_{i+1}}. \quad (96)$$

The bare interaction at level i is $\mathcal{G}(m_i, r)^{m_{i-1}/m_i}$. Iterating this procedure, we finally obtain the bare interaction of the most external reference points which is $\mathcal{G}(m_1, r)^{m/m_1}$. Therefore the interaction term per particle is

$$\begin{aligned} \frac{1}{2N} \int d\bar{x} d\bar{y} \rho(\bar{x}) \rho(\bar{y}) \left[\prod_{a=1}^m e^{-\beta v(x_a - y_a)} - 1 \right] &= \frac{\rho^2}{2N} \int dX^1 dY^1 \left[\mathcal{G}(m_1, X^1 - Y^1)^{m/m_1} - 1 \right] \\ &= \frac{\rho}{2} \int dr \left[\mathcal{G}(m_1, r)^{m/m_1} - 1 \right]. \end{aligned} \quad (97)$$

Before we show that these expressions give exactly the same result obtained before in the limit $d \rightarrow \infty$, let us consider the total “dressed” interaction between two i -level reference points. By dressed interaction we mean that we do not only integrate over the points “down the tree”, that are at level $j > i$, as we did before; we also integrate over all the other points. For the outermost reference points X^1, Y^1 , the dressed interaction is clearly given by

$$\mathcal{P}(m_1, X^1 - Y^1) = \mathcal{G}(m_1, X^1 - Y^1)^{m/m_1}, \quad (98)$$

as we discussed before. Now, if we consider the points at level 2, we have:

$$\mathcal{P}(m_2, r) = \mathcal{G}(m_2, r)^{m_1/m_2} \gamma_{\mathbb{D}_1 - \mathbb{D}_2}^d \otimes \mathcal{G}(m_1, r)^{m/m_1 - 1} = \mathcal{G}(m_2, r)^{m_1/m_2} \gamma_{\mathbb{D}_1 - \mathbb{D}_2}^d \otimes \frac{\mathcal{P}(m_1, r)}{\mathcal{G}(m_1, r)}. \quad (99)$$

The interpretation of this relation should be straightforward by looking at right panel of Fig. 2. In fact, the first term is the bare interaction that comes from points down the tree, while the second term is the contribution that comes from points up the tree, in which we divide \mathcal{P} by \mathcal{G} because we need to remove the contribution of the branch of the tree under consideration. Iterating, at level i we have

$$\mathcal{P}(m_i, r) = \mathcal{G}(m_i, r)^{m_{i-1}/m_i} \gamma_{\mathbb{D}_{i-1} - \mathbb{D}_i}^d \otimes \frac{\mathcal{P}(m_{i-1}, r)}{\mathcal{G}(m_{i-1}, r)}. \quad (100)$$

At level k this procedure gives the dressed interaction between the innermost reference points X^k, Y^k . The last step allows one to obtain the dressed correlations of two atoms x, y with $r = x - y$. This is the two-body effective potential $\phi_{\text{eff}}(r)$ of [11, 14] and we obtain

$$e^{-\phi_{\text{eff}}(r)} = e^{-\beta v(r)} \gamma_{\mathbb{D}_k}^d \otimes \frac{\mathcal{P}(m_k, r)}{\mathcal{G}(m_k, r)}. \quad (101)$$

One can easily check that in the 1RSB case this result gives back the effective potential used in [11, 14]. This result is particularly interesting for two reasons: on the one hand, in the limit $d \rightarrow \infty$ (or, in finite d , under the low-temperature approximation of Ref. [14]), the effective potential coincides with the pair correlation function of the glass, $g_{\text{g}}(r)$. On the other hand, in finite dimension one could plug this effective potential into some liquid theory integral equations to compute an approximation of the replicated entropy, following the strategy of [11]. We do not discuss this second issue here, leaving it for future work, and we keep our focus instead on the limit $d \rightarrow \infty$.

2. The limit $d \rightarrow \infty$

To take the $d \rightarrow \infty$ limit, we assume that the potential has the form $e^{-\beta v(r)} = e^{-\widehat{v}[d(|r|-D)/D]}$, and $e^{-\widehat{v}(h)}$ is a finite function⁶ when $d \rightarrow \infty$. The hard sphere potential, the only one that we consider in this paper, has this form with $e^{-\widehat{v}(h)} = \theta(h)$. Note, however, that the interaction potential enters only in the initial condition for the function $\mathcal{G}(1, r)$.

We now show briefly that in the limit $d \rightarrow \infty$ the equations we just derived give back Eq. (57). First of all, we note that all the interaction functions $\mathcal{G}(m_i, r)$ and $\mathcal{P}(m_i, r)$ are rotationally invariant and therefore depend only on $|r|$. Moreover, all these functions tend to 1 for $|r| \rightarrow \infty$ and they decrease fast to zero when $|r| \ll D$. Actually, as we show below, for $d \rightarrow \infty$ the growth of these functions from 0 to 1 happens on a scale $\sim 1/d$ around $|r| = D$. We therefore define $|r| = D(1 + h/d)$ and we consider $\mathcal{G}(m_i, h)$ and $\mathcal{P}(m_i, h)$ to be functions of h . We will see that with this convention, h is the same variable that enters in the equations of the previous sections.

Next, to obtain a non-trivial limit we scale the parameters introducing $\widehat{\Delta}_i = d^2 D_i / D^2$. Then, following exactly the strategy of [11, Appendix C.2.d] through the use of bipolar coordinates, one can see that in the limit $d \rightarrow \infty$, with the scaling $r = D(1 + h/d)$ and $u = D(1 + z/d)$, we have

$$\begin{aligned} \mathcal{G}(1, h) &= \gamma_{D^2 \widehat{\Delta}_k / d^2}^d \otimes e^{-\widehat{v}[d(|r|-D)/D]} = \int_0^\infty du \left(\frac{u}{r}\right)^{\frac{d-1}{2}} \frac{e^{-\frac{(r-u)^2}{2D_k}}}{\sqrt{2\pi D_k}} e^{-\frac{D_k}{8d^2 r u}} e^{-\widehat{v}[d(u-D)/D]} \\ &\sim \int_{-\infty}^\infty dz e^{(z-h)/2} \frac{e^{-\frac{(z-h)^2}{2\widehat{\Delta}_k}}}{\sqrt{2\pi \widehat{\Delta}_k}} e^{-\frac{\widehat{\Delta}_k}{8}} e^{-\widehat{v}(z)} = \int_{-\infty}^\infty dz \frac{e^{-\frac{(z-h-\widehat{\Delta}_k/2)^2}{2\widehat{\Delta}_k}}}{\sqrt{2\pi \widehat{\Delta}_k}} e^{-\widehat{v}(z)} \\ &= (\gamma_{\widehat{\Delta}_k} \star e^{-\widehat{v}})(h + \widehat{\Delta}_k/2) = g(1, h + \widehat{\Delta}_k/2) . \end{aligned} \quad (102)$$

With a similar reasoning, Eq. (96) becomes

$$\begin{aligned} \mathcal{G}(m_i, h) &= \gamma_{D_i - D_{i+1}}^d \otimes \mathcal{G}(m_{i+1}, h)^{m_i/m_{i+1}} = \int_{-\infty}^\infty dz \gamma_{\widehat{\Delta}_i - \widehat{\Delta}_{i+1}} [h - z + (\widehat{\Delta}_i - \widehat{\Delta}_{i+1})/2] \mathcal{G}(m_{i+1}, z)^{m_i/m_{i+1}} \\ &= \int_{-\infty}^\infty dz \gamma_{\widehat{\Delta}_i - \widehat{\Delta}_{i+1}} (h + \widehat{\Delta}_i/2 - z) \mathcal{G}(m_{i+1}, z - \widehat{\Delta}_{i+1}/2)^{m_i/m_{i+1}} . \end{aligned} \quad (103)$$

This equation coincides with Eq. (43) if one makes for all i the identification

$$\mathcal{G}(m_i, h) = g(m_i, h + \widehat{\Delta}_i/2) , \quad (104)$$

and recalling that for hard spheres $e^{-\widehat{v}(h)} = \theta(h)$. Hence the interaction term is (using that the solid angle is dV_d with V_d the volume of a unit sphere)

$$\begin{aligned} \frac{\rho}{2} \int dr \left[\mathcal{G}(m_1, r)^{m/m_1} - 1 \right] &= \frac{\rho d V_d}{2} \int_0^\infty dr r^{d-1} \left[g(m_1, h + \widehat{\Delta}_1/2)^{m/m_1} - 1 \right] \\ &= \frac{2^d \varphi}{2} \int_{-\infty}^\infty dh e^h \left[g(m_1, h + \widehat{\Delta}_1/2)^{m/m_1} - 1 \right] = \frac{d \widehat{\varphi}}{2} e^{-\widehat{\Delta}_1/2} \int_{-\infty}^\infty dh e^h \left[g(m_1, h)^{m/m_1} - 1 \right] , \end{aligned} \quad (105)$$

which provides the exact result of Eq. (57).

Next, we analyze the behavior of \mathcal{P} for $d \rightarrow \infty$. The initial condition from Eqs. (98) and (71) is

$$\mathcal{P}(m_1, h) = g(m_1, h + \widehat{\Delta}_1/2)^{m/m_1} = e^{-h - \widehat{\Delta}_1/2} P(m_1, h + \widehat{\Delta}_1/2) . \quad (106)$$

With a similar reasoning as before, one can show that identifying

$$\mathcal{P}(m_i, h) = e^{-h - \widehat{\Delta}_i/2} P(m_i, h + \widehat{\Delta}_i/2) \quad (107)$$

for all i , Eq. (100) becomes in fact identical to Eq. (72) in the limit $d \rightarrow \infty$. We obtain from this identification a deep physical interpretation of the function $P(m_i, h)$, which turns out to be related to the dressed interaction of the reference positions at level i , $\mathcal{P}(m_i, h)$, by Eq. (107).

⁶ Remember that in general we use a wide hat to denote quantities that are properly rescaled to be finite when $d \rightarrow \infty$.

Finally, we can write Eq. (101) for $d \rightarrow \infty$. We get

$$e^{-\phi_{\text{eff}}(h)} = e^{-\hat{v}(h)} \int_{-\infty}^{\infty} dz e^{z-h} \gamma_{\hat{\Delta}_k}(h-z) \frac{e^{-z-\hat{\Delta}_1/2} P(m_k, z)}{g(m_k, z)}. \quad (108)$$

This is a very important result because it allows one to obtain structural information about the pair correlation from the knowledge of the functions $P(m_i, h)$ and $g(m_i, h)$.

Part II

Extraction of the results from the equations

VI. SUMMARY OF THE EQUATIONS, AND A NUMERICALLY CONVENIENT FORMULATION

In the following sections, we will investigate the phase diagram that one obtains from the study of the k RSB equations, and we derive the scaling properties at large pressure. The way in which one has to extract physical information from the replicated entropy has been explained in many reviews [8, 10, 11, 30]. Although we will give additional details along the way, we assume that the reader is familiar with this kind of computations.

Before extracting the physics, let us summarize here the k RSB equations (57) together with the variational equations (71)-(72) and (73). These are

$$\begin{aligned}
\mathcal{S}_{k\text{RSB}} &= \sum_{i=1}^k \left(\frac{m}{m_i} - \frac{m}{m_{i-1}} \right) \log(\widehat{G}_i/m) - \widehat{\varphi} e^{-\widehat{\Delta}_1/2} \int_{-\infty}^{\infty} dh e^h \left\{ 1 - e^{mf(m_1, h)} \right\}, \\
\widehat{\Delta}_i &= \frac{\widehat{G}_i}{m_i} + \sum_{j=i+1}^k \left(\frac{1}{m_j} - \frac{1}{m_{j-1}} \right) \widehat{G}_j, \\
f(1, h) &= \log \gamma_{\widehat{\Delta}_k} \star \theta(h) = \log \Theta \left(\frac{h}{\sqrt{2\widehat{\Delta}_k}} \right), \\
f(m_i, h) &= \frac{1}{m_i} \log \left[\gamma_{\widehat{\Delta}_i - \widehat{\Delta}_{i+1}} \star e^{m_i f(m_{i+1}, h)} \right], \quad i = 1 \dots k-1, \\
P(m_1, h) &= e^h e^{mf(m_1, h)}, \\
P(m_i, h) &= \int dz P(m_{i-1}, z) e^{-m_{i-1} f(m_{i-1}, z)} \gamma_{\widehat{\Delta}_{i-1} - \widehat{\Delta}_i} (h-z) e^{m_{i-1} f(m_i, h)} \quad i = 2, \dots, k, \\
\frac{1}{\widehat{G}_i} &= \frac{\widehat{\varphi}}{2} e^{-\widehat{\Delta}_1/2} \int_{-\infty}^{\infty} dh \left\{ m_{i-1} P(m_i, h) f'(m_i, h)^2 - \sum_{j=1}^{i-1} (m_j - m_{j-1}) P(m_j, h) f'(m_j, h)^2 \right\}.
\end{aligned} \tag{109}$$

A. Scaled variables and the jamming limit

Because (as we will see below) we are mostly going to work at small m , and the jamming limit corresponds to $m \rightarrow 0$, it is convenient to write the equations in scaled variables that remain finite when $m \rightarrow 0$. These are $y_i = m_i/m$ (keeping in mind that $y_0 = 1$ and that $y_k = 1/m$ diverges with m and will play the role usually played by temperature), $\widehat{f}(y_i, h) = mf(m_i, h)$, $\widehat{\gamma}_i = \widehat{G}_i/m$, from which it follows that $\widehat{\Delta}_k = m\widehat{\gamma}_k$ while all the other $\widehat{\Delta}_i$ remain finite for $m \rightarrow 0$. It will also be convenient for numerical reasons to introduce $\widehat{P}(y_i, h) = e^{-\widehat{\Delta}_1/2} e^{-h} P(m_i, h)$. Note also that $\widehat{\Delta}_i - \widehat{\Delta}_{i+1} = (\widehat{\gamma}_i - \widehat{\gamma}_{i+1})/y_i$. In terms of these variables, and introducing auxiliary variables $\widehat{\kappa}_i$ (not to be confused with the exponent κ discussed above) we have:

$$\begin{aligned}
\mathcal{S}_{k\text{RSB}} &= \sum_{i=1}^k \left(\frac{1}{y_i} - \frac{1}{y_{i-1}} \right) \log \widehat{\gamma}_i - \widehat{\varphi} e^{-\widehat{\Delta}_1/2} \int_{-\infty}^{\infty} dh e^h \left\{ 1 - e^{\widehat{f}(y_1, h)} \right\}, \\
\widehat{\Delta}_i &= \frac{\widehat{\gamma}_i}{y_i} + \sum_{j=i+1}^k \left(\frac{1}{y_j} - \frac{1}{y_{j-1}} \right) \widehat{\gamma}_j, \\
\widehat{f}(1/m, h) &= m \log \Theta \left(\frac{h}{\sqrt{2m\widehat{\gamma}_k}} \right), \\
\widehat{f}(y_i, h) &= \frac{1}{y_i} \log \left[\gamma_{(\widehat{\gamma}_i - \widehat{\gamma}_{i+1})/y_i} \star e^{y_i \widehat{f}(y_{i+1}, h)} \right], \quad i = 1 \dots k-1, \\
\widehat{P}(y_1, h) &= e^{-\widehat{\Delta}_1/2} e^{\widehat{f}(y_1, h)},
\end{aligned}$$

$$\begin{aligned}
\widehat{P}(y_i, h) &= \int dz e^{z-h} \widehat{P}(y_{i-1}, z) e^{-y_{i-1} \widehat{f}(y_{i-1}, z)} \gamma_{(\widehat{\gamma}_{i-1} - \widehat{\gamma}_i)/y_{i-1}}(h-z) e^{y_{i-1} \widehat{f}(y_i, h)} \quad i = 2, \dots, k, \\
\widehat{\kappa}_i &= \frac{\widehat{\varphi}}{2} \int_{-\infty}^{\infty} dh e^h \widehat{P}(y_i, h) \widehat{f}'(y_i, h)^2, \\
\frac{1}{\widehat{\gamma}_i} &= y_{i-1} \widehat{\kappa}_i - \sum_{j=1}^{i-1} (y_j - y_{j-1}) \widehat{\kappa}_j.
\end{aligned}$$

To solve numerically these equations it is convenient to have some control on the asymptotic behavior of the functions when $h \rightarrow \pm\infty$. We start by the function $\widehat{f}(y_i, h)$. From the initial condition we see that $\widehat{f}(1/m, h \rightarrow \infty) = 0$ and $\widehat{f}(1/m, h \rightarrow -\infty) \sim -h^2/(2\widehat{\gamma}_k)$. Inserting these asymptotes in the evolution equation for $\widehat{f}(y_i, h)$, one can show that

$$\begin{aligned}
\widehat{f}(y_i, h \rightarrow -\infty) &\sim -h^2/(2\widehat{\gamma}_i), \\
\widehat{f}(y_i, h \rightarrow \infty) &= 0.
\end{aligned} \tag{110}$$

From this, we obtain that $\widehat{P}(y_1, h \rightarrow -\infty) = 0$ while $\widehat{P}(y_1, h \rightarrow \infty) = e^{-\widehat{\Delta}_1/2}$. As a consequence, from the recurrence equation for $\widehat{P}(y_i, h)$ one can show that

$$\begin{aligned}
\widehat{P}(y_i, h \rightarrow -\infty) &= 0, \\
\widehat{P}(y_i, h \rightarrow \infty) &= e^{-\widehat{\Delta}_i/2}.
\end{aligned} \tag{111}$$

To obtain a simpler asymptotic behavior it is convenient to make a change of variable:

$$\widehat{f}(y_i, h) = -\frac{h^2 \theta(-h)}{2\widehat{\gamma}_i} + \widehat{j}(y_i, h), \tag{112}$$

in such a way that the leading asymptotic term of $\widehat{f}(y_i, h)$ in Eq. (110) is subtracted from $\widehat{j}(y_i, h)$. Then we have

$$\begin{aligned}
\mathcal{S}_{k\text{RSB}} &= \sum_{i=1}^k \left(\frac{1}{y_i} - \frac{1}{y_{i-1}} \right) \log \widehat{\gamma}_i - \widehat{\varphi} e^{-\widehat{\Delta}_1/2} \int_{-\infty}^{\infty} dh e^h \left\{ 1 - e^{-\frac{h^2 \theta(-h)}{2\widehat{\gamma}_1} + \widehat{j}(y_1, h)} \right\}, \\
\widehat{\Delta}_i &= \frac{\widehat{\gamma}_i}{y_i} + \sum_{j=i+1}^k \left(\frac{1}{y_j} - \frac{1}{y_{j-1}} \right) \widehat{\gamma}_j, \\
\widehat{j}(1/m, h) &= m \log \Theta \left(\frac{h}{\sqrt{2m\widehat{\gamma}_k}} \right) + \frac{h^2 \theta(-h)}{2\widehat{\gamma}_k}, \\
\widehat{j}(y_i, h) &= \frac{1}{y_i} \log \left[\int_{-\infty}^{\infty} dz K_{\widehat{\gamma}_i, \widehat{\gamma}_{i+1}, y_i}(h, z) e^{y_i \widehat{j}(y_{i+1}, z)} \right], \quad i = 1 \dots k-1, \\
\widehat{P}(y_1, h) &= e^{-\widehat{\Delta}_1/2 - \frac{h^2 \theta(-h)}{2\widehat{\gamma}_1} + \widehat{j}(y_1, h)}, \\
\widehat{P}(y_i, h) &= \int dz K_{\widehat{\gamma}_{i-1}, \widehat{\gamma}_i, y_{i-1}}(z, h) \widehat{P}(y_{i-1}, z) e^{z-h} e^{-y_{i-1} \widehat{j}(y_{i-1}, z) + y_{i-1} \widehat{j}(y_i, h)} \quad i = 2, \dots, k, \\
\widehat{\kappa}_i &= \frac{\widehat{\varphi}}{2} \int_{-\infty}^{\infty} dh e^h \widehat{P}(y_i, h) \left(-\frac{h \theta(-h)}{\widehat{\gamma}_i} + \widehat{j}'(y_i, h) \right)^2, \\
\frac{1}{\widehat{\gamma}_i} &= y_{i-1} \widehat{\kappa}_i - \sum_{j=1}^{i-1} (y_j - y_{j-1}) \widehat{\kappa}_j.
\end{aligned} \tag{113}$$

where

$$K_{\widehat{\gamma}, \widehat{\gamma}', y}(h, z) = \frac{\exp \left[-\frac{y}{2} \left(\frac{(z-h)^2}{\widehat{\gamma} - \widehat{\gamma}'} - \frac{h^2 \theta(-h)}{\widehat{\gamma}} + \frac{z^2 \theta(-z)}{\widehat{\gamma}'} \right) \right]}{\sqrt{2\pi(\widehat{\gamma} - \widehat{\gamma}')/y}} \tag{114}$$

is *not* a symmetric function of h and z , nor a function of $h - z$. However, the advantage of this formulation is that the kernel K is an almost Gaussian function which is well behaved, and all the other functions that appear in the integrals are smooth. This allows for a stable numerical evaluation of the integrals.

Note that Eqs. (113) admit a perfectly smooth $m \rightarrow 0$ limit. First of all one has to set $1/y_k = m$, $\widehat{\Delta}_k = 0$. Then, using the large λ development of $\Theta(-\lambda/\sqrt{2})$, one can easily show that

$$\lim_{\mu \rightarrow 0} \Theta \left(\frac{z}{\sqrt{\mu}} \right)^\mu = e^{-z^2 \theta(-z)}, \quad (115)$$

and therefore $\widehat{j}(y_k, h) = 0$. All the other equations remain identical to the case $m > 0$.

B. The continuum limit

It will be convenient for later purposes to write explicitly the continuum limit of the equations in terms of scaled variables. These are

$$\begin{aligned} \mathcal{S}_{\infty\text{RSB}} &= - \int_1^{1/m} \frac{dy}{y^2} \log[\gamma(y)] - \widehat{\varphi} e^{-\Delta(1)/2} \int_{-\infty}^{\infty} dh e^h [1 - e^{-\frac{h^2 \theta(-h)}{2\gamma(1)} + \widehat{j}(1,h)}], \\ \Delta(y) &= \frac{\gamma(y)}{y} - \int_y^{1/m} \frac{dz}{z^2} \gamma(z), \quad \Leftrightarrow \quad \gamma(y) = y\Delta(y) + \int_y^{1/m} dz \Delta(z), \\ \widehat{j}(1/m, h) &= m \log \Theta \left(\frac{h}{\sqrt{2m\gamma(1/m)}} \right) + \frac{h^2 \theta(-h)}{2\gamma(1/m)}, \\ \frac{\partial \widehat{j}(y, h)}{\partial y} &= \frac{1}{2} \frac{\dot{\gamma}(y)}{y} \left[-\frac{\theta(-h)}{\gamma(y)} + \frac{\partial^2 \widehat{j}(y, h)}{\partial h^2} - 2y \frac{h\theta(-h)}{\gamma(y)} \frac{\partial \widehat{j}(y, h)}{\partial h} + y \left(\frac{\partial \widehat{j}(y, h)}{\partial h} \right)^2 \right], \\ \widehat{P}(1, h) &= e^{-\Delta(1)/2 - \frac{h^2 \theta(-h)}{2\gamma(1)} + \widehat{j}(1,h)}, \\ \frac{\partial \widehat{P}(y, h)}{\partial y} &= -\frac{1}{2} \frac{\dot{\gamma}(y)}{y} e^{-h} \left\{ \frac{\partial^2 [e^h \widehat{P}(y, h)]}{\partial h^2} - 2y \frac{\partial}{\partial h} \left[e^h \widehat{P}(y, h) \left(-\frac{h\theta(-h)}{\gamma(y)} + \frac{\partial \widehat{j}(y, h)}{\partial h} \right) \right] \right\}, \\ \kappa(y) &= \frac{\widehat{\varphi}}{2} \int_{-\infty}^{\infty} dh e^h \widehat{P}(y, h) \left(-\frac{h\theta(-h)}{\gamma(y)} + \widehat{j}'(y, h) \right)^2, \\ \frac{1}{\gamma(y)} &= y\kappa(y) - \int_1^y dz \kappa(z). \end{aligned} \quad (116)$$

Having formulated the k RSB equations in a convenient way, we now proceed to extract the physical results from them. However, because the numerical solution of these equations is not trivial, we first investigate a certain number of asymptotic limits in which analytical results can be obtained.

VII. PERTURBATIVE 2RSB SOLUTION AROUND THE GARDNER LINE

The Gardner transition [35] separates the region where the 1RSB solution is stable from the one where it is unstable. In our problem, the 1RSB solution is stable in a certain region of the phase diagram, and it becomes unstable on a line that has been computed and characterized in the previous paper of this series [2]. The aim of this section, following the analysis of [33], is to perform a perturbative computation around the Gardner line, in the region where the 1RSB solution is unstable, and discuss the existence of a 2RSB (or fullRSB) solution. In Sec. VII A we perform the perturbative computation and show that a 2RSB solution only exists in a certain region of the Gardner line; in Sec. VII B we discuss the behavior of the perturbative solution at large densities and pressures.

We start our analysis of the k RSB equations by examining what happens around the Gardner transition line that has been computed in [2]. We will follow closely the analysis of Refs. [31, 33]. Fig. 3 reports a schematic phase diagram in the $\widehat{\varphi}$, m plane. The reader should keep in mind that $m \propto 1/p$ where p is the reduced pressure [2]. Let us summarize briefly the phase diagram. A 1RSB solution exists above the 1RSB dynamical line, i.e. for $\widehat{\varphi} > \widehat{\varphi}_d^{\text{1RSB}}(m)$ or equivalently $m > m_d^{\text{1RSB}}(\widehat{\varphi})$. Above the Gardner line, i.e. for $m \geq m_G(\widehat{\varphi})$ or $\widehat{\varphi} > \widehat{\varphi}_G(m)$, this 1RSB solution is stable [2] and one can extract the physical results from it [11]. Below this line, the 1RSB solution is unstable and we look for a k RSB solution with $k > 1$. Since the instability is due to a vanishing mode [2], we expect that the 1RSB solution will transform continuously in a k RSB solution with $k > 1$, and we therefore start by looking at the

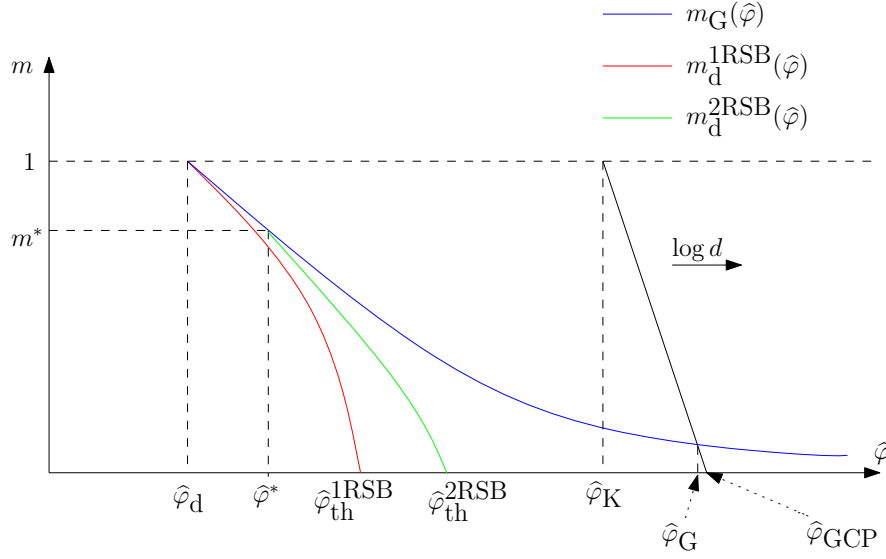


FIG. 3: Schematic phase diagram in the $(m, \hat{\varphi})$ plane.

new solution by doing perturbation theory around the 1RSB solution in the vicinity of the Gardner line. Based on the analogy with spin glass models [33], we expect the new solution to be a fullRSB one, but in perturbation theory it is enough to consider a 2RSB solution because the breaking is small and the two perturbative computations give identical results [65].

A. Development around the 1RSB solution

We have found in [2] that the instability of the 1RSB solution is due to the vanishing of the “replicon” eigenvalue $\lambda_R(m)$. It is therefore natural to consider a perturbation of the 1RSB matrix that is proportional to the subspace associated with the vanishing mode. We need to consider the cubic expansion in this direction and check if the cubic terms can stabilize the negative quadratic part. Hence we consider a perturbative 2RSB matrix of the form:

$$\begin{aligned} \alpha_{ab} &= \alpha_{ab}^{\text{1RSB}} + \delta\alpha_{ab} , \\ \delta\alpha_{ab} &= \delta\hat{\alpha}_1(1 - \delta_{ab}) \left(\frac{m - m_1}{1 - m_1} I_{ab}^{m_1} + I_{ab}^m - I_{ab}^{m_1} \right) \equiv \delta\hat{\alpha}_1 r_{ab} \end{aligned} \quad (117)$$

(remember that the matrices $I_{ab}^{m_i}$ are defined in Sec. III C). The matrix $\delta\hat{\alpha}$ belongs to the replicon subspace [66]. It has been shown in [66] that the cubic terms of the expansion of the 2RSB entropy around the 1RSB solution are eight, but if the perturbation matrix $\delta\hat{\alpha}$ is in the replicon subspace, only the two terms proportional to the coefficients w_1 and w_2 that have been analyzed in [2] survive. In practice we have

$$\begin{aligned} s[\hat{\alpha}^{\text{1RSB}} + \delta\hat{\alpha}] &= s[\hat{\alpha}^{\text{1RSB}}] + \frac{1}{2}\lambda_R(m) \sum_{a \neq b} \delta\alpha_{ab}^2 + \frac{1}{6} \left[w_1(m) \text{Tr} \delta\hat{\alpha}^3 + w_2(m) \sum_{a \neq b} \delta\alpha_{ab}^3 \right] \\ &= s[\hat{\alpha}^{\text{1RSB}}] + \frac{1}{2}\hat{\lambda}_R(m, m_1) \delta\hat{\alpha}_1^2 + \frac{1}{6}W[w_1(m), w_2(m), m, m_1] \delta\hat{\alpha}_1^3 . \end{aligned} \quad (118)$$

where $\lambda_R(m)$ is the replicon eigenvalue that has been computed in [2]. The relation between $\lambda_R(m)$ and $\hat{\lambda}_R(m, m_1)$ can be exploited to obtain the replicon eigenvalue from the 2RSB entropy and it gives

$$\hat{\lambda}_R(m, m_1) = \frac{m(1-m)(m-m_1)}{1-m_1} \lambda_R(m) = \left. \frac{d^2 s[\hat{\alpha}^{\text{1RSB}} + \delta\hat{\alpha}]}{d\delta\hat{\alpha}_1^2} \right|_{\delta\hat{\alpha}_1=0} . \quad (119)$$

It expresses the fact that the replicon eigenvalue can be obtained from the second derivative with respect to $\delta\hat{\alpha}_1$ of the replicated entropy computed on a matrix of the form (117). We want now to express W explicitly in terms of w_1

and w_2 that we have already computed in [2]. Note that $w_1(m)$ and $w_2(m)$ depend only on m and not on m_1 as a consequence of the fact that they are computed on a 1RSB matrix that does not depend on m_1 . To do this one can use the following relations between matrices \hat{I}^{m_i} :

$$(\hat{I}^{m_i})^2 = m_i \hat{I}^{m_i}, \quad \hat{I}^m \hat{I}^{m_1} = \hat{I}^{m_1} \hat{I}^m = m_1 \hat{I}^m, \quad (120)$$

to obtain that the matrix \hat{r} defined in (117) satisfies

$$\text{Tr } \hat{r}^3 = \frac{m(m_1 - m)(m - 1)}{(m_1 - 1)^2} (mm_1 + m_1 - 2m), \quad \sum_{a \neq b} r_{ab}^3 = \frac{m(m_1 - m)(m - 1)}{(m_1 - 1)^2} (1 + m - 2m_1), \quad (121)$$

and therefore

$$W[w_1, w_2, m, m_1] = \frac{m(m_1 - m)(m - 1)}{(m_1 - 1)^2} [w_1(m) (mm_1 + m_1 - 2m) + w_2(m)(1 + m - 2m_1)]. \quad (122)$$

To obtain the perturbative 2RSB solution in the $(m, \hat{\varphi})$ plane we search for a non trivial stationary point solution for the expression (118). The trivial 1RSB solution $\delta\hat{\alpha}_1 = 0$ can always be found but it is unstable below the Gardner line where $\lambda_R(m) < 0$. To find the non-trivial solution we first optimize over $\delta\hat{\alpha}_1$ and then we optimize over the breaking point m_1 . The saddle point equation for $\delta\hat{\alpha}_1$ gives

$$\delta\hat{\alpha}_1 = -\frac{2\hat{\lambda}_R}{W}. \quad (123)$$

The entropy as a function of m_1 is obtained by plugging the above expression in (118) and it gives

$$s[\hat{\alpha}^{1\text{RSB}} + \delta\hat{\alpha}] = s[\hat{\alpha}^{1\text{RSB}}] - \frac{1}{3} \frac{\hat{\lambda}_R^3(m, m_1)}{W^2(m, m_1)} \quad (124)$$

Now we should search for the extremum in m_1 . We obtain that the breaking point is

$$m_1 = \frac{w_2(m)}{w_1(m)} \equiv \lambda(m), \quad (125)$$

where $\lambda(m)$ is the Mode-Coupling theory exponent parameter that has been discussed in [2]. However, as it is usual in replica computations, the saddle point solution for the breaking point should satisfy $m < m_1 < 1$. This implies that a 2RSB solution exists only if

$$m \leq \frac{w_2(m)}{w_1(m)} \equiv \lambda(m). \quad (126)$$

Note that, because we are perturbing around the 1RSB solution close to the Gardner line where the replicon mode vanishes, all the quantities $\hat{\lambda}_R(m)$, $w_1(m)$ and $w_2(m)$ are computed on the Gardner line.

We now follow the discussion of [33]. We know that at $m = 1$ the Gardner line corresponds to the dynamical transition point and at that point $\lambda(m = 1) = \lambda_{\text{MCT}} = 0.70698 < 1 = m$ [2]. Hence, by continuity, close to $m = 1$ we have $\lambda(m) < m$ and there is no non-trivial 2RSB solution. We conclude, following [33], that in this region only the 1RSB solution exists down to the Gardner line, and there is no other solution below the Gardner line. However, the condition (126) tells us that there might exist a point in the $(m, \hat{\varphi})$ plane where

$$m^* = \lambda(m^*), \quad (127)$$

so that below this point a perturbative 2RSB solution can be found. The point m^* can be computed using the expressions for $w_1(m)$ and $w_2(m)$ that we computed in [2]. The numerical solution of equation (127) gives

$$m^* \simeq 0.414 \implies \hat{\varphi}^* \simeq 5.84. \quad (128)$$

We therefore obtain the schematic phase diagram represented in Fig. 3, which is strongly similar to the one found in [33] for the Ising p -spin glass model. For $m > m^*$ or $\hat{\varphi} < \hat{\varphi}^*$, no solution exist below the Gardner line, which therefore delimits the region where the only non-trivial 1RSB solution exists. Instead, for $m < m^*$ or $\hat{\varphi} > \hat{\varphi}^*$ a non-trivial k RSB solution with $k > 1$ exists below the Gardner line. It is reasonable to expect that this solution will exist in a finite region below the Gardner line. The region of existence of the 2RSB solution should be delimited by a dynamical line $\hat{\varphi}_d^{2\text{RSB}}(m)$ or $m_d^{2\text{RSB}}(\hat{\varphi})$, shifted with respect to the 1RSB dynamical line (see Fig. 3 for a schematic drawing of this line). We will show in Sec. VIII C how this line can be defined. Note however that the instability of the replicon mode suggests that the 2RSB solution is also unstable towards 3RSB and so on, until the correct fullRSB solution is found.

B. Asymptotic expression for $\lambda(m)$ at large densities on the Gardner line

In this section we compute the asymptotic behavior of $\lambda(m)$ for $m \rightarrow 0$ or $\widehat{\varphi} \rightarrow \infty$ on the Gardner line. The importance of this computation is twofold. First, we want to check that the condition $m < \lambda(m)$ holds for all $m < m^*$ on the Gardner line, which implies that a non-trivial 2RSB solution exists for all $\widehat{\varphi} > \widehat{\varphi}^*$. Second, we have shown that the breaking point of the 2RSB solution is $m_1 = \lambda(m)$ on the Gardner line. Actually this is true also if we perform a perturbative fullRSB calculation around the instability line [65]. It follows that the asymptotic computation of $\lambda(m)$ tells us what is the behavior of the breaking point at large densities, which will be useful to investigate the general properties of the k RSB solutions.

In the following we rely heavily on the notations and results of [2, Sec.V and VI]. Let us first recall the expression for $\lambda(m)$, which can be written as

$$\lambda(m) = \frac{-\hat{w}_2^{(1)}(\widehat{A}_G(m), m)}{\frac{2}{\widehat{\varphi}_G(m)} - \hat{w}_1^{(1)}(\widehat{A}_G(m), m)} \quad (129)$$

where $\widehat{\varphi}_G(m)$ is the Gardner line, $\widehat{A}_G(m)$ is the 1RSB cage radius on the Gardner line, and

$$\begin{aligned} \hat{w}_1^{(1)}(\widehat{A}_G(m), m) &= -\langle \Theta_0^{m-1}(\lambda) \Gamma_1(\lambda, m) \rangle_{\widehat{A}_G(m)} \\ \hat{w}_2^{(1)}(\widehat{A}_G(m), m) &= \frac{1}{2} \langle \Theta_0^{m-1}(\lambda) \Gamma_2(\lambda, m) \rangle_{\widehat{A}_G(m)} \end{aligned} \quad (130)$$

with

$$\begin{aligned} \Gamma_2(\lambda, m) &= \left[2 \left(\frac{\Theta_1(\lambda)}{\Theta_0(\lambda)} \right)^3 - 3 \frac{\Theta_1(\lambda)\Theta_2(\lambda)}{\Theta_0^2(\lambda)} + \frac{\Theta_3(\lambda)}{\Theta_0(\lambda)} \right] \left[2\lambda^3 + 2(m-6) \left(\frac{\Theta_1(\lambda)}{\Theta_0(\lambda)} \right)^3 + \right. \\ &\quad \left. + 3 \frac{\Theta_1(\lambda)}{\Theta_0(\lambda)} \left[4\lambda \frac{\Theta_1(\lambda)}{\Theta_0(\lambda)} - (m-4) \frac{\Theta_2(\lambda)}{\Theta_0(\lambda)} \right] - 6\lambda \left(\lambda \frac{\Theta_1(\lambda)}{\Theta_0(\lambda)} + \frac{\Theta_2(\lambda)}{\Theta_0(\lambda)} \right) + (m-2) \frac{\Theta_3(\lambda)}{\Theta_0(\lambda)} \right], \\ \Gamma_1(\lambda, m) &= \left[1 + \frac{\Theta_1^2(\lambda)}{\Theta_0^2(\lambda)} - \frac{\Theta_2(\lambda)}{\Theta_0(\lambda)} \right]^2 \left[(m-3\lambda^2) + (m-6) \frac{\Theta_1^2(\lambda)}{\Theta_0^2(\lambda)} + 6\lambda \frac{\Theta_1(\lambda)}{\Theta_0(\lambda)} - (m-3) \frac{\Theta_2(\lambda)}{\Theta_0(\lambda)} \right], \end{aligned} \quad (131)$$

where the functions $\Theta_k(\lambda) = \frac{1}{\sqrt{2\pi}} \int_x^\infty dy y^k e^{-y^2/2}$ have been defined in [2, Eq. (41)-(43)] and

$$\langle O(x) \rangle_A = \int_{-\infty}^{\infty} \frac{dx}{\sqrt{2\pi}} O(x) e^{-\frac{1}{2}(x+\sqrt{2A})^2}. \quad (132)$$

Following the analysis and the notations of [2, Sec.V and VI], at the instability line we have $\widehat{\varphi}_G(m) = 1/\mathcal{F}_m(\widehat{A}_G(m))$, where $\widehat{A}_G(m)$ satisfies the equation $2\mathcal{F}_m(\widehat{A}_G(m)) = -\Lambda_m(\widehat{A}_G(m))$ and

$$\begin{aligned} \Lambda_m(\widehat{A}_G(m)) &= \langle \mathcal{L}(\lambda, m) \rangle_{\widehat{A}_G(m)} \\ \mathcal{L}(\lambda, m) &= \Theta_0^{m-1}(\lambda) \left[\left(\frac{\Theta_1(\lambda)}{\Theta_0(\lambda)} \right)^2 - \lambda \frac{\Theta_1(\lambda)}{\Theta_0(\lambda)} \right] \left[2 - 2\lambda^2 + (m-4) \left(\frac{\Theta_1(\lambda)}{\Theta_0(\lambda)} \right)^2 + (6-m)\lambda \frac{\Theta_1(\lambda)}{\Theta_0(\lambda)} \right]. \end{aligned} \quad (133)$$

It follows that the expression for λ can be put in the form

$$\lambda(m) = \frac{\hat{w}_2^{(1)}(\widehat{A}_G(m), m)}{\Lambda_m(\widehat{A}_G(m)) + \hat{w}_1^{(1)}(\widehat{A}_G(m), m)}. \quad (134)$$

In [2, Sec. V D] it was shown that in the limit $m \rightarrow 0$, $\sqrt{\widehat{A}_G(m)} \simeq 0.8m$. This means that we can hope to expand the numerator and the denominator in powers of $\sqrt{\widehat{A}_G}$.

$$\begin{aligned} \hat{w}_2^{(1)}(\widehat{A}_G(m), m) &= w_2^{(0)}(m) + \sqrt{\widehat{A}_G(m)} w_2^{(1)}(m) + \widehat{A}_G(m) w_2^{(2)}(m) + \dots \\ \hat{w}_1^{(1)}(\widehat{A}_G(m), m) &= w_1^{(0)}(m) + \sqrt{\widehat{A}_G(m)} w_1^{(1)}(m) + \widehat{A}_G(m) w_1^{(2)}(m) + \dots \\ \Lambda_m(\widehat{A}_G(m)) &= \Lambda^{(0)}(m) + \sqrt{\widehat{A}_G(m)} \Lambda^{(1)}(m) + \widehat{A}_G(m) \Lambda^{(2)}(m) + \dots \end{aligned} \quad (135)$$

Let us study the numerator first. It happens that $w_2^{(0)}(m) = 0$ with very good numerical accuracy, and the equality can be probably demonstrated by a series of integrations by parts (see [2] for a similar computation). The first order term (multiplied by 2 for convenience) can be written as

$$2w_2^{(1)}(m) = \int_{-\infty}^{\infty} \frac{d\lambda}{\sqrt{2\pi}} e^{-\lambda^2/2} (-\lambda\sqrt{2}) \Theta_0(\lambda)^{m-1} \Gamma_2(\lambda, m). \quad (136)$$

As it was discussed in [2], the behavior of the integral depends on how the function inside behaves as $\lambda \rightarrow \infty$ for small m . We have two possibilities: the integral decays as λ^α with $\alpha > 1$ and in that case the integral is convergent; on the other case, we have a divergent contribution that has to be studied looking at the limit $m \rightarrow 0$. To see which of the two behaviors happens we develop asymptotically the integrand

$$e^{-\lambda^2/2} (-\lambda\sqrt{2}) \Theta_0^{m-1}(\lambda) \Gamma_2(\lambda, m) \sim e^{-m\lambda^2/2} (-\lambda\sqrt{2}) (\lambda\sqrt{2\pi})^{1-m} \left(\frac{2m}{\lambda^6} - \frac{12(4m-1)}{\lambda^8} + \dots \right) \quad (137)$$

from which it follows that the integral is finite at $m = 0$ and it is given by

$$2w_2^{(1)}(0) = \int_{-\infty}^{\infty} \frac{d\lambda}{\sqrt{2\pi}} e^{-\lambda^2/2} (-\lambda\sqrt{2}) \Theta_0^{-1}(\lambda) \Gamma_2(\lambda, 0) \simeq -0.134 \quad (138)$$

Let us now study the denominator. Also in this case the zeroth order term is zero with very good accuracy. The first order term of the denominator is

$$\begin{aligned} 2\Lambda^{(1)}(m) + 2w_1^{(1)}(m) &= \int_{-\infty}^{\infty} \frac{d\lambda}{\sqrt{2\pi}} (-\lambda\sqrt{2}) e^{-\lambda^2/2} \Theta_0^{m-1}(\lambda) [\mathcal{L}(\lambda, m) + \Gamma_1(\lambda, m)] \\ &\sim \int_{-\infty}^{\infty} \frac{d\lambda}{\sqrt{2\pi}} e^{-m\lambda^2/2} (\lambda\sqrt{2\pi})^{1-m} (-\lambda\sqrt{2}) \left[\frac{m}{\lambda^2} + \frac{2-8m}{\lambda^4} + \dots \right]. \end{aligned} \quad (139)$$

Also in this case the integral is finite at $m \rightarrow 0$ and it is given by

$$2\Lambda^{(1)}(0) + 2w_1^{(1)}(0) = \int_{-\infty}^{\infty} \frac{d\lambda}{\sqrt{2\pi}} e^{-\lambda^2/2} (-\lambda\sqrt{2}) \Theta_0^{-1}(\lambda) [\mathcal{L}(\lambda, 0) + \Gamma_1(\lambda, 0)] \simeq -1.067. \quad (140)$$

We therefore obtain the final result

$$\lim_{m \rightarrow 0} \lambda(m) = 0.124, \quad (141)$$

which shows that $\lambda(m)$ has a finite limit on the Gardner line and therefore the condition $m < \lambda(m)$ holds for all $m < m^*$.

VIII. THE JAMMING LIMIT OF THE 2RSB SOLUTION

The opposite limit, with respect to the perturbative computation of Sec. VII, in which the problem simplifies a lot is the jamming limit $m \rightarrow 0$. In this limit, pressure diverges and one approaches the jamming point where particles are in contact. This has been investigated in full details at the 1RSB level [11, 14]: at the 1RSB level, in the limit $m \rightarrow 0$ the parameter $\widehat{\gamma}_1 = 2\widehat{\alpha}_1$ remains finite, in such a way that the mean square displacement in the glass, $\widehat{\Delta}_1 = m\widehat{\gamma}_1$ vanishes proportionally to m , $\widehat{\Delta}_1 \sim m \sim 1/p$.

In this section we discuss what happens at the 2RSB level. This is interesting because it allows us to determine the endpoint of the 2RSB dynamical line, which corresponds to the 2RSB threshold $\widehat{\varphi}_{\text{th}}^{2\text{RSB}}$, see Fig. 3. In general, we can expect (based on the experience accumulated on the spin glass models [30]) that the 2RSB computation is an extremely good quantitative approximation for the fullRSB result as far as thermodynamic quantities are concerned, therefore the 2RSB threshold should be a very good approximation of the fullRSB one. Moreover, we will encounter here most of the numerical difficulties that will also be relevant for the study of the fullRSB solution.

In Sec. VIII A we obtain the expression of the 2RSB entropy and the associated variational equations in the limit $m \rightarrow 0$. In Sec. VIII B we show that the variational equations can be solved analytically in a systematic high density expansion. In Sec. VIII C we discuss the results of a numerical solution of the variational equations; we show that the numerical results are consistent with the high density expansion, and we discuss how the 2RSB threshold is computed. Finally, in Sec. VIII D we summarize the phase diagram obtained from the 2RSB solution.

A. The 2RSB equations at $m = 0$

In order to discuss the behavior of the 2RSB entropy at small m , it is convenient to make a change of variables as follows. We eliminate $\widehat{\gamma}_2$ and m_1 in favor of

$$\begin{aligned}\eta &= 1 - \frac{\widehat{\gamma}_2}{\widehat{\gamma}_1}, \\ \nu &= \frac{m}{m_1} = \frac{1}{y_1}.\end{aligned}\tag{142}$$

In terms of the variables $\widehat{\gamma}_1$, η , ν , and using Eqs. (33) we can reconstruct the other parameters as follows:

$$\begin{aligned}m_1 &= m/\nu, \\ \widehat{\gamma}_2 &= \widehat{\gamma}_1(1 - \eta), \\ \widehat{\Delta}_1 &= m\widehat{\gamma}_1(1 - \eta) + \widehat{\gamma}_1\eta\nu, \\ \widehat{\Delta}_2 &= m\widehat{\gamma}_1(1 - \eta).\end{aligned}\tag{143}$$

Furthermore, from the condition that $\widehat{\Delta}_1 \geq \widehat{\Delta}_2 \geq 0$ we see that $\eta \in [0, 1]$, while from $1 \geq m_1 \geq m$ we have that $\nu \in [m, 1]$. Writing the entropy (56) in terms of these variables, and writing explicitly the convolutions with some simple changes of variables, we obtain

$$\begin{aligned}s_{2\text{RSB}} &= 1 - \log \rho + \frac{d}{2}m \log m + \frac{d}{2}(m - 1) \log(\pi e D^2/d^2) \\ &\quad + \frac{d}{2} \left\{ (m - 1) \log \widehat{\gamma}_1 + (m - \nu) \log(1 - \eta) - \widehat{\varphi} \sqrt{\nu\eta\widehat{\gamma}_1} e^{-\widehat{\gamma}_1[m(1-\eta)+\eta\nu]/2} \int_{-\infty}^{\infty} dx e^{x\sqrt{\nu\eta\widehat{\gamma}_1}} [1 - (I_2^m(x))^\nu] \right\} \\ I_2^m(x) &= \int_{-\infty}^{\infty} \mathcal{D}z \Theta^{m/\nu} \left[\sqrt{\frac{\nu}{m} \frac{\eta}{1-\eta}} \frac{x-z}{\sqrt{2}} \right]\end{aligned}\tag{144}$$

As we will see later, this expression is also convenient to perform a numerical computation of the optimal values of the parameters $\widehat{\gamma}_1$, η , ν .

We now want to check that Eq. (144) has a finite limit $m \rightarrow 0$ if all the other parameters $\widehat{\gamma}_1, \eta, \nu$ are fixed (i.e. they do not scale with m). Note that in this limit both $\eta, \nu \in [0, 1]$ and moreover, according to Eq. (143), $\widehat{\Delta}_2 \rightarrow 0$ while $\widehat{\Delta}_1$ remains finite. The limit $m \rightarrow 0$ of Eq. (144) can be taken easily. The only non-trivial part is the function $I_2^m(x)$. Using Eq. (115), we have

$$\begin{aligned}I_2(x) &= \lim_{m \rightarrow 0} I_2^m(x) = \int_{-\infty}^{\infty} \mathcal{D}z \exp \left[-\frac{\eta}{2(1-\eta)} (x-z)^2 \theta(z-x) \right] \\ &= \Theta \left(\frac{x}{\sqrt{2}} \right) + e^{-\frac{\eta}{2}x^2} \sqrt{1-\eta} \Theta \left(-\sqrt{\frac{1-\eta}{2}}x \right),\end{aligned}\tag{145}$$

and therefore

$$\begin{aligned}\lim_{m \rightarrow 0} s_{2\text{RSB}} &= 1 - \log \rho - \frac{d}{2} \log(\pi e D^2/d^2) \\ &\quad + \frac{d}{2} \left\{ -\log \widehat{\gamma}_1 - \nu \log(1 - \eta) - \widehat{\varphi} \sqrt{\eta\nu\widehat{\gamma}_1} e^{-\widehat{\gamma}_1\eta\nu/2} \int dx e^{x\sqrt{\eta\nu\widehat{\gamma}_1}} [1 - I_2(x)^\nu] \right\} \\ I_2(x) &= \Theta \left(\frac{x}{\sqrt{2}} \right) + e^{-\frac{\eta}{2}x^2} \sqrt{1-\eta} \Theta \left(-\sqrt{\frac{1-\eta}{2}}x \right).\end{aligned}\tag{146}$$

We see that we obtain a finite limit that corresponds to the complexity at $m = 0$ [11], and we also conclude that the three parameters $\widehat{\gamma}_1, \eta, \nu$ have finite values at $m = 0$. From this, we reach the important physical conclusion that the mean square displacement *inside a glass*, $\widehat{\Delta}_2$, vanishes at jamming, as it should, but at the same time, the mean square displacement *between different sub-glasses inside a meta-glass remains finite*. Hence, sub-glasses inside a meta-glass are microscopically distinct. Finally, we note that m_1 vanishes proportionally to m because ν is finite.

B. The high density limit of the 2RSB solution at $m = 0$

The expression (146) is still quite difficult to handle numerically. Therefore, before discussing the numerical optimization it is convenient to obtain some asymptotic results for large density. We first observe that in the 1RSB case $\hat{\gamma}_1 \sim \hat{\varphi}^{-2}$ and we therefore expect the same scaling also in the 2RSB case. Furthermore, on the Gardner transition line we showed in section VII that $m_1 = \lambda(m) \rightarrow 0.124$ and that $m \sim 1.98\hat{\varphi}^{-2}$, hence $\nu = m/m_1 \sim 16.0\hat{\varphi}^{-2}$. We therefore seek for a small $\hat{\gamma}_1$ and small ν expansion of Eq. (146). Because both $\hat{\gamma}_1$ and ν are of the same order of magnitude, we use $1/\hat{\varphi}$ as the small expansion parameter. Note that we write $\hat{\gamma}_1, \nu \sim \mathcal{O}(2)$ to indicate that these quantities are of order 2 in $1/\hat{\varphi}$, and similarly for other quantities.

According to the definition in Eq. (54), the part of the entropy that has to be optimized is

$$\mathcal{S}_{2\text{RSB}} = -\log \hat{\gamma}_1 - \nu \log(1 - \eta) - \hat{\varphi} \mathcal{I} , \quad (147)$$

and we have to expand the integral

$$\mathcal{I} = \sqrt{\hat{\gamma}_1 \eta \nu} \int_{-\infty}^{\infty} dx e^{x\sqrt{\hat{\gamma}_1 \eta \nu} - \hat{\gamma}_1 \eta \nu / 2} [1 - I_2(x)^\nu] . \quad (148)$$

When ν is small, it is very useful to separate two contributions to this integral as follows:

$$\begin{aligned} \mathcal{I} &= \mathcal{I}^{(a)} + \mathcal{I}^{(n)} \\ \mathcal{I}^{(n)} &= \sqrt{\hat{\gamma}_1 \eta \nu} \int_{-\infty}^{\infty} dx e^{x\sqrt{\hat{\gamma}_1 \eta \nu} - \hat{\gamma}_1 \eta \nu / 2} [\theta(-x)e^{-\frac{\eta}{2}x^2\nu} \sqrt{1-\eta}^\nu + \theta(x) - I_2(x)^\nu] \\ &= \sqrt{\hat{\gamma}_1 \eta \nu} e^{-\hat{\gamma}_1 \eta \nu / 2} \int_0^{\infty} dx \left[e^{x\sqrt{\hat{\gamma}_1 \eta \nu}} (1 - I_2(x)^\nu) + e^{-x\sqrt{\hat{\gamma}_1 \eta \nu}} (e^{-\frac{\eta}{2}x^2\nu} \sqrt{1-\eta}^\nu - I_2(-x)^\nu) \right] \\ \mathcal{I}^{(a)} &= \sqrt{\hat{\gamma}_1 \eta \nu} \int_{-\infty}^0 dx e^{x\sqrt{\hat{\gamma}_1 \eta \nu} - \hat{\gamma}_1 \eta \nu / 2} [1 - e^{-\frac{\eta}{2}x^2\nu} \sqrt{1-\eta}^\nu] \\ &= \sqrt{\hat{\gamma}_1 \eta} \int_{-\infty}^0 dy e^{y\sqrt{\hat{\gamma}_1 \eta} - \hat{\gamma}_1 \eta \nu / 2} [1 - e^{-\frac{\eta}{2}y^2} \sqrt{1-\eta}^\nu] \\ &= e^{-\hat{\gamma}_1 \eta \nu / 2} [1 - e^{\hat{\gamma}_1 / 2} \sqrt{\pi \hat{\gamma}_1 / 2} (1 - \eta)^{\nu/2} (1 - \text{erf}(\sqrt{\hat{\gamma}_1 / 2}))] \end{aligned} \quad (149)$$

The term $\mathcal{I}^{(a)}$ can be easily handled and expanded in a power series of ν and $\hat{\gamma}_1$. Moreover, the integrand of $\mathcal{I}^{(n)}$ is well behaved at large $|x|$ (it decays as a Gaussian) for all values of ν , therefore we can expand the integrand.

We can expand $\mathcal{I}^{(n)}$ as follows

$$\begin{aligned} \mathcal{I}^{(n)} &= e^{-\hat{\gamma}_1 \eta \nu / 2} \int_0^{\infty} dx \sum_{l=0}^{\infty} \frac{x^l}{l!} (\hat{\gamma}_1 \eta \nu)^{(l+1)/2} \sum_{k=1}^{\infty} \frac{\nu^k}{k!} \left\{ -\log I_2(x)^k + (-1)^l \left[\left(\frac{1}{2} \log(1-\eta) - \frac{\eta}{2} x^2 \right)^k - \log I_2(-x)^k \right] \right\} \\ &= e^{-\hat{\gamma}_1 \eta \nu / 2} \sum_{l=0}^{\infty} \sum_{k=1}^{\infty} \frac{1}{l! k!} (\hat{\gamma}_1 \eta \nu)^{(l+1)/2} \nu^k \mathcal{I}_{l,k}(\eta) , \\ \mathcal{I}_{l,k}(\eta) &= \int_0^{\infty} dx x^l \left\{ -\log I_2(x)^k + (-1)^l \left[\left(\frac{1}{2} \log(1-\eta) - \frac{\eta}{2} x^2 \right)^k - \log I_2(-x)^k \right] \right\} \end{aligned} \quad (150)$$

The functions $\mathcal{I}_{l,k}(\eta)$ are defined by well convergent integrals, hence they are well behaved functions of η and they can be differentiated as many times as one wishes by exchanging the derivative with the integration over x . In this way, expanding all the variables in powers of $1/\hat{\varphi}$ as follows,

$$\begin{aligned} \hat{\gamma}_1 &= \sum_{k=2}^{\infty} \hat{\gamma}_{1,k} \hat{\varphi}^{-k} , \\ \nu &= \sum_{k=2}^{\infty} \nu_k \hat{\varphi}^{-k} , \\ \eta &= \sum_{k=0}^{\infty} \eta_k \hat{\varphi}^{-k} , \end{aligned} \quad (151)$$

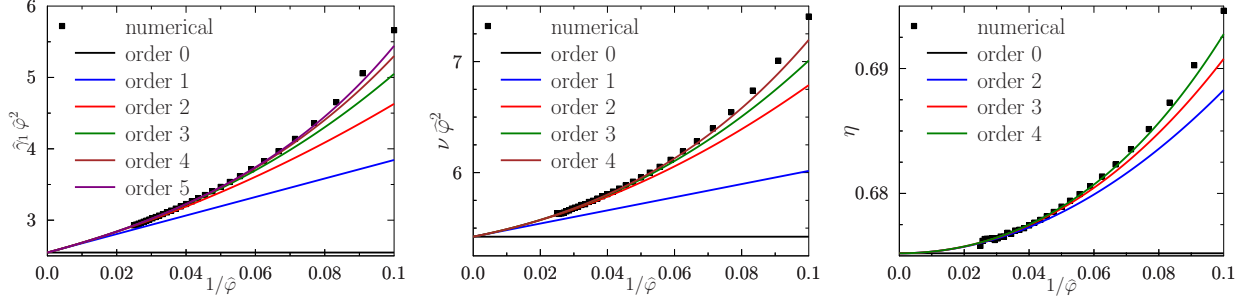


FIG. 4: Results for $\hat{\gamma}_1$, ν and η in the high density expansion at $m = 0$. Full lines are the analytical results at different orders in the small $1/\hat{\varphi}$ expansion. Points are the result of a direct numerical optimization of the 2RSB entropy at $m = 0$.

one can perform a systematic expansion of the entropy in powers of $1/\hat{\varphi}$ and determine the coefficients $\hat{\gamma}_{1,k}$, ν_k , η_k by optimizing order by order in inverse density. This computation can be very easily performed with the help of some algebraic manipulation software (we used Mathematica). Below we just give an example of the lowest orders in the computation.

At the lowest order we have, recalling that $\mathcal{O}(n)$ denotes an order n in $1/\hat{\varphi}$:

$$\begin{aligned} \mathcal{I}^{(n)} &= \nu^{3/2} \sqrt{\hat{\gamma}_1 \eta} \mathcal{I}_{0,1}(\eta) + \mathcal{O}(6) , \\ \mathcal{I}_{0,1}(\eta) &= \int_0^\infty dx \left[-\log I_2(x) + \frac{1}{2} \log(1-\eta) - \frac{\eta}{2} x^2 - \log I_2(-x) \right] . \end{aligned} \quad (152)$$

and

$$\mathcal{I}^{(a)} = -\sqrt{\pi \hat{\gamma}_1 / 2} + \hat{\gamma}_1 - \sqrt{\pi (\hat{\gamma}_1 / 2)^3} - \frac{1}{2} \sqrt{\frac{\pi \hat{\gamma}_1}{2}} \nu \log(1-\eta) + \frac{1}{3} \hat{\gamma}_1^2 + \frac{1}{2} \hat{\gamma}_1 \nu (\log(1-\eta) - \eta) + \mathcal{O}(5) . \quad (153)$$

Collecting all together and rearranging the terms in increasing order in the expansion we have

$$\begin{aligned} \mathcal{S}_{2\text{RSB}} &= -\log \hat{\gamma}_1 + \hat{\varphi} \sqrt{\pi \hat{\gamma}_1 / 2} - \hat{\varphi} \hat{\gamma}_1 + \left(-\nu \log(1-\eta) + \hat{\varphi} \sqrt{\pi (\hat{\gamma}_1 / 2)^3} + \frac{1}{2} \hat{\varphi} \sqrt{\frac{\pi \hat{\gamma}_1}{2}} \nu \log(1-\eta) \right) \\ &\quad - \hat{\varphi} \left(\frac{1}{3} \hat{\gamma}_1^2 + \frac{1}{2} \hat{\gamma}_1 \nu (\log(1-\eta) - \eta) + \nu^{3/2} \sqrt{\hat{\gamma}_1 \eta} \mathcal{I}_{0,1}(\eta) \right) + \mathcal{O}(4) \end{aligned} \quad (154)$$

We have now to optimize Eq. (154) order by order. At the leading order we obtain an equation for $\hat{\gamma}_1$ which coincides with the 1RSB one:

$$-\frac{2}{\hat{\gamma}_1} + \frac{1}{2} \hat{\varphi} \sqrt{\frac{2\pi}{\hat{\gamma}_1}} = 0 \quad \Rightarrow \quad \hat{\gamma}_1 = \frac{8}{\pi} \hat{\varphi}^{-2} + \mathcal{O}(3) \quad \Rightarrow \quad \hat{\gamma}_{1,2} = \frac{8}{\pi} . \quad (155)$$

We therefore have to look for a solution of the form $\hat{\gamma}_1 = \frac{8}{\pi} \hat{\varphi}^{-2} + \hat{\gamma}_{1,3} \hat{\varphi}^{-3} + \mathcal{O}(4)$. Plugging this in Eq. (154) and expanding we get

$$\mathcal{S}_{2\text{RSB}} = \text{const.} + \left(-\hat{\gamma}_{1,3} + \frac{\pi^2}{256} \hat{\gamma}_{1,3}^2 \right) \hat{\varphi}^{-2} + \mathcal{O}(3) \quad (156)$$

which allows to determine $\hat{\gamma}_{1,3} = 128/\pi^2$. Finally we look for $\hat{\gamma}_1 = \frac{8}{\pi} \hat{\varphi}^{-2} + (128/\pi^2) \hat{\varphi}^{-3} + \hat{\gamma}_{1,4} \hat{\varphi}^{-4} + \mathcal{O}(5)$ and $\nu = \nu_2 \hat{\varphi}^{-2} + \mathcal{O}(3)$, plug this in Eq. (154) and expand to get

$$\mathcal{S}_{2\text{RSB}} = \text{const.} - \frac{2}{3\pi} \left(-6\nu_2(\eta + \log(1-\eta)) + 3\sqrt{2\pi\eta} \nu_2^{3/2} h(\eta) \right) \hat{\varphi}^{-3} + \mathcal{O}(4) \quad (157)$$

This function must be optimized numerically and we obtain $\nu_2 = 5.4226$ and $\eta_0 = 0.6752$. We therefore obtain the asymptotic 2RSB solution for $m = 0$ and $\hat{\varphi} \rightarrow \infty$:

$$\begin{aligned} \hat{\gamma}_1 &= \frac{8}{\pi} \hat{\varphi}^{-2} + (128/\pi^2) \hat{\varphi}^{-3} + \mathcal{O}(4) , \\ \nu &= 5.4226 \hat{\varphi}^{-2} + \mathcal{O}(3) , \\ \eta &= 0.6752 + \mathcal{O}(1) , \end{aligned} \quad (158)$$

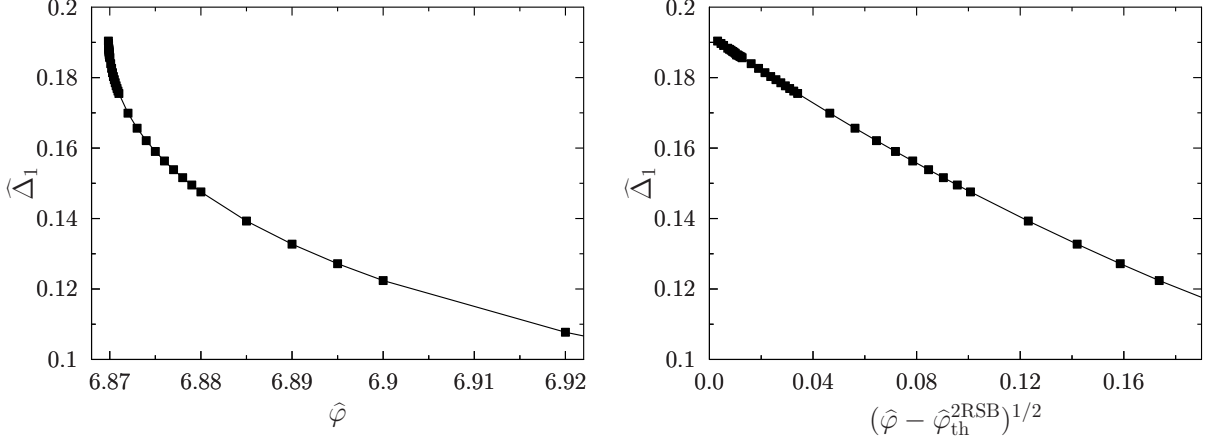


FIG. 5: The inter-state overlap of the 2RSB solution at $m = 0$, $\hat{\Delta}_1 = \hat{\gamma}_1 \eta \nu$ as a function of $\hat{\varphi}$. A square-root singularity is seen, and the singular point can be located to $\hat{\varphi}_{\text{th}}^{\text{2RSB}} = 6.86984$.

and

$$s[\hat{\alpha}_{2RSB}] = s[\hat{\alpha}_{1RSB}] - \frac{d}{2} 1.03416 \hat{\varphi}^{-3} + \mathcal{O}(4) . \quad (159)$$

This last result shows that at the 2RSB level the value of $\hat{\varphi}_{\text{GCP}}$, which corresponds to the point where the complexity (equal to the replicated entropy) at $m = 0$ vanishes, is slightly reduced with respect to the 1RSB level. However, this happens only at subdominant orders in large d , because the dominant orders are defined by a term $\log d$ that comes from the ideal gas term [11].

Higher orders in the calculation can be easily obtained by iterating the above procedure. This requires adding more terms in the expansion in Eq. (154) which can be easily automatized with Mathematica. In Fig. 4 we report the results of the calculation done at order 11 in density, which allows to obtain $\hat{\gamma}_1$ to order $\hat{\varphi}^{-7}$, ν to order $\hat{\varphi}^{-6}$ and η to order $\hat{\varphi}^{-4}$. The results are in perfect agreement with a numerical optimization of the 2RSB entropy (146) at $m = 0$, that we describe in Sec. VIII C.

We expect that this strategy to construct a high density expansion (which corresponds to the small cage expansion of [11] in the 1RSB case) could be generalized to $m > 0$ and to k RSB solutions with $k > 2$ with a little bit of additional work. However, having tested the accuracy of our numerical optimization code, we do not pursue this strategy further and we turn to the discussion of the numerical results.

C. Numerical solution of the 2RSB equations at $m = 0$: the 2RSB threshold

We report here results from the full numerical optimization of the 2RSB entropy at $m = 0$, given in Eq. (146). The code we used makes explicit use of the decomposition (149), in such a way that $\mathcal{I}^{(a)}$ is computed easily and $\mathcal{I}^{(n)}$ is a numerically stable integral (some care should be taken to write the error functions in a numerically stable way). Taking derivatives with respect to η and $\hat{\gamma}_1$, we obtain recurrence equations for these quantities, that we do not report because they are the specialization of Eqs. (113) to the case $k = 2$ and $m = 0$. For each fixed value of density $\hat{\varphi}$ and breaking point $\nu = 1/y_1$, these two equations can be solved by iteration to obtain η , $\hat{\gamma}_1$, and the entropy s_{2RSB} .

We make now a few remarks on the 2RSB equation at $m = 0$:

- When $\nu = 1$ (corresponding to $m_1 = m$), the 2RSB entropy reduces to the 1RSB one, function of $\hat{\gamma}_2 = \hat{\gamma}_1(1 - \eta)$.
- Similarly, when $\nu \rightarrow 0$ (corresponding to $m_1 = 1$), the 2RSB entropy reduces to the 1RSB one, function of $\hat{\gamma}_1$.
- Finally, when $\eta \rightarrow 0$ (corresponding to $\hat{\gamma}_1 = \hat{\gamma}_2$), one again recovers the 1RSB entropy.

Let us call $f(\nu, \eta; \hat{\varphi}) = \min_{\hat{\gamma}_1} s_{2RSB}$. This function has to be minimized with respect to $\{\nu, \eta\} \in [0, 1]^2$. Based on the considerations above, $f(\nu, \eta; \hat{\varphi})$ is a constant equal to the 1RSB value of the free energy when $\nu = 0$, $\nu = 1$ or $\eta = 0$, i.e. on three sides of the box $[0, 1]^2$. Moreover its derivative in $\eta = 0$ is always strictly negative (except for $\nu = 0$ and $\nu = 1$) as a consequence of the instability of the replicon mode (it is easy to see that the replicon is

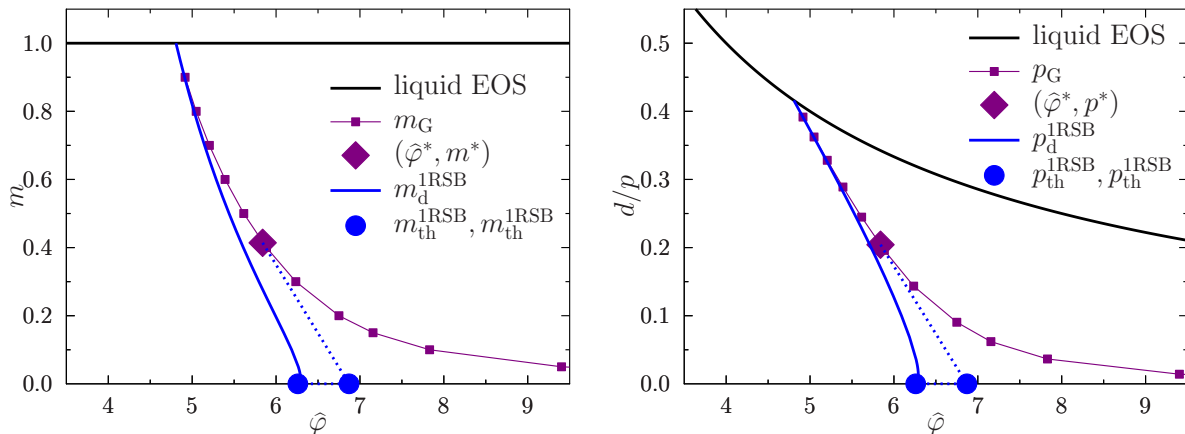


FIG. 6: Phase diagram in the $(m, \hat{\varphi})$ plane (left) and in the $(d/p, \hat{\varphi})$ plane (right). In both cases the black full line corresponds to the liquid state, the purple line is the Gardner line, the large purple diamond is the point $(m^*, \hat{\varphi}^*)$ in Eq. (128), the blue line is the 1RSB dynamical line, and the two blue dots are the 1RSB and 2RSB thresholds. The blue dashed line is just a straight line joining the point $(m^*, \hat{\varphi}^*)$ with the 2RSB threshold; it is drawn as a guide to the eye and should be a decent approximation to the 2RSB dynamical line at finite pressure or finite m .

related to the derivative with respect to η of $s_{2\text{RSB}}$. We conclude that a minimum must exist at non trivial values of ν and η (remember that as usual in replica computations, the entropy should be minimized and not maximized [30]). However, it is also important to remark that for some values of the parameters $\{\nu, \eta\}$ the solution for $\hat{\gamma}_1$ might not exist formally corresponding to $\hat{\gamma}_1 = \infty$, which corresponds to losing the non-trivial 2RSB solution to a trivial solution where all replicas are uncorrelated.

The best way to find the minimum is to optimize over $\hat{\gamma}_1$ and η at fixed ν and plot the resulting entropy $s_{2\text{RSB}}$ as a function of ν to find the minimum, recalling that based on the above considerations we must have $s_{2\text{RSB}} = s_{1\text{RSB}}$ at $\nu = 0, 1$. We performed this procedure at high density (up to $\hat{\varphi} = 40$) and compared the results to the high density expansion of Sec. VIII B, finding excellent agreement and confirming therefore the validity of our numerical code, see Fig. 4. We note however that solving the equations in the very high density regime is hard and the data are quite noisy, especially for η .

We then focus on the low density regime. We observe that, upon decreasing $\hat{\varphi}$, a secondary maximum appears when the 2RSB entropy is plotted as a function of ν . At a critical density $\hat{\varphi}_{\text{th}}^{2\text{RSB}}$, the physical minimum coalesces with this secondary maximum and disappears. Below this point, the 2RSB solution does not exist anymore. This does not contradict the previous statement, that a minimum should exist for $\{\nu, \eta\} \in [0, 1]^2$. In fact, when the maximum and minimum disappear, we also observe that in a region of values of ν the solution for $\hat{\gamma}_1$ and η does not exist, which means that the 2RSB is not defined.

If we follow the values of the parameters $\hat{\gamma}_1$, ν and η corresponding to the physical 2RSB solution, we see that they display a square root singularity on approaching $\hat{\varphi}_{\text{th}}^{2\text{RSB}}$ from above, which confirms that when the maximum and minimum coalesce, a longitudinal mode of the 2RSB solution vanishes signaling the singularity that marks the disappearance of the solution. This is illustrated in Fig. 5 using a physical quantity, the inter-state overlap $\hat{\Delta}_1$, but the same behavior is observed in all the three parameters $\hat{\gamma}_1$, ν and η . We conclude therefore that $\hat{\varphi}_{\text{th}}^{2\text{RSB}} = 6.86984$ can be taken as a definition of the threshold state within a 2RSB calculation. We stress once again that, however, we expect that the 2RSB solution is unstable and we expect that one should perform a fullRSB calculation to obtain the correct value of the threshold, following [33]. The same analysis could be repeated at $m > 0$ but we do not report the calculation here.

D. The 2RSB phase diagram

1. Phase diagram in the $(m, \hat{\varphi})$ plane

In Fig. 6 we summarize the phase diagram that we can infer from the previous discussions. A schematic version of this phase diagram was already presented in Ref. [2, Fig. 1], and here we substantiate this proposal with actual computations. At the 1RSB level, the dynamical line ends at $\hat{\varphi}_{\text{th}}^{1\text{RSB}} = 6.25967$, as computed in Ref. [11]. However,

we find here that this 1RSB dynamical line falls into the unstable region and therefore has no physical meaning. The 2RSB calculation indeed gives a higher value for the threshold point, $\widehat{\varphi}_{\text{th}}^{2\text{RSB}} = 6.86984$. We expect that a dynamical line $\widehat{\varphi}_d^{2\text{RSB}}(m)$ connects the 2RSB threshold to the point $(m^*, \widehat{\varphi}^*)$ defined in Sec. VII A, as illustrated in the schematic Fig. 3. We did not compute this line, but its location can be reasonably approximated by joining the two points by a straight line, as we did in Fig. 6. By analogy with spin-glass systems, we expect that further RSB will not strongly affect the location of the dynamical line, so the 2RSB computation should give a good approximation of the exact result. This dynamical line and the Gardner line, that join at the point $(m^*, \widehat{\varphi}^*)$, delimit the region of existence of the fullRSB solution.

The 1RSB solution remains correct around the liquid phase (corresponding to $m = 1$) so that when glassy states form, they have a 1RSB structure (as described in [11]). They only undergo the Gardner transition at higher densities. In the region where the 1RSB solution is stable, all the results of Ref. [11] remain valid. In particular, note that the Kauzmann point [11], depicted schematically in Fig. 3, shifts to infinite density on the scale of Fig. 6 and for that reason it is not depicted in the figure. This point nonetheless falls within the region where the 1RSB solution is stable and therefore none of its properties is changed with respect to the discussion of Ref. [11]. The glass close packing (GCP) point introduced in [11], corresponding to the densest amorphous packing that can be obtained by compressing liquid configurations, is also located at infinite density ($\widehat{\varphi} \propto \log d$) on the $m = 0$ (infinite pressure) line of Fig. 6. Because the Gardner transition occurs at infinite pressure when $\widehat{\varphi} \rightarrow \infty$, the equilibrium *ideal* glass only undergoes the Gardner transition exactly at infinite pressure, when GCP is reached. The GCP point somehow lies exactly on the Gardner line, which may explain why previous results obtained in [11] for GCP (like the fact that the GCP point is isostatic) were quite accurate despite neglecting the Gardner transition. We would like to stress, however, that experiments and numerical simulations are typically conducted in the vicinity of the dynamical line, and therefore never approach the Kauzmann nor the GCP points.

2. Phase diagram in the $(1/p, \widehat{\varphi})$ plane: isocomplexity assumption

It would be nice to convert the $(m, \widehat{\varphi})$ phase diagram into a physical $(1/p, \widehat{\varphi})$ phase diagram where p is the reduced pressure of the glassy states visited at a given m and $\widehat{\varphi}$. Doing this exactly requires a so-called “state following” calculation where we adiabatically follow the evolution of a given state in density to compute the pressure. Although this is certainly possible, we do not report this computation here and we resort to a much simpler “isocomplexity” assumption [11, 31] where we assume that states can be followed by fixing the value of the complexity. If this is the case, we can reason as follows, see [11] for a more detailed discussion. First we recall that $s_{2\text{RSB}} = ms^* + \Sigma(s^*)$, where s^* is the internal entropy of the state and $\Sigma(s^*)$ the associated complexity. Then, we note that the value of m corresponding to a given level of complexity Σ_g is given by the point where

$$\frac{1}{m}[s_{2\text{RSB}} - \Sigma_g] = s^* + \frac{1}{m}[\Sigma(s^*) - \Sigma_g] \quad (160)$$

is maximum with respect to m . In fact the maximum condition

$$-m^2 \frac{d}{dm} \left\{ s^* + \frac{1}{m} [\Sigma(s^*) - \Sigma_g] \right\} = \Sigma(s^*) - \Sigma_g = 0 \quad (161)$$

is equivalent to the isocomplexity condition. Let us call the solution $m_g(\widehat{\varphi})$. We also note that the corresponding internal entropy of the state is

$$s_g = \frac{1}{m} [s_{2\text{RSB}} - \Sigma_g] \Big|_{m=m_g(\widehat{\varphi})}. \quad (162)$$

It follows that the pressure of the glass is

$$p_g = -\widehat{\varphi} \frac{ds_g}{d\widehat{\varphi}} = -\frac{\widehat{\varphi}}{m_g(\widehat{\varphi})} \frac{\partial s_{2\text{RSB}}}{\partial \widehat{\varphi}} \Big|_{m=m_g(\widehat{\varphi})} = \frac{1}{m_g} \left[1 + \frac{d}{2} \widehat{\varphi} \mathcal{F}(2\hat{\alpha}^*) \right], \quad (163)$$

where $\mathcal{F}(2\hat{\alpha}^*)$ is the interaction part of the entropy computed in the matrix $\hat{\alpha}^*$ corresponding to the 2RSB solution at m_g . This formula generalizes the one in [2, Eq. (17)], it reduces to that one for the equilibrium glass which corresponds to the choice $\Sigma_g = 0$, and it allows us to convert the $(m, \widehat{\varphi})$ phase diagram into a pressure-density one under the isocomplexity approximation. Note that we must scale pressure by dimension plotting d/p to obtain a finite result for $d \rightarrow \infty$ as it is evident from Eq. (163). The result is shown in Fig. 6 and is qualitatively similar to the $(m, \widehat{\varphi})$ one.

IX. CRITICAL SCALING OF THE FULLRSB SOLUTION AT JAMMING ($m = 0$)

In the previous section we have delimited approximately the region where a non-trivial k RSB solution with $k > 1$ is found. We now assume that this phase is a fullRSB phase, which we confirm below through a numerical solution of Eq. (113), and that the 2RSB calculation provides a quite good approximation to the fullRSB one, which is usually correct in spin glasses. Then the fullRSB region is, in Fig. 6, the one below the Gardner line, at densities above the 2RSB dynamical line that connects the 2RSB threshold at $m = 0$ (or infinite pressure) and the point $(m^*, \widehat{\varphi}^*)$. We are now in the position to explore the scaling of the fullRSB solution in the jamming limit $m \rightarrow 0$. This limit is formally very similar to the zero-temperature limit in the Sherrington-Kirkpatrick model which has been thoroughly investigated in the past [30, 63, 67–69], and we follow here a very similar strategy.

Our results can be considered as a generalization of the arguments of Pankov [68] to the more complex case under investigation, as it will be clear below. Our starting point are Eq. (113) and its continuum version Eq. (116), and we begin the discussion by making some conjectures on the behavior of these equations for $m = 0$ and large y . These conjectures are partly based on the results of the numerical solution of the equations, that we discuss later, and partly on physical intuition. The aim of this section will be to show that they are indeed correct.

In Sec. IX A and IX B we will show that in the limit $m \rightarrow 0$ (in which the variable y extends from 1 to ∞) a scaling regime of Eq. (113) and Eq. (116) appears, and is characterized by non-trivial scaling exponents. In Sec. IX C, we consider a simplified set of equations (a toy model) for which the scaling regime can be fully characterized, that is instructive to discuss the scaling regime of the complete equations. In Sec. IX D, we extend the results of the toy model to the complete fullRSB equations. Finally, in Sec. IX E we determine analytically all the critical exponents that characterize the scaling regime.

A. Scaling of $\Delta(y)$, and asymptotic scaling of $\widehat{P}(y, h)$ for $h \rightarrow -\infty$

We look for an asymptotic solution at large y characterized by $\Delta(y) \sim \Delta_\infty y^{-\kappa}$. From the relation between $\Delta(y)$ and $\gamma(y)$ in Eq. (116) it follows that $\gamma(y) \sim \gamma_\infty y^{-c}$ with $c = \kappa - 1$ and $\gamma_\infty = \frac{\kappa}{\kappa-1} \Delta_\infty$. We will later show that the exponent c is close to 1/2.

Before studying the full scaling of $\widehat{P}(y, h)$, let us look to its asymptotic behavior at $h \rightarrow -\infty$, which provides some very useful insight. First, we note that $\widehat{P}(y_i, h) \sim A_i e^{B_i h - h^2 D_i}$ when $h \rightarrow -\infty$. In fact, this is true for y_1 , and the iteration (113) for $\widehat{P}(y_i, h)$ preserves this asymptotic behavior. From the analysis of Eq. (113) in the limit $h \rightarrow -\infty$, we obtain the discrete recurrence equations

$$\begin{aligned} D_i &= \frac{D_{i-1} y_{i-1} \gamma_{i-1}^2}{\gamma_i [2D_{i-1} \gamma_{i-1} (\gamma_{i-1} - \gamma_i) + y_{i-1} \gamma_i]} , \\ B_i &= \frac{y_{i-1} \gamma_{i-1} + B_{i-1} y_{i-1} \gamma_{i-1}}{2D_{i-1} \gamma_{i-1} (\gamma_{i-1} - \gamma_i) + y_{i-1} \gamma_i} - 1 , \\ A_i &= A_{i-1} \sqrt{D_i / D_{i-1}} \exp \left[\frac{(1 + B_{i-1})^2 \gamma_{i-1} (\gamma_{i-1} - \gamma_i)}{2[2D_{i-1} \gamma_{i-1} (\gamma_{i-1} - \gamma_i) + y_{i-1} \gamma_i]} \right] , \end{aligned} \quad (164)$$

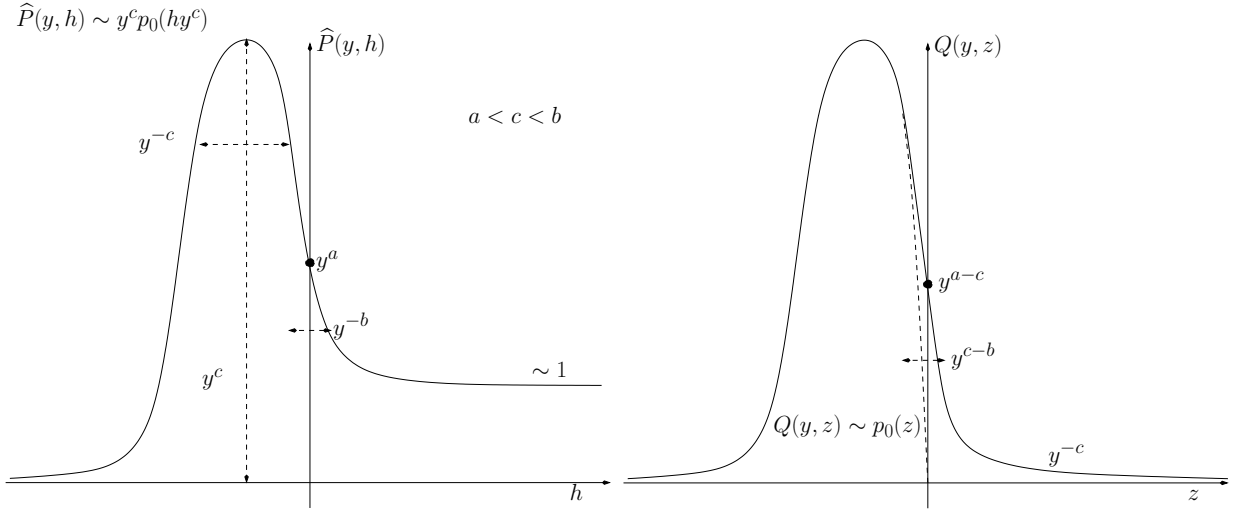
which in the continuum limit become

$$\begin{aligned} \dot{D} &= \frac{2D\dot{\gamma}}{y} (D - y/\gamma) , \\ \dot{B} &= \frac{(-y\dot{\gamma} + 2D\gamma\dot{\gamma})}{y\gamma} (1 + B) , \\ \dot{A} &= A \left(-\frac{(1+B)^2 \dot{\gamma}}{2y} + \frac{D\dot{\gamma}}{y} - \frac{\dot{\gamma}}{\gamma} \right) . \end{aligned} \quad (165)$$

Note in fact that Eqs. (165) can also be obtained directly from the continuum equation for $\widehat{P}(y, h)$. Under the assumption that $\gamma(y) \sim \gamma_\infty y^{-c}$ with $0 < c < 1$, Eqs. (165) admit a solution with $D(y) \sim D_\infty y^{2c}$, $B \sim B_\infty y^c$ and $A(y) \sim A_\infty y^c$ for $y \rightarrow \infty$. Hence we conclude that for $h \rightarrow -\infty$ and large y we have

$$\widehat{P}(y_i, h) \sim A_\infty y^c e^{B_\infty h y^c - D_\infty h^2 y^{2c}} = y^c p_0(h y^c) \quad (166)$$

with $p_0(z \rightarrow -\infty) = A_\infty \exp(B_\infty z - D_\infty z^2)$.

FIG. 7: Scaling of $\widehat{P}(y, h)$ and $Q(y, z)$.

B. Complete scaling of $\widehat{P}(y, h)$

Let us conjecture that the scaling of Eq. (166) holds for all $h < 0$. This means that for $h < 0$ and large y , $\widehat{P}(y, h) \sim y^c$ diverges, while we know from Eq. (111) that for large $h > 0$, $\widehat{P}(y, h) \sim \exp(-\Delta(y)/2)$, therefore it remains finite for large y . Combining this information we expect that, on increasing h from $-\infty$, $\widehat{P}(y, h)$ increases up to a value $\approx y^c$ on a scale $|h| \approx y^{-c}$, it reaches a peak and then it decreases fast around $h \approx 0$ to approach its asymptotic limit $\exp(-\Delta(y)/2) \approx 1$ at $h \rightarrow \infty$.

It is natural therefore to conjecture that the decrease from the peak down to values of order 1 happens around $h \sim 0$ on another scale $|h| \approx y^{-b}$ with $b > c$, which matches between the behavior at $h < 0$ and $h > 0$. We pose that in this regime $\widehat{P}(y, h \sim 0) \sim y^a$ with $a < c$. In summary, we have

$$\widehat{P}(y, h) \sim \begin{cases} y^c p_0(hy^c) & \text{for } h \sim -y^{-c} \\ y^a p_1(hy^b) & \text{for } |h| \sim y^{-b} \\ p_2(h) & \text{for } h \gg y^{-b} \end{cases} \quad (167)$$

with the condition $a < c < b$, and this scaling is illustrated in Fig. 7.

Assuming this scaling, we can match the different regimes. Note first that obviously the scaling (167) requires that $p_0(z = 0) = 0$. We can assume that $p_0(z) \sim |z|^\theta$ for small z . Then, to match with $p_1(z)$, we must assume that $p_1(z \rightarrow -\infty) \sim |z|^\theta$ too. Matching requires that $y^c |hy^c|^\theta \sim y^a |hy^b|^\theta$, therefore $c(1+\theta) = a+b\theta$, which implies $\theta = \frac{c-a}{b-c}$. Similarly, in order to match with the regime of positive h , we must have $p_1(z \rightarrow \infty) \sim z^{-\alpha}$, and $y^a (hy^b)^{-\alpha} \sim O(1)$, from which we obtain that $a - b\alpha = 0$, hence $\alpha = a/b$, and $p_2(h) \sim h^{-\alpha}$ for $h \rightarrow 0$. In summary, we obtain the following scaling relations between exponents⁷:

$$\alpha = \frac{a}{b} \quad \theta = \frac{c-a}{b-c} \quad \kappa = c + 1. \quad (168)$$

We will see later that the exponents α, θ, κ are directly related to the scaling of physical observables (the cage radius and the pair correlation function).

Eq. (167) suggests to define the scaled variable $z = hy^c$ and the functions

$$\begin{aligned} H(y_i, z) &= y_i \widehat{j}(y_i, zy_i^{-c}), & \Leftrightarrow & \widehat{j}(y_i, h) = \frac{1}{y_i} H(y_i, hy_i^c), \\ Q(y_i, z) &= y_i^{-c} \widehat{P}(y_i, zy_i^{-c}), & \Leftrightarrow & \widehat{P}(y_i, h) = y_i^c Q(y_i, hy_i^c). \end{aligned} \quad (169)$$

⁷ The reader should not confuse the exponent α introduced here with the previously used matrix $\hat{\alpha}$.

In terms of $Q(y, z)$, the scaling (167) becomes

$$Q(y, z) \sim \begin{cases} p_0(z) & \text{for } z < 0, \\ y^{a-c} p_1(z y^{b-c}) & \text{for } |z| \sim y^{-b+c}, \\ 0 & \text{for } z > 0. \end{cases} \quad (170)$$

A plot of $Q(y, z)$ is a scaled plot of $y^{-c} \widehat{P}(y, h)$ versus $z = h y^c$; this plot approaches a master function $p_0(z)$ at negative z , while around $z = 0$ there is a region where $|z| \approx y^{-b+c}$, in which $Q(y, z) \approx y^{a-c}$ is small, which matches the scaling function $p_0(z)$ for negative z with the behavior $Q \sim y^{-c} \widehat{P}(y, h) \rightarrow 0$ at positive z .

With this change of variable, the leading terms at large y in the continuum equation for $Q(y, z)$ are

$$\dot{Q}(y, z) = -\frac{\dot{\gamma}(y)}{2} y^{2c-1} Q''(y, z) - \left(\frac{c}{y} + \frac{\dot{\gamma}(y)}{\gamma(y)} \theta(-z) \right) [z Q(y, z)]' + \dot{\gamma}(y) y^{2c-1} [Q(y, z) H'(y, z)]'. \quad (171)$$

C. A toy model

Before analyzing the complete fullRSB equations, we discuss here a toy model that gives a lot of insight about how the scaling of $Q(y, z)$ can be studied analytically. The toy model is obtained as a strong simplification of Eq. (171), obtained by *setting* $\gamma(y) = y^{-c}$ for all $y \in [1, \infty)$, and $H = 0$. We have $\dot{\gamma}(y) = -c y^{-1-c}$ and $\dot{\gamma}(y)/\gamma(y) = -c/y$, therefore we obtain

$$\dot{Q}(y, z) = \frac{c}{2y^{2-c}} Q''(y, z) - \frac{c}{y} \theta(z) [z Q(y, z)]', \quad (172)$$

and we keep a generic initial condition $Q(1, z) = Q_i(z)$. Eq. (172) is a Fokker-Planck equation with diffusion and drift, and it corresponds to the Langevin equation

$$\frac{dz}{dy} = \frac{cz}{y} \theta(z) + \frac{\sqrt{c}}{y^{(2-c)/2}} \eta(y) \quad (173)$$

where $\eta(y)$ is a white noise with $\langle \eta(y) \eta(y') \rangle = \delta(y - y')$. The Langevin equation shows that on the $z > 0$ side, the random walkers drift towards $z = \infty$, and for this reason $Q(y, z) \rightarrow 0$ for large y . Instead, for $z < 0$ the equation corresponds to a simple random walk with a diffusion coefficient that is reduced when y grows.

1. Scaling in the matching region

The numerical study of Eq. (172) is straightforward and shows that $Q(y, z)$ satisfies the scaling (170). To obtain analytical insight on the scaling, we plug the *ansatz* $Q(y, z) = y^{a-c} p_1(z y^{b-c})$ in Eq. (172); then we see that a non-trivial equation is obtained only if $b = (1 + c)/2$, otherwise the diffusion term has a different scaling from the other terms. Calling $t = z y^{b-c} = h y^b$, with $b = (1 + c)/2$, one obtains a simple differential equation for the master function $p_1(t)$:

$$\frac{c}{2} p_1''(t) = (a - c \theta(-t)) p_1(t) + \left(\frac{1+c}{2} - c \theta(-t) \right) t p_1'(t). \quad (174)$$

This equation admits solutions with the correct asymptotic behavior of $p_1(t)$. In fact, one can show that for $t \rightarrow \infty$ there is a solution $p_1(t) \sim t^{-\alpha}$ with $\alpha = a/b$, and for $t \rightarrow -\infty$ there is a solution $p_1(t) \sim |t|^\theta$, with $\theta = (c-a)/(b-c) = 2(c-a)/(1-c)$. However, a solution that has *both* correct asymptotic behaviors does not exist for generic values of a . Imposing the existence of a solution with the correct asymptotes therefore defines the value of a as a function of c , which can be easily determined with very high precision by solving Eq. (174) numerically and using a bisection method to find the correct a . As an example, we obtain $a(c = 0.5) = 0.38923 \dots$ and $a(c = 0.4) = 0.29110 \dots$. A decent fit to have an idea of the trend is $a(c) \approx 0.53c + 0.49c^2$, but of course one needs a much higher precision on a to have the correct behavior of $p_1(t)$. Note that a is not a simple rational function of c , because the condition that determines it is quite involved. The solution for $p_1(t)$ corresponding to this value of a gives the scaling function in the matching regime.

In Fig. 8 we compare the results of this scaling analysis with direct numerical resolution of Eq. (172) for $c = 1/2$. We chose initial condition $Q_i(z) = 1$ and solved numerically Eq. (172). For large y , we observe the appearance of a scaling regime around $z = 0$. Note that other initial conditions can be considered and the choice does not affect the scaling around $z = 0$. In the scaling regime, we find excellent agreement with the predictions of the scaling analysis presented above, as discussed in the caption of Fig. 8.

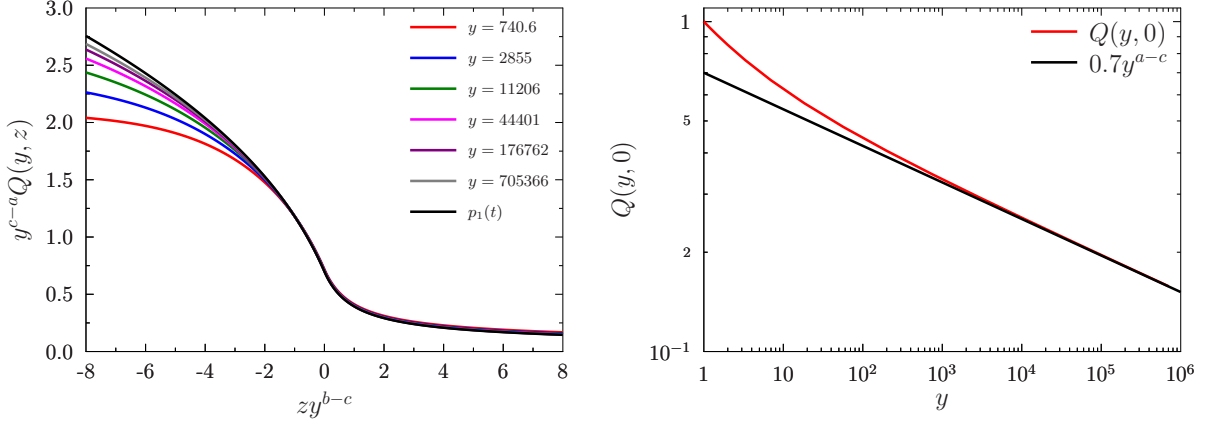


FIG. 8: (Left) Scaling plot of $y^{c-a}Q(y, z)$ with $c = 1/2$, $b = 3/4$ and $a = 0.38923\dots$ versus $t = zy^{b-c}$ for different values of y in the toy model Eq. (172), compared with the solution for $p_1(t)$ with the same a . The agreement is excellent. (Right) Plot of $Q(y, z = 0)$ versus y which shows that $Q(y, z = 0) \sim y^{a-c}$ as expected.

2. Computation of $p_0(z)$

We know that $Q(y \rightarrow \infty, z) = p_0(z)$ for $z < 0$, while $Q(y \rightarrow \infty, z)$ vanishes for $z > 0$. To compute the function $p_0(z)$ it is convenient to change variables to $\tau = 1 - y^{c-1}$, and write Eq. (172) for $z < 0$ as

$$\frac{\partial Q(\tau, z)}{\partial \tau} = \frac{c}{2(1-c)} Q''(\tau, z) = \frac{D}{2} Q''(\tau, z), \quad (175)$$

which is the standard diffusion equation. The corresponding Green's function is

$$G(\tau, z - z') = \frac{1}{\sqrt{2\pi D\tau}} e^{-\frac{(z-z')^2}{2D\tau}}, \quad (176)$$

with $G(\tau = 0, z - z') = \delta(z - z')$. We look for a solution of Eq. (175) in the region $z < 0$. We start by constructing a solution that satisfies the boundary condition $Q(\tau = 0, z) = Q_i(z)$ and $Q(\tau, z = 0) = 0$. It has the form

$$Q_{\text{reg}}(\tau, z) = \int_{-\infty}^0 dz' [G(\tau, z - z') - G(\tau, z + z')] Q_i(z'). \quad (177)$$

The regions $z < 0$ and $z > 0$ admit different solutions, and we know that $Q(y, z = 0) \sim y^{a-c}$ hence $Q(\tau, z = 0) \sim (1-\tau)^{(c-a)/(1-c)} = (1-\tau)^{\theta/2}$ using the relations $b = (1+c)/2$ and $\theta = (c-a)/(b-c) = 2(c-a)/(1-c)$. Therefore, we should add a second contribution to $Q_{\text{reg}}(\tau, z)$ in order to match the boundary condition at $z = 0$. This contribution can be chosen, for $z < 0$, as

$$\begin{aligned} Q_{\text{sing}}(\tau, z) &= \int_0^\tau dt G(\tau - t, z) B(1 - t) = \int_0^\tau dt \frac{B(1 - t)}{\sqrt{2\pi D(\tau - t)}} e^{-\frac{z^2}{2D(\tau - t)}} \\ &= \int_{1-\tau}^1 ds \frac{B(s)}{\sqrt{2\pi D[s - (1 - \tau)]}} e^{-\frac{z^2}{2D[s - (1 - \tau)]}} = \int_{1-\tau}^1 ds \frac{s^{(\theta-1)/2} \mathcal{B}(s)}{\sqrt{2\pi D[s - (1 - \tau)]}} e^{-\frac{z^2}{2D[s - (1 - \tau)]}}. \end{aligned} \quad (178)$$

In fact, it is a solution of Eq. (175), such that $Q_{\text{sing}}(\tau = 0, z) = 0$, hence it does not affect the initial condition in $\tau = 0$.

We want to show that choosing $B(s) = s^{(\theta-1)/2} \mathcal{B}(s)$, where $\mathcal{B}(s) = \mathcal{B}_0 + \mathcal{B}_1 s + \dots$ is an analytic function of s , such that

$$Q_{\text{sing}}(\tau = 1, z = 0) = \int_0^1 \frac{ds}{\sqrt{2\pi D} s^{1-\theta/2}} \mathcal{B}(s) = 0, \quad (179)$$

provides a solution with the correct scaling $Q(\tau, z = 0) \sim (1 - \tau)^{\theta/2}$. The function $\mathcal{B}(s)$ should be determined from

the matching with the solution at $z > 0$, but this is not relevant for the rest of this discussion⁸. In fact, for $z = 0$ we have at leading order for small $\epsilon = 1 - \tau$, using Eq. (179)

$$\begin{aligned} Q_{\text{sing}}(\tau, z = 0) &= \int_{\epsilon}^1 ds \frac{s^{(\theta-1)/2} \mathcal{B}(s)}{\sqrt{2\pi D[s-\epsilon]}} = \int_0^{1-\epsilon} ds \frac{(s+\epsilon)^{(\theta-1)/2} \mathcal{B}(s+\epsilon)}{\sqrt{2\pi Ds}} \sim \int_0^1 ds \frac{(s+\epsilon)^{(\theta-1)/2} \mathcal{B}(s)}{\sqrt{2\pi Ds}} \\ &= \int_0^1 ds \frac{\mathcal{B}(s)}{\sqrt{2\pi Ds}} \left[(s+\epsilon)^{(\theta-1)/2} - s^{(\theta-1)/2} \right] \sim \int_0^1 ds \frac{\mathcal{B}_0 + \mathcal{B}_1 s + \dots}{\sqrt{2\pi D} s^{1-\theta/2}} \left[(1+\epsilon/s)^{(\theta-1)/2} - 1 \right] \\ &\sim \mathcal{B}_0 \epsilon^{\theta/2} \int_0^{1/\epsilon} \frac{du}{\sqrt{2\pi D} u^{1-\theta/2}} \left[(1+1/u)^{(\theta-1)/2} - 1 \right] \propto (1-\tau)^{\theta/2}, \end{aligned} \quad (180)$$

and repeating the same argument at vanishingly small z we obtain

$$\begin{aligned} Q_{\text{sing}}(\tau, z) &\sim \int_0^1 ds \frac{\mathcal{B}_0 + \mathcal{B}_1 s + \dots}{\sqrt{2\pi D} s^{1-\theta/2}} \left[(1+\epsilon/s)^{(\theta-1)/2} - 1 \right] e^{-\frac{z^2}{2Ds}} \\ &\sim \mathcal{B}_0 \epsilon^{\theta/2} \int_0^{1/\epsilon} \frac{du}{\sqrt{2\pi D} u^{1-\theta/2}} \left[(1+1/u)^{(\theta-1)/2} - 1 \right] e^{-\frac{z^2}{2Du}} = (1-\tau)^{\theta/2} q[z/(1-\tau)^{1/2}], \end{aligned} \quad (181)$$

which translated back to the variable y implies, recalling that $b - c = (1 - c)/2$,

$$Q_{\text{sing}} = y^{a-c} q[zy^{b-c}], \quad (182)$$

as expected from Eq. (170). Finally, using again Eq. (179), we have that for small z

$$\begin{aligned} Q_{\text{sing}}(\tau = 1, z) &= \int_0^1 ds \frac{s^{(\theta-1)/2} \mathcal{B}(s)}{\sqrt{2\pi Ds}} e^{-\frac{z^2}{2Ds}} = \int_0^1 \frac{ds}{\sqrt{2\pi D} s^{1-\theta/2}} \left[e^{-\frac{z^2}{2Ds}} - 1 \right] (\mathcal{B}_0 + \mathcal{B}_1 s + \dots) \\ &\sim \mathcal{B}_0 z^{\theta} \int_0^{1/z^2} \frac{du}{\sqrt{2\pi D} u^{1-\theta/2}} \left[e^{-\frac{1}{2Bu}} - 1 \right]. \end{aligned} \quad (183)$$

We conclude that, even if the function $\mathcal{B}(s)$ remains undetermined by this analysis, the resulting function $Q(\tau, z) = Q_{\text{reg}}(\tau, z) + Q_{\text{sing}}(\tau, z)$ has all the correct scaling properties. The resulting function $p_0(z)$ is given by

$$p_0(z) = Q(\tau = 1, z) = \int_{-\infty}^0 dz' [G(1, z - z') - G(1, z + z')] Q_i(z') + \int_0^1 ds \frac{s^{(\theta-1)/2} \mathcal{B}(s)}{\sqrt{2\pi Ds}} e^{-\frac{z^2}{2Ds}}, \quad (184)$$

which shows that *the function $p_0(z)$ depends on non-universal details of the evolution of $Q(y, z)$, such as the initial condition $Q_i(z)$ and the function $\mathcal{B}(s)$.*

3. Summary

From the analysis of the toy model Eq. (172), we obtain several important informations:

- In the matching regime, the scaling is controlled by a universal function $p_1(t)$, solution of Eq. (174), with exponents $b = (1 + c)/2$ and $a(c)$ determined by the condition that $p_1(t)$ has the correct asymptotic behavior. However, the exponent c remains underdetermined by this analysis, with the only condition that $a < c < b$ which implies $c \in [0, 1]$.
- There is no hope of computing $p_0(z)$ from scaling arguments, because this function depends on non-universal quantities that contain information on the whole evolution of $Q(y, z)$. Hence we have to obtain it through the full numerical solution of the equation for $Q(y, z)$.

These informations are very useful to understand the complete fullRSB equations.

⁸ One can choose for illustrative purposes $\mathcal{B}(s) = -\mathcal{B}_0[1 - s(2 + \theta)/\theta]$, which has the required properties.

D. Scaling of the functions $\hat{j}(y, h)$ and $\hat{P}(y, h)$ in the matching region

Using the analogy with the toy model investigated in the previous section, we can start to discuss the asymptotic scaling of the solution of the complete fullRSB equations. We consider first the equation for $\hat{j}(y, h)$. For $m = 0$, its initial condition for $y = \infty$ becomes $\hat{j}(y, h) = 0$, see Eq. (113). One can show from Eq. (113) that

$$\hat{j}(y_i, h \rightarrow -\infty) = \sum_{j=i}^{k-1} \frac{1}{2y_j} \log(\hat{\gamma}_{j+1}/\hat{\gamma}_j), \quad (185)$$

and in the continuum limit

$$\hat{j}(y, h \rightarrow -\infty) = \int_y^\infty \frac{du \dot{\gamma}(u)}{2u \gamma(u)}; \quad (186)$$

this relation can also be derived directly from Eq. (116). Similarly, one can easily show that $\hat{j}(y, h \rightarrow \infty) = 0$ for all y .

At large y , under the assumption that $\gamma(y) \sim \gamma_\infty y^{-c}$, we then have $\hat{j}(y, h \rightarrow -\infty) \sim -c/(2y)$. We therefore conjecture the scaling form

$$\hat{j}(y, h) = -\frac{c}{2y} J(hy^b/\sqrt{\gamma_\infty}), \quad H(y, z) = -\frac{c}{2} J(zy^{b-c}/\sqrt{\gamma_\infty}), \quad (187)$$

and we insert it in Eq. (116) for $\hat{j}(y, h)$. As in the case of the toy model, the only choice that leads to a non-trivial equation is $b = (1 + c)/2$, which leads to the following equation for $J(t)$ with $t = hy^b/\sqrt{\gamma_\infty} = zy^{b-c}/\sqrt{\gamma_\infty}$:

$$\frac{c}{2} J''(t) = tJ'(t) \left(-\frac{1+c}{2} + c\theta(-t) \right) + J(t) - \theta(-t) + \frac{c^2}{4} J'(t)^2. \quad (188)$$

This equation must be solved with boundary conditions $J(-\infty) = 1$ and $J(\infty) = 0$, which can be done easily by a shooting method and leads to a unique solution for each value of c .

We consider next the scaling of $\hat{P}(y, h)$ in the intermediate scaling regime that matches around $h = 0$. According to Eq. (167) and (170), we have $\hat{P}(y, h) = y^a p_1(hy^b/\sqrt{\gamma_\infty})$ and $Q(y, z) = y^{a-c} p_1(zy^{b-c}/\sqrt{\gamma_\infty})$, and we added here the term $\sqrt{\gamma_\infty}$ because in this way the dependence on γ_∞ disappears from the scaling equations. We choose again $b = (1 + c)/2$, because, as in the case of the toy model, it is the only choice that leads to a non-trivial equation for $p_1(t)$, that depends in a non-trivial way on the function $J(t)$ that varies on the same scale. If we call once again $t = zy^{b-c}/\sqrt{\gamma_\infty} = hy^b/\sqrt{\gamma_\infty}$, we plug the scaling form of $Q(y, z)$ in Eq. (171), and we use Eq. (187), then we obtain, at the leading order

$$\frac{c}{2} p_1''(t) = (a - c\theta(-t)) p_1(t) + \left(\frac{1+c}{2} - c\theta(-t) \right) t p_1'(t) - \frac{c^2}{2} [p_1'(t)J'(t) + p_1(t)J''(t)], \quad (189)$$

which correctly coincides with Eq. (174) of the toy model if one chooses $J = 0$. Note that for $|t| \rightarrow \infty$, $J' \sim J'' \rightarrow 0$, therefore one can repeat the same analysis as for Eq. (174) to show that Eq. (189) admits solutions with the correct asymptotic behavior of $p_1(t)$, namely $p_1(t \rightarrow \infty) \sim t^{-\alpha}$ with $\alpha = a/b$, and $p_1(t \rightarrow -\infty) \sim |t|^\theta$, with $\theta = (c-a)/(b-c)$. Like for Eq. (174), a solution that has both correct asymptotic behaviors exists only for a specific value of a , that can be determined through a bisection method.

In summary, for given c and $b = (1 + c)/2$, we have to solve the two Eqs. (188) and (189) with their appropriate boundary condition. As in the toy model, this fixes the value of a as a function of c . We find that the presence of $J \neq 0$ is only a small perturbation of Eq. (189) with respect to Eq. (174), and the resulting values of a are just slightly smaller than the ones of the toy model.

E. Determination of the critical exponents

Up to now the exponent c has remained undetermined. In this section, we derive a condition that allows us to determine c and from it a and b , hence obtaining analytical predictions for all the critical exponents.

1. Some exact relations

We start by deriving a few useful exact relations, following [33]. To do so, we introduce

$$\tilde{f}(y, h) = \gamma(y)\hat{f}(y, h) = -\frac{h^2\theta(-h)}{2} + \gamma(y)\hat{j}(y, h) \quad (190)$$

and we consider the equation for $\kappa(y)$ in Eq. (116), which is:

$$\kappa(y) = \frac{\hat{\varphi}}{2\gamma^2(y)} \int_{-\infty}^{\infty} dh e^h \hat{P}(y, h) \tilde{f}'(y, h)^2 . \quad (191)$$

We take the derivative with respect to y , and using the equation of motion (116) for $\hat{P}(y, h)$ and $\hat{f}(y, h)$ we obtain

$$\dot{\kappa}(y) = -\frac{\hat{\varphi}\dot{\gamma}(y)}{2y\gamma^2(y)} \int_{-\infty}^{\infty} dh e^h \hat{P}(y, h) \tilde{f}''(y, h)^2 . \quad (192)$$

From the relation between $\kappa(y)$ and $\gamma(y)$ we have $\dot{\kappa}(y) = -\frac{\dot{\gamma}(y)}{y\gamma^2(y)}$, so we obtain the exact expression

$$1 = \frac{\hat{\varphi}}{2} \int_{-\infty}^{\infty} dh e^h \hat{P}(y, h) \tilde{f}''(y, h)^2 . \quad (193)$$

Note that to derive Eq. (193) we have assumed that $\dot{\kappa}(y) \neq 0$ in a finite interval of y . Hence, for any finite k RSB solution, Eq. (193) does not hold because $\dot{\kappa}(y) = 0$ except in a finite number of isolated points. For a fullRSB solution, instead, Eq. (193) holds for all y . Indeed, if $\dot{\kappa}(y) = 0$ then $\hat{P}(y, h)$ and $\tilde{f}''(y, h)$ do not depend on y , hence if Eq. (193) holds in the region where $\dot{\kappa}(y) \neq 0$, it must also hold (trivially) where $\dot{\kappa}(y) = 0$.

If we derive once more Eq. (193) with respect to y , we obtain (using once more the equations of motion)

$$0 = \int_{-\infty}^{\infty} dh e^h \hat{P}(y, h) \left[2 \left(\tilde{f}''(y, h)^2 + \tilde{f}'''(y, h)^3 \right) - \frac{\gamma(y)}{y} \tilde{f}'''(y, h)^2 \right] , \quad (194)$$

from which it follows that

$$y = \frac{\gamma(y)}{2} \frac{\int_{-\infty}^{\infty} dh e^h \hat{P}(y, h) \tilde{f}'''(y, h)^2}{\int_{-\infty}^{\infty} dh e^h \hat{P}(y, h) \left(\tilde{f}''(y, h)^2 + \tilde{f}'''(y, h)^3 \right)} . \quad (195)$$

Note that Eq. (195) can only hold in the region where $\dot{\kappa}(y) \neq 0$; this is obvious because the right hand side is constant when $\dot{\kappa}(y) = 0$.

2. Scaling regime

These equations have important consequences in the scaling regime. First of all, Eq. (193) is a kind of normalization condition for $\hat{P}(y, h)$. In the limit $y \rightarrow \infty$, at the leading order we have $\tilde{f}''(y, h) = -\theta(-h)$, and using Eq. (167) one can show that Eq. (193) becomes

$$1 = \frac{\hat{\varphi}}{2} \int_{-\infty}^0 dz p_0(z) , \quad (196)$$

which will be crucial, in the following, to obtain isostaticity. Also, in the same regime $\tilde{f}'(y, h) = -h\theta(-h)$ and Eq. (191) gives

$$\kappa_{\infty} = \kappa(y \rightarrow \infty) = \frac{\hat{\varphi}}{2\gamma_{\infty}^2} \int_{-\infty}^0 dz p_0(z) z^2 . \quad (197)$$

Eq. (195), instead, receives non-vanishing contributions only from the matching regime, both in the numerator and in the denominator, as one can check that the other contributions vanish. In the matching regime for large y , using $\gamma(y) \sim \gamma_{\infty} y^{-c}$ and Eq. (187), one can show easily that

$$\begin{aligned} \tilde{f}''(y, h) &= -\theta(-t) - \frac{c}{2} J''(t) , \\ \tilde{f}'''(y, h) &= \frac{y^{(1+c)/2}}{\sqrt{\gamma_{\infty}}} \frac{d}{dt} \left[-\theta(-t) - \frac{c}{2} J''(t) \right] . \end{aligned} \quad (198)$$

Plugging this in Eq. (195), we get

$$\frac{1}{2} = \frac{\int_{-\infty}^{\infty} dt p_1(t) [\theta(-t) + \frac{c}{2} J''(t)]^2 [\theta(t) - \frac{c}{2} J''(t)]}{\int_{-\infty}^{\infty} dt p_1(t) [\frac{d}{dt} (\theta(-t) + \frac{c}{2} J''(t))]^2}. \quad (199)$$

Now, remember that for a given c , we can determine a , b , $J(t)$ and $p_1(t)$ through Eqs. (188) and (189). Hence, Eq. (199) becomes a condition on the exponent c . Solving this condition numerically, and also using Eq. (168), we obtain the values of the exponents:

$$\begin{aligned} a &= 0.29213\dots & b &= 0.70787\dots & c &= 0.41574\dots, \\ \alpha &= 0.41269\dots & \theta &= 0.42311\dots & \kappa &= 1.41574\dots. \end{aligned} \quad (200)$$

The precision of the determination of these exponents depends on the cutoffs that are used to discretize Eqs. (188) and (189): we estimate (conservatively) that the error in Eq. (200) is smaller than ± 1 on the last reported digit. These are our analytic predictions for the scaling exponents, and they complete the analysis of the scaling regime of Eq. (116). Note that within our error we find that $a = 1 - b$, which, together with $b = (1 + c)/2$, implies the relation $\alpha = 1/(2 + \theta)$ that has been derived in [25] using scaling arguments. We will come back on this point later. In the next sections we test the correctness of our scaling analysis, and we relate these exponents to observable quantities.

X. NUMERICAL TEST OF THE CRITICAL SCALING OF THE FULLRSB SOLUTION

Having obtained analytical results for the exponents that characterize the asymptotic scaling of the fullRSB solution at jamming, we now solve the fullRSB numerically to test them and check the pre-asymptotic corrections.

We consider Eq. (113) at $m = 0$, which means that $y_k = \infty$ and $\hat{j}(y_k, h) = 0$, and we solve the recurrence equations numerically. We use here a different code than in the 2RSB computation, which is not optimized to work at large densities, hence it does not make use of the decomposition (149). This code just solves the equations by iterating them, carefully taking into account the behavior of the various functions for $h \rightarrow \pm\infty$. The code can work for any number k of RSB. Note that even if $m = 0$, numerically solving the equations necessitates working at finite k , hence we effectively introduce a cutoff $y_{k-1} = y_{\max}$ which is akin to a finite m (we will come back to this point later). To study the fullRSB solution at $m = 0$ we therefore have to set y_{\max} and k to be as large as possible. Cutoffs are also used to discretize the integrals, but we checked that the results we report are independent of their choice so we do not further discuss this issue below.

In the following, all numerical results are obtained for $\hat{\varphi} = 10$, which is a value large enough that we are sure to be above the threshold, but low enough that our code works well.

A. Dependence on the cutoffs k and y_{\max}

We start our discussion with a brief study of the dependence of the function $\Delta(y)$ on the cutoffs k and y_{\max} . For our numerical studies, we chose logarithmically spaced y_i , between $y_1 = 1$ and $y_{k-1} = y_{\max}$. In Fig. 9 results for several k at fixed y_{\max} , and for fixed k at several y_{\max} , show that we can reach the limit where both k and y_{\max} can be considered as infinite. Clearly, $\Delta(y)$ is a non-trivial continuous function of y , which confirms that we are in a fullRSB phase, as we conjectured at the beginning of Sec. IX. Our results are also perfectly compatible with the expected behavior at large y , $\Delta(y) \sim \Delta_{\infty} y^{-\kappa}$ with κ given in Eq. (200). A deviation is observed for values of y close to the cutoff at y_{\max} , but the value of y at which we observe the deviation grows proportionally to y_{\max} . This observation will be important later. Note that in the region where this deviation is observed, we expect that $\Delta(y)$ should tend to be approximately constant. The reason why this is not the case is that the convergence of our code to the fixed point of Eq. (113) is very slow in that region. We could perform more iterations to observe full convergence but we did not do so, because this calculation is computationally hard and because the behavior of this cutoff-dependent region is irrelevant for our analysis.

B. Test of the critical exponents

We now perform a more detailed test of the critical scaling derived in Sec. IX using the data with the largest available cutoff, $y_{\max} = 10000$, and $k = 100$. In Fig. 10 we plot γ as a function of y^{-c} and Δ as a function of y^{-c-1} ;

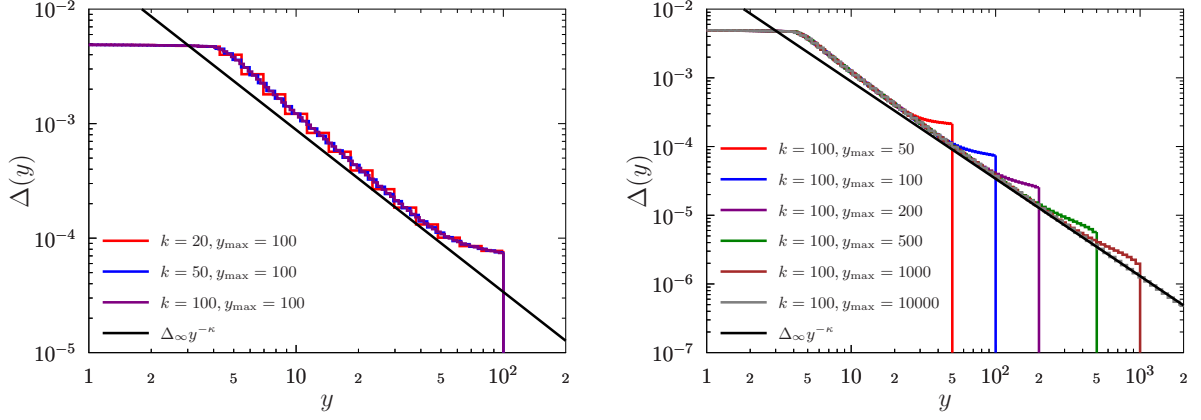


FIG. 9: The function $\Delta(y)$ at $m = 0$ and $\hat{\varphi} = 10$. In left panel we report results for fixed $y_{\max} = 100$ and $k = 20, 50, 100$, which show that $k = 100$ is large enough to be considered infinite. In right panel we report results for fixed $k = 100$ and $y_{\max} = 50, 100, 200$, which show that for large y_{\max} the cutoff at large y disappears. The power law regime $\Delta(y) \sim \Delta_{\infty} y^{-\kappa}$ with $\Delta_{\infty} \approx 0.023$ and κ given in Eq. (200) is approached at large y .

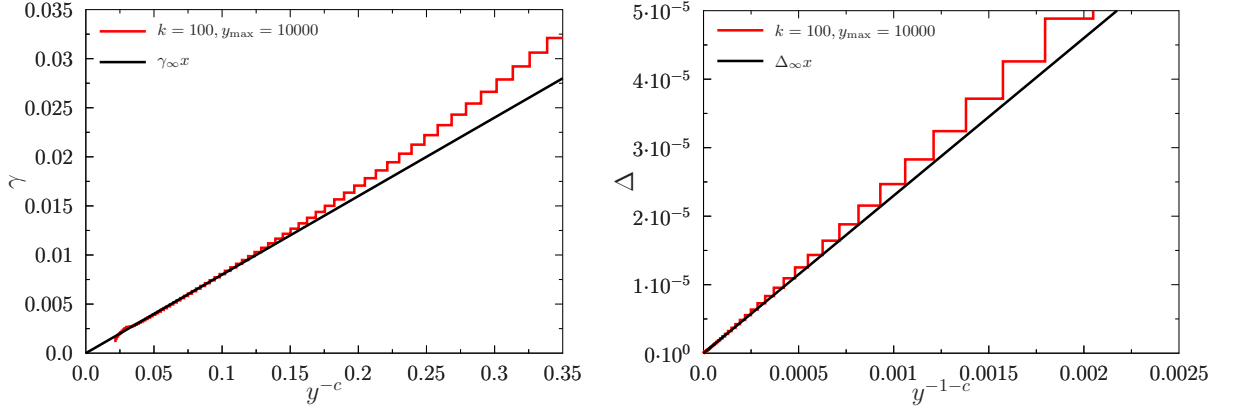


FIG. 10: Plot of γ versus y^{-c} (left), and of Δ versus y^{-1-c} (right), with c given in Eq. (200). The linear fits give $\gamma_{\infty} \approx 0.080$ and $\Delta_{\infty} = \frac{c}{c+1} \gamma_{\infty} \approx 0.023$.

the plots are linear at large y and provide an estimate of $\gamma_{\infty} \approx 0.080$ and $\Delta_{\infty} = \frac{c}{c+1} \gamma_{\infty} \approx 0.023$, which is also perfectly compatible with Fig. 9.

Having an estimate of γ_{∞} , we can test the scaling of Eq. (187), see Fig. 11, and the scaling in Eq. (167), see Fig. 12. In both cases we find excellent agreement between the analytical results of Sec. IX and the numerical solution of the equations.

XI. CRITICAL SCALING OF PHYSICAL OBSERVABLES

We have confirmed that the asymptotic solution of Eqs. (113) and (116) found in Sec. IX is realized by the numerical solution of the fullRSB equations. We now start to investigate the physical consequences, in particular to identify observables that display critical scaling controlled by the exponents in Eq. (200).

In Sec. XI A we show that the exponent κ is related to the scaling of the cage radius with pressure. In Sec. XI B we discuss the scaling of the pair correlation function of the glass on approaching jamming and we show that it is determined by the exponents α and θ . In Sec. XI C we show that the distribution of forces in the packing can be obtained from the pair correlation function and that it is characterized by the exponent θ . Finally, in Sec. XI D we show that the fullRSB solution predicts that jammed packings are isostatic, i.e. particles touch on average $2d$ other particles.

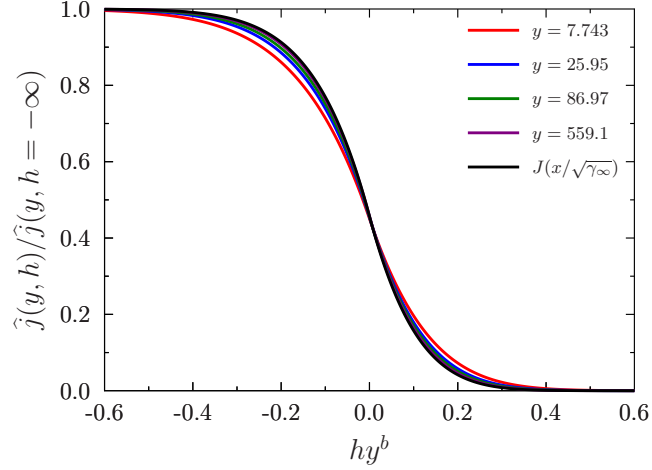


FIG. 11: Scaling plot of the function $\hat{j}(y, h)$ according to Eq. (187). We plot $\hat{j}(y, h)/\hat{j}(y, h \rightarrow -\infty)$ versus hy^b , with b given in Eq. (200). We also report the (properly scaled) solution $J(z)$ of Eq. (188) corresponding to the choice of exponents in Eq. (200). On increasing y the curves approach the master function.

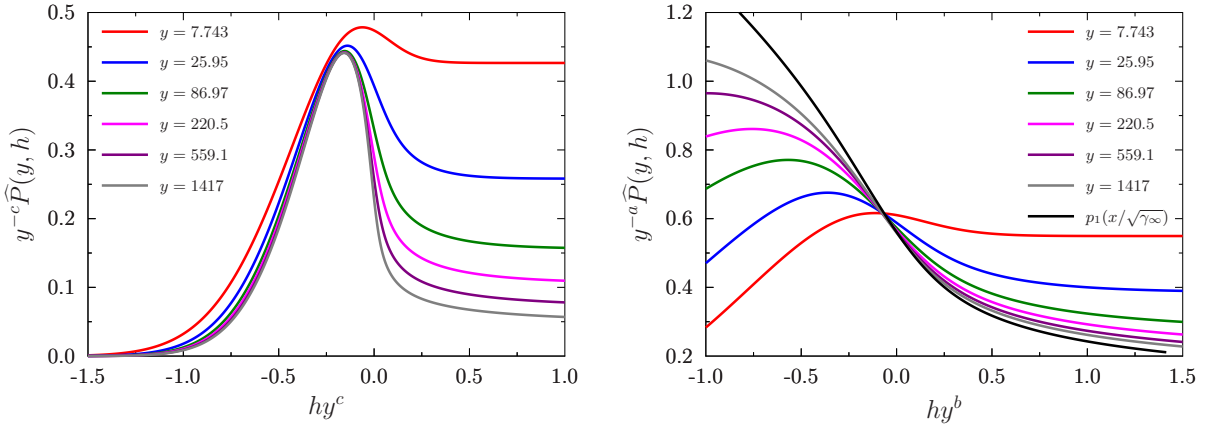


FIG. 12: Test of Eq. (167) and (170), with exponents given by Eq. (200). (Left) Convergence to the function $Q(y, z)$ to $p_0(z)$. (Right) Scaling in the region around $h = 0$ where $\hat{P}(y, h) \sim y^a p_1(hy^b)$, compared with the solution $p_1(z)$ of Eq. (189).

A. Scaling of the cage radius with pressure

First, we discuss the physical meaning of the exponent κ . We have already explained that finite pressures are equivalent to finite m with $m \sim 1/p$. Moreover, we see from Eq. (113) that a finite (small) m is equivalent to a cutoff for $\Delta(y)$ at $y_{\max} \sim 1/m \sim p$. In fact, the only difference between the equations at finite m and the ones at $m = 0$ with a cutoff at y_{\max} is the initial condition for $\hat{j}(y, h)$, which is non-vanishing (but small) for finite small m . However, this difference is completely irrelevant because the scaling regime is universal and independent of the initial conditions. From this argument we conclude that the intra-state cage radius (or mean square displacement, or Debye-Waller factor) scales as $\hat{\Delta}_{\text{EA}} \sim \Delta(y \propto 1/m) \propto m^\kappa \propto p^{-\kappa}$, which provides a way to measure the exponent κ . Note that instead, at any level of k RSB with finite k , we have $\hat{\Delta}_{\text{EA}} = \hat{\Delta}_k \propto m \propto 1/p$ as in the 1RSB solution. As in the Sherrington-Kirkpatrick model, the presence of a fullRSB solution is the signature of a marginally stable phase where the scaling of the intra-state overlap is changed.

B. Pair correlation function

We now want to study the scaling of the effective potential given by Eq. (108), that in $d \rightarrow \infty$ coincides with the glass correlation function⁹ $g(r)$ as a function of $h = d(r - D)/D$ (recall that $m_k = 1$ and $y_k = 1/m$):

$$\begin{aligned} e^{-\phi_{\text{eff}}(h)} &= \theta(h) \int_{-\infty}^{\infty} dz e^{z-h} \gamma_{\widehat{\Delta}_k}(h-z) \frac{e^{-z-\widehat{\Delta}_k/2} P(m_k, z)}{g(m_k, z)} = \theta(h) \int_{-\infty}^{\infty} dz e^{z-h} \gamma_{\widehat{\Delta}_k}(h-z) \frac{\widehat{P}(y_k, z)}{\Theta\left(z/\sqrt{2\widehat{\Delta}_k}\right)} \\ &= \theta(h) \int_{-\infty}^{\infty} dz \frac{\gamma_{\widehat{\Delta}_k}(h + \widehat{\Delta}_k - z)}{\Theta\left(z/\sqrt{2\widehat{\Delta}_k}\right)} \widehat{P}(y_k, z) e^{\widehat{\Delta}_k/2}. \end{aligned} \quad (201)$$

1. Finite k RSB

Before looking at the fullRSB solution, it is instructive to examine what happens at any finite level of k RSB. In that case, when $m \rightarrow 0$, we have $\widehat{\Delta}_k \sim m$ and $\widehat{P}(m_k, h)$ tends to a finite function for all h . In this situation, if $h > 0$, the kernel $\gamma_{\widehat{\Delta}_k}(h + \widehat{\Delta}_k - z)$ forces $|z - h| \sim m^{1/2} \rightarrow 0$, hence $z > 0$. The function $\Theta\left(z/\sqrt{2\widehat{\Delta}_k}\right) \rightarrow 1$, and we conclude that

$$e^{-\phi_{\text{eff}}(h)} = \widehat{P}(y_k, h) e^{\widehat{\Delta}_k/2}. \quad (202)$$

In particular, in the 1RSB case, $\widehat{P}(y_1, h) e^{\widehat{\Delta}_1/2} = 1$ and the effective potential is 1 corresponding to no correlations at all for any $h > 0$. Note however that for $k > 1$ RSB, the function $\widehat{P}(y_k, h)$ has qualitatively the shape of Fig. 7, although the peak is not divergent. We therefore obtain that the glass correlation has a peak for small h .

On top of that, there is a highly non-trivial behavior when $h \sim m$ [11]. In fact, in that regime z is not always positive. The positive part of the integral over z gives a small contribution, but for negative z the function Θ can be computed in large and negative arguments where it goes to zero. This small denominator changes completely the behavior of the function inducing a large peak. In this regime, defining $\lambda = h/m$, making use of the expansion of the error function $\Theta(s \rightarrow \infty) \sim \frac{e^{-s^2}}{2\sqrt{\pi}|s|}$ [11], and omitting subleading terms, we get:

$$e^{-\phi_{\text{eff}}(h)} = \int_{-\infty}^0 dz \frac{e^{-\frac{(m\lambda + \widehat{\Delta}_k - z)^2}{2\widehat{\Delta}_k}}}{\sqrt{2\pi\widehat{\Delta}_k}} |z| e^{\frac{z^2}{2\widehat{\Delta}_k}} \sqrt{\frac{2\pi}{\widehat{\Delta}_k}} \widehat{P}(y_k, z) = \int_{-\infty}^0 dz |z| \frac{1}{\widehat{\Delta}_k} e^{z\left(\frac{m\lambda}{\widehat{\Delta}_k} + 1\right)} \widehat{P}(y_k, z). \quad (203)$$

Now, using that $\widehat{\Delta}_k = m\widehat{\gamma}_k$, and that $\widehat{\gamma}_k$ remains finite for $m \rightarrow 0$, we have

$$e^{-\phi_{\text{eff}}(h)} = \frac{1}{m} \int_{-\infty}^0 dz |z| \frac{1}{\widehat{\gamma}_k} e^{z\left(\frac{\lambda}{\widehat{\gamma}_k} + 1\right)} \widehat{P}(y_k, z) = \frac{1}{m\widehat{\gamma}_k} \mathcal{F}_k\left(\frac{\lambda}{\widehat{\gamma}_k}\right) = \frac{1}{m\widehat{\gamma}_k} \mathcal{F}_k\left(\frac{h}{m\widehat{\gamma}_k}\right), \quad (204)$$

which shows that the contact value of the pair correlation $g(r)$ diverges as $1/m$ and the peak is characterized by a scaling function¹⁰ \mathcal{F}_k on a scale $h \sim m$. This function is finite for $\lambda = 0$ (remember that $P(y_k, z)$ is a finite function, and it decays as a Gaussian for large z), while for $\lambda \rightarrow \infty$ it decays as $1/\lambda^2$, because $P(y_k, z)$ is finite in $z = 0$. These results were already derived in [11] at the 1RSB level.

2. FullRSB

Let us now see how this scenario is profoundly modified in the fullRSB case. As discussed in Sec. XIA, at finite m the scaling discussed in Sec. IX holds, but there is a cutoff at $y = x_{\text{max}}/m$ with some constant factor x_{max} , after

⁹ The reader should not confuse this function, which is a standard object of liquid theory [70] with the auxiliary function $g(m, h)$ that has been introduced above.

¹⁰ We called the scaling function \mathcal{F}_k to keep the same notation used in previous papers [11]. This function should not be confused with the function $\mathcal{F}(\widehat{\Delta})$ that has been introduced in the expression of the replicated entropy at the beginning of the paper.

which $\Delta(y)$ is constant, and so is $\widehat{P}(y, h)$. Therefore, $\widehat{\Delta}_k \sim \Delta_\infty (m/x_{\max})^{1+c}$. At the same time, $\widehat{P}(y_k, h)$ is not finite anymore: it satisfies the scaling (167) and in particular for $h < 0$ we have

$$\widehat{P}(y_k, h) \sim (x_{\max}/m)^c p_0(h(x_{\max}/m)^c). \quad (205)$$

The reasoning that leads to Eq. (203) still holds, but now we have to take into account these modifications. We get, calling $t = -z(x_{\max}/m)^c$,

$$\begin{aligned} e^{-\phi_{\text{eff}}(h)} &= \int_{-\infty}^0 dz |z| \frac{1}{\Delta_\infty (m/x_{\max})^{1+c}} e^{z \left(\frac{m\lambda}{\Delta_\infty (m/x_{\max})^{1+c}} + 1 \right)} (x_{\max}/m)^c p_0(z(x_{\max}/m)^c) \\ &= \frac{x_{\max}}{m\Delta_\infty} \int_0^\infty dt t p_0(-t) e^{-t \frac{\lambda x_{\max}}{\Delta_\infty}} = \frac{x_{\max}}{m\Delta_\infty} \int_0^\infty dt t p_0(-t) e^{-t \frac{hx_{\max}}{m\Delta_\infty}}. \end{aligned} \quad (206)$$

The divergent part of the pressure is given by the contact value of $g(r)$, hence

$$p = 1 + 2^{d-1} \varphi g(D) \sim \frac{d}{2} \widehat{\varphi} e^{-\phi_{\text{eff}}(0)} = \frac{d}{2} \widehat{\varphi} \frac{x_{\max}}{m\Delta_\infty} \int_0^\infty dt t p_0(-t) = \frac{dx_{\max}}{m\Delta_\infty} \frac{\int_0^\infty dt t p_0(-t)}{\int_0^\infty dt p_0(-t)} \equiv \frac{dx_{\max}}{m\Delta_\infty} \bar{t}, \quad (207)$$

where we made use of Eq. (196) and introduced \bar{t} . Note that this result confirms that the pressure is indeed proportional to $1/m$ as we have already discussed above. Eq. (206) can therefore be written as

$$\frac{g(r)}{g(D)} = \frac{e^{-\phi_{\text{eff}}(h)}}{e^{-\phi_{\text{eff}}(0)}} = \frac{\int_0^\infty dt t p_0(-t) e^{-t \frac{hx_{\max}}{m\Delta_\infty}}}{\int_0^\infty dt t p_0(-t)} = \frac{\int_0^\infty dt t p_0(-t) e^{-\frac{t}{\bar{t}} \frac{hp}{d}}}{\int_0^\infty dt t p_0(-t)}. \quad (208)$$

We now define the scaling variable $\lambda = (hp)/d = p(r - D)/D$ and the function

$$P_\infty(f) = \frac{p_0(-f\bar{t})}{\int_0^\infty df f p_0(-f\bar{t})}, \quad (209)$$

and we obtain the final result

$$\frac{g(r)}{g(D)} = \int_0^\infty df f P_\infty(f) e^{-\lambda f} \equiv \mathcal{F}_\infty(\lambda) = \mathcal{F}_\infty\left(p \frac{r - D}{D}\right). \quad (210)$$

Note that the function $P_\infty(f)$ is normalized in such a way that

$$\int_0^\infty df P_\infty(f) = \int_0^\infty df f P_\infty(f) = 1, \quad (211)$$

therefore $\mathcal{F}_\infty(\lambda = 0) = 1$ as it should. Furthermore, because $p_0(z) \sim |z|^\theta$ for small z , one has $P_\infty(f) \sim f^\theta$ for small f and $\mathcal{F}_\infty(\lambda) \sim \lambda^{-2-\theta}$ for large λ , which provides a way to measure θ from the scaling of the contact peak of the pair correlation function.

Finally, Eq. (202) remains true also in the fullRSB case, but we have seen that the function $p_2(h)$ that describes the behavior of $\widehat{P}(y_k, h)$ at finite h diverges as $h^{-\alpha}$ when $h \rightarrow 0$. We therefore *predict* that the pair correlation function, at jamming, should diverge as $h^{-\alpha}$ for $h \rightarrow 0^+$, which provides a way to measure the exponent α .

C. Force distribution

It has been shown in [44] that the function $P(f)$ that enters in the scaling function $\mathcal{F}(\lambda)$ in Eq. (210) is exactly the probability distribution of the forces between particles. Here forces are scaled by the average force, in such a way that the average force is 1, which is consistent with the normalization (211). Obviously, we cannot compute directly $P(f)$ for hard spheres, because forces between hard particles are due to collisions: they have dynamical origin and cannot be obtained through a static computation without making assumptions about the connection between structure and forces [21, 44].

Interestingly, however, in the case of soft harmonic spheres the forces are simply linear functions of the overlaps, and therefore their distribution $P(f)$ is related to $g(r)$ by a straightforward relation [27]. In Appendix A we present a simple extension of the theory to soft harmonic spheres, following [14], that allows us to compute $P(f)$ directly.

Because the distribution of forces at jamming is only determined by the contact network [25, 28], $P(f)$ must be the same if one approaches jamming from below using hard spheres or from above using soft spheres. Indeed, as in the 1RSB case [27], we find that the soft sphere computation gives the result in Eq. (209), thus identifying $P_\infty(f)$ with the (scaled) force distribution at jamming in the fullRSB solution. This result provides an independent proof of the relation (210) between $P(f)$ and $\mathcal{F}(\lambda)$ derived in [44].

Note that a similar manipulation starting from Eq. (204) shows that at any finite level of k RSB

$$P_k(f) = \frac{e^{-\bar{t}f} \widehat{P}(y_k, -f\bar{t})}{\int_0^\infty df f e^{-\bar{t}f} \widehat{P}(y_k, -f\bar{t})}, \quad (212)$$

with \bar{t} defined by the same normalization condition as in Eq. (211). The resulting force distribution is finite for $f \rightarrow 0$ and decays as a Gaussian at large forces, as found at the 1RSB level in [11]. At the fullRSB level, thanks to the appearance of the scaling regime, Eq. (212) becomes Eq. (209). This is very interesting, because for finite forces we obtain a function that is still qualitatively similar to the k RSB result (it is close to a Gaussian), but for small forces we have a large deviation and in particular $P_\infty(f) \sim f^\theta$ with θ given in Eq. (200). As noted in [25], the opening of this ‘‘pseudogap’’ in the force distribution is exactly the same phenomenon as the opening of a pseudogap in the frozen field distributions of the SK model [63, 71], and it fully reflects the presence of fullRSB.

D. Isostaticity

Finally, we can compute the integral of the delta peak to obtain the coordination number. The number of neighbors at distance h is

$$Z(h) = \rho V_d d \int_0^{1+h/d} ds s^{d-1} e^{-\phi_{\text{eff}}} = d\widehat{\varphi} \int_{-\infty}^h du e^u e^{-\phi_{\text{eff}}(u)} = d\widehat{\varphi} \int_0^h du e^u e^{-\phi_{\text{eff}}(u)} \quad (213)$$

The rise of $Z(h)$ from 0 to the plateau happens on the scale $\lambda = h/m$. We obtain therefore for the contact number, using Eq. (206):

$$z = d\widehat{\varphi} \int_0^\infty d\lambda \frac{x_{\text{max}}}{\Delta_\infty} \int_0^\infty dt t p_0(-t) e^{-t \frac{\lambda x_{\text{max}}}{\Delta_\infty}} = d\widehat{\varphi} \int_0^\infty dt p_0(-t). \quad (214)$$

Now, we know from Eq. (196) that $\int_0^\infty dt p_0(-t) = 2/\widehat{\varphi}$, we therefore *predict* that jammed packings are isostatic with $z = 2d$, independently of their density. Note that isostaticity appears as a direct consequence of Eq. (193).

XII. MARGINAL STABILITY

In this section we want to prove that the fullRSB solution is marginally stable. This means that the matrix of small fluctuations around the optimum selected by the variational equations has at least one zero eigenvalue. The complete proof of this statement in the case of the SK model has been given in [39–42]. Here we do not discuss the complete calculation of all the eigenvalues but we focus our attention to the one that is responsible for the marginal stability of the fullRSB state. We consider the replicon eigenvalue that is responsible for the stability of the fullRSB solution with respect to small fluctuations of the mean square displacement matrix that are localized in the innermost blocks.

We start the computation from the replicated entropy defined by Eq. (1). We want to study the eigenvalues of the matrix defined by

$$M_{ab;cd}^{(k)} = \frac{2}{d} \frac{\partial^2 s}{\partial \Delta_{a<b} \partial \Delta_{c<d}} = \frac{\partial^2}{\partial \Delta_{a<b} \partial \Delta_{c<d}} \left[\log \det(\hat{\alpha}^{m,m}) - \widehat{\varphi} \mathcal{F}(\hat{\Delta}), \right] \quad (215)$$

where all the four indexes a, b, c, d are in the same innermost block in a k RSB ansatz and the derivatives are computed on the k RSB solution. We follow the same convention as in [2] by assuming that the variation of Δ_{ab} also induces an identical variation of Δ_{ba} , thereby preserving the symmetry of the matrix. We denote this ‘‘symmetric’’ derivative by $\partial/\partial \Delta_{a<b}$. Replica symmetry implies that all the innermost blocks are equivalent, and that the form of the stability matrix in each of these blocks is

$$M_{ab;cd}^{(k)} = M_1 \left(\frac{\delta_{ac} \delta_{bd} + \delta_{ad} \delta_{bc}}{2} \right) + M_2 \left(\frac{\delta_{ac} + \delta_{bd} + \delta_{ad} + \delta_{bc}}{4} \right) + M_3. \quad (216)$$

The replicon eigenvalue responsible for the stability of the innermost states is given by [35, 66]

$$\lambda_R^{(k)} = M_1 . \quad (217)$$

If we consider a k RSB matrix and make a variation of the innermost element $\widehat{\Delta}_k$, we have (here B denotes one of the innermost blocks)

$$\begin{aligned} \frac{2}{d} \frac{\partial^2 s}{\partial \widehat{\Delta}_k^2} &= \frac{m}{m_{k-1}} \sum_{a \neq b, c \neq d \in B} \frac{2}{d} \frac{\partial^2 s}{\partial \Delta_{ab} \partial \Delta_{cd}} + \frac{m}{m_{k-1}} \left(\frac{m}{m_{k-1}} - 1 \right) [m_{k-1}(m_{k-1} - 1)]^2 \frac{2}{d} \frac{\partial^2 s}{\partial \Delta_{ab} \partial \Delta_{cd}} \Big|_{a \neq b \in B, c \neq d \in B' \neq B} \\ &= \frac{1}{4} m(m_{k-1} - 1) M_1 + O((m_{k-1} - 1)^2) , \end{aligned} \quad (218)$$

where in the first step we used that $\frac{\partial^2 s}{\partial \Delta_{ab} \partial \Delta_{cd}}$ is independent of the choice of indexes if they belong to different blocks, and in the second step we used Eq. (216) and neglected higher orders in $m_{k-1} - 1$. This is due to the fact that eventually we want to take the continuum limit $k \rightarrow \infty$ in which $m_{k-1} - 1 \rightarrow 0$, and we only want to keep the leading order. The factor $1/4$ in the second line comes from the symmetrization of the derivative. We therefore obtain the result for the replicon eigenvalue in the continuum limit

$$\lambda_R = \frac{4}{m(m_{k-1} - 1)} \frac{2}{d} \frac{\partial^2 s}{\partial \widehat{\Delta}_k^2} = \frac{4}{m(m_{k-1} - 1)} \frac{\partial^2}{\partial \widehat{\Delta}_k^2} \left[\log \det(\hat{\alpha}^{m,m}) - \widehat{\varphi} \mathcal{F}(\widehat{\Delta}) \right] . \quad (219)$$

For the first term (the entropic term) we use the k RSB expression given in Eq. (39). We have

$$\frac{\partial}{\partial \widehat{\Delta}_k} \log \det(\hat{\alpha}^{m,m}) = \frac{1}{\widehat{\Delta}_k} \left(\frac{m}{m_k} - \frac{m}{m_{k-1}} \right) + O((m_{k-1} - 1)^2) \quad (220)$$

and

$$\frac{\partial^2}{\partial \widehat{\Delta}_k^2} \log \det(\hat{\alpha}^{m,m}) = -\frac{1}{\widehat{\Delta}_k^2} \left(\frac{m}{m_k} - \frac{m}{m_{k-1}} \right) + O((m_{k-1} - 1)^2) , \quad (221)$$

so that the contribution to the replicon of the entropic term is in the continuum limit (remember that $m_k = 1$ and $m_{k-1} \rightarrow 1$):

$$\lambda_R^{(E)} = -\frac{4}{\Delta(1)^2} . \quad (222)$$

We have now to compute the interaction part of the replicon eigenvalue. This can be done following exactly the same lines of Sec. IV A. The result is

$$\begin{aligned} \lambda_R^{(I)} &= 2 \int_{-\infty}^{\infty} dh e^h \frac{d}{dh} \left[\gamma_{-\widehat{\Delta}_1} \star \left[P(1, h) \left[\frac{(g''(1, h))^2}{g^2(1, h)} - 2 \frac{(g'(1, h))^2 g''(1, h)}{g^3(1, h)} + \frac{(g'(1, h))^4}{g^4(1, h)} \right] \right] \right] \\ &= 2 \int_{-\infty}^{\infty} dh e^h \gamma_{-\widehat{\Delta}_1} \star \left[\frac{d}{dh} \left[P(1, h) (f''(1, h))^2 \right] \right] = -2 \int_{-\infty}^{\infty} dh e^h \widehat{P} \left(\frac{1}{m}, h \right) (f''(1, h))^2 . \end{aligned} \quad (223)$$

Putting all the pieces together, we obtain

$$\lambda_R = -\frac{4}{\Delta(1)^2} + 2\widehat{\varphi} \int dh e^h \widehat{P} \left(\frac{1}{m}, h \right) (f''(1, h))^2 . \quad (224)$$

By using the fact that $\Delta(1) = m\gamma(1/m)$, and $f(1, h) = \widehat{f}(1/m, h)/m$ we can rewrite this expression in the following form

$$\lambda_R = -\frac{4}{m^2 \gamma(1/m)^2} \left[1 - \frac{\widehat{\varphi}}{2} \gamma(1/m)^2 \int_{-\infty}^{\infty} dh e^h \widehat{P}(1/m, h) \widehat{f}''(1/m, h)^2 \right] . \quad (225)$$

Eq. (193) with $y = 1/m$ therefore implies that $\lambda_R = 0$ everywhere in the fullRSB phase, which shows the marginal stability of the fullRSB solution. This result is important because we have shown in the previous sections that Eq. (193) is the key ingredient to obtain the critical exponents at jamming. This means that the marginal stability of the fullRSB solution plays a prominent role in characterizing the properties of the jamming transition.

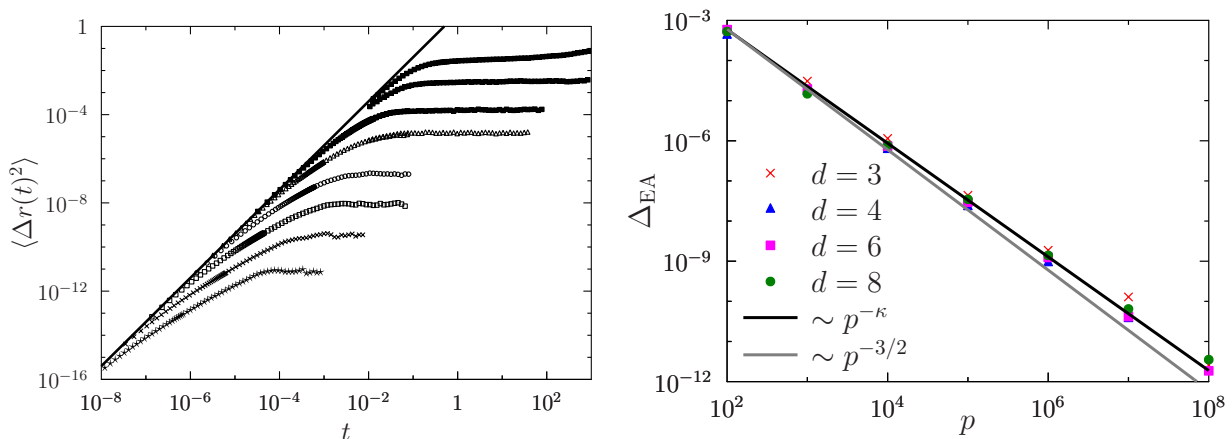


FIG. 13: (Left) Time evolution of the mean-square displacement in the equilibrated liquid at $\varphi = 0.405$ as well as in the glass for different $p = 10^2$ – 10^8 . (Right) Pressure evolution of the Debye-Waller factor Δ_{EA} in $d = 3, 4, 6, 8$. The black line is a power-law with exponent κ given by Eq. (200). For comparison, we also show a power-law $p^{-3/2}$ as a grey line.

XIII. COMPARISON WITH RESULTS OF MOLECULAR DYNAMICS SIMULATIONS IN FINITE DIMENSIONS

The scaling of the fullRSB solution provides a number of predictions for the critical scaling at the jamming transition. It predicts that packings are isostatic with average contact number $z = 2d$, that the cage radius scales as $\Delta_{EA} \sim p^{-\kappa}$, that the correlation function at jamming diverges on approaching contact as $(r - D)^{-\alpha}$, that the contact peak of the correlation function, on approaching jamming, has a scaling form given by Eq. (210) (see also [11]) with a scaling function $\mathcal{F}_\infty(\lambda) \sim \lambda^{-2-\theta}$ at large λ , and that the force distribution is characterized by $P_\infty(f) \sim f^\theta$ for small f . The exponents κ, α, θ are given in Eq. (200).

Some of these predictions have already been verified in the past using molecular dynamics simulation. In particular isostaticity is a well-known property of jammed packings (see [11, 46, 72] for reviews). Also, the exponent α in $g(r) \sim (r - D)^{-\alpha}$ has been independently measured with good precision by a number of groups [27, 28, 44, 73, 74] and its mostly accepted value $\alpha \approx 0.42$ is perfectly compatible with the prediction in Eq. (200).

The scaling of $\Delta_{EA} \sim p^{-\kappa}$ has been studied in [21–23, 26] and the data were found to be compatible with $\kappa = 3/2$, which is slightly different from our prediction, and had been proposed in [20, 23] using a scaling argument based on marginal stability. To check whether the numerical data are also compatible with our prediction for κ , we performed additional molecular dynamics simulations. Hard-sphere systems in $d=3, 4, 6$, and 8 with $N=8000$ particles are simulated under periodic boundary conditions using a modified version of the event-driven molecular dynamics code described in Refs. [12, 13, 73]. We consider monodisperse spheres with unit mass and unit diameter D and unit mass m , hence time is expressed in units of $\sqrt{\beta m D^2}$ at fixed unit inverse temperature β . Hard sphere glasses are obtained using a Lubachevski-Stillinger algorithm initiated in the low-density fluid state with a slow growth rate $\dot{\gamma} = 3 \times 10^{-4}$. The fluid then falls out of equilibrium near the dynamical transition. Using these configurations, the mean-square displacement $\langle \Delta r^2(t) \rangle = \langle 1/N \sum_i [r_i(t) - r_i(0)]^2 \rangle$ is obtained, and reported in Fig. 13. The rattlers, which are identified as the particles having fewer than $d + 1$ contacts at $p = 10^{10}$ (following Ref. [27]), are removed when analyzing systems at $p \gtrsim 10^5$. The long-time mean square displacement plateau provides $\langle \Delta r^2(t \rightarrow \infty) \rangle = d \Delta_{EA}$, where the Debye-Waller factor Δ_{EA} is an estimate of the average cage size in the glass [13]. Using this approach, we find that in all dimensions the exponent κ is close to $3/2$, but the data are better described by our predicted value of κ , see Fig. 13. Note that the theoretical prediction is that $\Delta_{EA} = \hat{\Delta}_{EA}/d^2$ should decrease as d^2 (at fixed $\hat{\varphi}$), while in Fig. 13 we see that Δ_{EA} is roughly independent of dimension in the range of d we investigated. This discrepancy is probably due to the fact that the numerically investigated dimensions are quite far from the asymptotic $d \rightarrow \infty$ limit (as far as prefactors are concerned), as it has been already noted in [12, 13]. An approximate analytical computation of the prefactor Δ_∞ of the $p^{-\kappa}$ scaling in finite d is certainly possible and would shed light on this issue.

The measure of the exponent θ is more problematic. In fact, previous attempts at measuring θ using different techniques reported results in the range $0.2 \div 0.45$ [27, 28]. In [28] it has been shown that the behavior of the force distribution $P(f)$ at small forces is dominated by two different ways in which the force network responds to an external perturbation: extended modes and local buckling modes. According to the results of [28, 43], extended modes give an exponent $\theta_e = 1/\alpha - 2$, which perfectly agrees with our results given in Eq. (200). Buckling modes, instead, give

an exponent $\theta_b = 1 - 2\alpha$ and using the value of α predicted by our theory in Eq. (200), one obtains $\theta_b = 0.17462$, which agrees with the numerical value reported in [28, 43]. According to the analysis of [28], in presence of both modes the force distribution is dominated by the smallest exponent, hence $\theta = \min\{\theta_b, \theta_e\} = 0.17462$ is the value that enters in $P(f)$. However, in our approach we do not see any trace of the buckling modes and $P(f)$ is characterized by the exponent θ associated with extended modes. This is probably due to the fact that buckling modes disappear in large dimensions, similarly to what happens to rattlers [27]. A careful numerical investigation of this effect would be important.

XIV. CONCLUSIONS

We have derived the fullRSB equations that describe infinite-dimensional hard spheres (and, *en passant*, more general potentials). We have shown that a marginal fullRSB phase exists at high pressure and that it correctly *predicts* isostaticity and the critical exponents κ, α, θ associated with the jamming transition, unlike the 1RSB solution. The predicted values of the exponents are given in Eq. (200). These predictions have been reviewed and compared with numerical simulations in Sec. XIII.

Of course, a lot of work is still needed to understand and characterize this phase. Let us summarize a certain number of research directions that should be explored in the near future:

- The exponents κ , α and θ recently attracted a lot of attention because they are related to the marginal mechanical stability of the packing in real space [20, 25, 28, 43, 75]. Furthermore, the analysis of [25, 28, 43] predicts two scaling relations, $\alpha = 1/(2 + \theta)$ and $\kappa = 2 - 2/(3 + \theta)$, that are exactly verified by our predicted exponents, see Eq. (200). Within the present approach, the critical regime around jamming emerges as a consequence of a marginal stability in phase space, a consequence of the vanishing of the replicon eigenvalue of the fullRSB solution [30, 40]. The scaling relations $\alpha = 1/(2 + \theta)$ and $\kappa = 2 - 2/(3 + \theta)$ can be derived from Eq. (168), using $b = (1 + c)/2$ (which we proved) and $a + b = 1$, a relation that we were not able to prove but holds within arbitrary numerical precision, see Eq. (200). It seems therefore that our approach, based on phase-space marginality, and the approach of [25, 28, 43], based on marginal mechanical stability, are intimately related, and making this connection more explicit would be extremely interesting.
- In [28] it was claimed that another exponent θ_b , associated to local buckling modes, controls the behavior of the small force distribution, and this exponent is smaller than θ and verifies a different scaling relation, see the discussion in Sec. XIII. Yet we do not see any trace of the exponent θ_b in our $d = \infty$ solution. Clarifying this point is therefore of crucial importance. It might be possible that the modes leading to the exponent θ_b disappear in the limit $d \rightarrow \infty$. This could be checked through numerical simulations.
- An important technical issue is to perform a state following calculation [57, 76]. Such a computation would allow one to compute the Gardner transition and the fullRSB phase for a given glass phase, which would facilitate the comparison with numerical simulations.
- Following [47–49], one can hope to compute exactly the shear modulus, which is another important observable showing anomalous scaling at the jamming transition [18, 77]. This is particularly interesting in light of the recent numerical results of [78], which show some possible direct observations of fullRSB effects.
- It could be possible to compute the distribution of avalanche sizes, following [50], who performed a similar computation in the Sherrington-Kirkpatrick model.
- Although in this paper we focused only on hard spheres, the computations can be easily extended to soft spheres, in order to study the complete scaling on both sides of the jamming transition [14, 26]. A preliminary and incomplete account of this extension is reported in Appendix A. It would also be interesting to check what is the temperature scale of the Gardner transition in thermal systems.
- The results should be extended to finite dimensional systems (still within a mean-field approximation) by using the effective potential approximation scheme of [11, 14]. This would be extremely important, as it would allow one to compute precise numbers (e.g. for the distribution of mean-square displacements among different states) to be compared with numerical simulations and experiments.
- It would be very important to understand how truly finite dimensional corrections around the mean field approximation, i.e. critical fluctuations in a renormalization group approach, affect the scenario proposed in this paper. Some attempts to study this problem have been made e.g. in [79–81].

- The most important point is, however, the study of the off-equilibrium dynamics, that is still poorly understood in presence of fullRSB effects even in spin glass models [31–33]. In this paper, we assumed that, since fullRSB seems to characterize all glasses at high enough pressure, it will be present in whatever state is reached by the off-equilibrium dynamics. However, how this is realized precisely, and which are the dynamical signatures of fullRSB in the context of structural glasses, remains an open problem.

Acknowledgments

We are very indebted to Silvio Franz for an extremely useful discussion about the recursive procedure to write the replicated free energy in the Sherrington-Kirkpatrick model; to Carolina Brito, Eric DeGiuli, Edan Lerner and Matthieu Wyart, for many important exchanges related to their work [28, 43], and for sharing with us unpublished material, that was particularly useful to detect an error in the original version of Appendix A; and to Florent Krzakala, Federico Ricci-Tersenghi, and Tommaso Rizzo for many important discussions on the Gardner transition and fullRSB equations in the p -spin model, including their numerical resolution, that settled the basis for this work. We also very warmly thank Ludovic Berthier, Giulio Biroli, and Hajime Yoshino for many interesting exchanges related to this work.

P.U. acknowledges the Physics Department of the University of Rome “La Sapienza” and the Laboratoire de Physique Théorique et Modèles Statistiques of the University of Paris-Sud 11 where part of this work has been done.

Financial support was provided by the European Research Council through ERC grant agreement no. 247328 and ERC grant NPRGGLASS. PC acknowledges Sloan Foundation support.

Appendix A: Extension to soft spheres

We consider a system of soft spheres interacting through the potential $v(r) = \epsilon(1 - |r|/D)^2\theta(1 - |r|/D)$. Introducing $h = d(|r| - D)/D$ we have

$$e^{-\beta v(r)} = e^{-\beta\epsilon(1-|r|/D)^2\theta(1-|r|/D)} = e^{-(\beta\epsilon/d^2)h^2\theta(-h)} = e^{-\hat{\beta}h^2\theta(-h)} = e^{-\hat{v}(h)}, \quad (\text{A1})$$

where we introduced a scaled temperature $\hat{\beta} = \beta\epsilon/d^2$. Note that if we want to keep $\hat{\beta}$ finite, we have $\beta\epsilon \sim d^2$ hence the soft sphere system is effectively at a very low temperature; for this reason the soft sphere system is close to a hard sphere one and neglecting higher order virial diagrams is correct as in the case of hard spheres. The equations for soft spheres have been derived in Sec. V: they are identical to Eq. (113), with only a difference in the initial condition for $\hat{f}(y, h)$, which can be deduced from Eq. (102) and becomes¹¹:

$$g(m_k, h) = \gamma_{\hat{\Delta}_k} \star e^{-\hat{v}(h)}, \quad \hat{f}(y_k, h) = m \log \gamma_{m\hat{\gamma}_k} \star e^{-\hat{v}(h)}. \quad (\text{A2})$$

The effective potential in Eq. (108), similarly to Eq. (201), has the following expression:

$$e^{-\phi_{\text{eff}}(h)} = e^{-\hat{v}(h)} \int_{-\infty}^{\infty} dz e^{z-h} \gamma_{\hat{\Delta}_k}(h-z) \frac{e^{-z-\hat{\Delta}_1/2} P(m_k, z)}{g(m_k, z)} = e^{-\hat{v}(h)} \int_{-\infty}^{\infty} dz \frac{\gamma_{\hat{\Delta}_k}(h+\hat{\Delta}_k-z)}{\gamma_{m\hat{\gamma}_k} \star e^{-\hat{v}(z)}} \hat{P}(y_k, z) e^{\hat{\Delta}_k/2}. \quad (\text{A3})$$

In the case of soft spheres, the jamming limit can be approached from above by an appropriate scaling of the parameters [14]. First, the zero-temperature soft sphere limit is obtained by letting $m \rightarrow 0$ with $\hat{T} = 1/\hat{\beta} = m\tau$ and fixed τ . After this limit has been taken, the jamming point is approached from above by letting $\tau \rightarrow 0$.

1. The zero temperature limit

We now focus on the zero-temperature soft sphere limit. To take this limit we have to compute

$$\hat{f}(y_k, h) = m \log \gamma_{m\hat{\gamma}_k} \star e^{-\hat{\beta}h^2\theta(-h)} \quad (\text{A4})$$

¹¹ Remember that according to our definitions, $m_k = 1$, $\hat{\Delta}_k = m\hat{\gamma}_k$, $y_k = m_k/m = 1/m$, and $\hat{f}(y_k, h) = y_k^{-1} \log g(m_k, h)$.

in the limit where $m \rightarrow 0$ and $\hat{\beta} = 1/(m\tau)$. Note that it is natural to assume that $\hat{\gamma}_k$ remains finite in this limit: therefore, $\Delta_{\text{EA}} = \hat{\Delta}_k \sim m \sim T$ vanishes proportionally to temperature, as found numerically in [26]. We have

$$\gamma_{m\hat{\gamma}_k} \star e^{-\hat{\beta}h^2\theta(-h)} = \int_{-\infty}^{\infty} dz \frac{e^{-\frac{(h-z)^2}{2m\hat{\gamma}_k} - \frac{1}{m\tau}z^2\theta(-z)}}{\sqrt{2\pi m\hat{\gamma}_k}} \quad (\text{A5})$$

which for $m \rightarrow 0$ can be evaluated by a saddle-point. For $h > 0$, the saddle point is $z^* = h > 0$, while for $h < 0$ it is $z^* = h/(1 + 2\hat{\gamma}_k/\tau) < 0$. In both cases therefore the integral is strongly peaked around z^* . Because the integral is quadratic, computing the corrections to the saddle point is equivalent to replacing $\theta(-z)$ with $\theta(-h)$, and we obtain

$$\gamma_{m\hat{\gamma}_k} \star e^{-\hat{\beta}h^2\theta(-h)} \sim \int_{-\infty}^{\infty} dz \frac{e^{-\frac{(h-z)^2}{2m\hat{\gamma}_k} - \frac{1}{m\tau}z^2\theta(-h)}}{\sqrt{2\pi m\hat{\gamma}_k}} = \begin{cases} e^{-\frac{1}{m(2\hat{\gamma}_k+\tau)}h^2} \left(1 + \frac{2\hat{\gamma}_k}{\tau}\right)^{-1/2} & \text{for } h < 0 \\ 1 & \text{for } h > 0 \end{cases} \quad (\text{A6})$$

For $m \rightarrow 0$, one therefore obtains

$$\hat{f}(y_k, h) = -\frac{1}{2\hat{\gamma}_k + \tau} h^2 \theta(-h) . \quad (\text{A7})$$

This is therefore the appropriate initial condition for $\hat{f}(y_k, h)$ for soft spheres at $T = 0$. Note that the asymptotic behavior is therefore modified with respect to the hard sphere case. As in hard spheres, inserting these asymptotes in the evolution equation for $\hat{f}(y_i, h)$, one can show that Eq. (110) becomes

$$\hat{f}(y_i, h \rightarrow -\infty) \sim -\frac{h^2}{2\hat{\gamma}_i + \tau} . \quad (\text{A8})$$

The correct definition of $\hat{j}(y_i, h)$ is therefore

$$\hat{f}(y_i, h) = -\frac{h^2\theta(-h)}{2\hat{\gamma}_i + \tau} + \hat{j}(y_i, h) . \quad (\text{A9})$$

It is also convenient to define $\hat{\gamma}_i^\tau = \hat{\gamma}_i + \tau/2$. Then Eqs. (113) become, recalling that $y_k = 1/m$ is formally infinite:

$$\begin{aligned} \mathcal{S}_{\text{kRSB}} &= \sum_{i=1}^k \left(\frac{1}{y_i} - \frac{1}{y_{i-1}} \right) \log(\hat{\gamma}_i^\tau - \tau/2) - \hat{\varphi} e^{-\hat{\Delta}_1/2} \int_{-\infty}^{\infty} dh e^h \left\{ 1 - e^{-\frac{h^2\theta(-h)}{2\hat{\gamma}_1^\tau} + \hat{j}(y_1, h)} \right\} , \\ \hat{\Delta}_i &= \frac{\hat{\gamma}_i^\tau}{y_i} + \sum_{j=i+1}^k \left(\frac{1}{y_j} - \frac{1}{y_{j-1}} \right) \hat{\gamma}_j^\tau , \\ \hat{j}(y_k, h) &= 0 , \\ \hat{j}(y_i, h) &= \frac{1}{y_i} \log \left[\int_{-\infty}^{\infty} dz K_{\hat{\gamma}_i^\tau, \hat{\gamma}_{i+1}^\tau, y_i}(h, z) e^{y_i \hat{j}(y_{i+1}, z)} \right] , \quad i = 1 \dots k-1 , \\ \hat{P}(y_1, h) &= e^{-\hat{\Delta}_1/2 - \frac{h^2\theta(-h)}{2\hat{\gamma}_1^\tau} + \hat{j}(y_1, h)} , \\ \hat{P}(y_i, h) &= \int dz K_{\hat{\gamma}_{i-1}^\tau, \hat{\gamma}_i^\tau, y_{i-1}}(z, h) \hat{P}(y_{i-1}, z) e^{z-h} e^{-y_{i-1} \hat{j}(y_{i-1}, z) + y_{i-1} \hat{j}(y_i, h)} \quad i = 2, \dots, k , \\ \hat{\kappa}_i &= \frac{\hat{\varphi}}{2} \int_{-\infty}^{\infty} dh e^h \hat{P}(y_i, h) \left(-\frac{h\theta(-h)}{\hat{\gamma}_i^\tau} + \hat{j}(y_i, h) \right)^2 , \\ \frac{1}{\hat{\gamma}_i^\tau - \tau/2} &= y_{i-1} \hat{\kappa}_i - \sum_{j=1}^{i-1} (y_j - y_{j-1}) \hat{\kappa}_j , \end{aligned} \quad (\text{A10})$$

where the kernel K is the same as the one for hard spheres given in Eq. (114). We notice that, in terms of $\hat{\gamma}_i^\tau$, these equations are almost identical to the ones of hard spheres, except for slight modifications to the first and last equations. When $\tau = 0$, the equations correctly give back the HS equations for $m \rightarrow 0$ [14, 27]. In the continuum

limit the equations above become

$$\begin{aligned}
\mathcal{S}_{\infty\text{RSB}} &= - \int_1^\infty \frac{dy}{y^2} \log \left[\gamma_\tau(y) - \frac{\tau}{2} \right] - \widehat{\varphi} e^{-\Delta(1)/2} \int_{-\infty}^\infty dh e^h [1 - e^{-\frac{h^2 \theta(-h)}{2\widehat{\gamma}_\tau(1)} + \widehat{j}(1,h)}] , \\
\Delta(y) &= \frac{\gamma_\tau(y)}{y} - \int_y^\infty \frac{dz}{z^2} \gamma_\tau(z) , \quad \Leftrightarrow \quad \gamma_\tau(y) = y\Delta(y) + \int_y^\infty dz \Delta(z) , \\
\lim_{y \rightarrow \infty} \widehat{j}(y, h) &= 0 , \\
\frac{\partial \widehat{j}(y, h)}{\partial y} &= \frac{1}{2} \frac{\dot{\gamma}_\tau(y)}{y} \left[-\frac{\theta(-h)}{\gamma_\tau(y)} + \frac{\partial^2 \widehat{j}(y, h)}{\partial h^2} - 2y \frac{h\theta(-h)}{\gamma_\tau(y)} \frac{\partial \widehat{j}(y, h)}{\partial h} + y \left(\frac{\partial \widehat{j}(y, h)}{\partial h} \right)^2 \right] , \\
\widehat{P}(1, h) &= e^{-\Delta(1)/2 - \frac{h^2 \theta(-h)}{2\widehat{\gamma}_\tau(1)} + \widehat{j}(1,h)} , \\
\frac{\partial \widehat{P}(y, h)}{\partial y} &= -\frac{1}{2} \frac{\dot{\gamma}_\tau(y)}{y} e^{-h} \left\{ \frac{\partial^2 [e^h \widehat{P}(y, h)]}{\partial h^2} - 2y \frac{\partial}{\partial h} \left[e^h \widehat{P}(y, h) \left(-\frac{h\theta(-h)}{\gamma_\tau(y)} + \frac{\partial \widehat{j}(y, h)}{\partial h} \right) \right] \right\} , \\
\kappa(y) &= \frac{\widehat{\varphi}}{2} \int_{-\infty}^\infty dh e^h \widehat{P}(y, h) \left(-\frac{h\theta(-h)}{\gamma_\tau(y)} + \widehat{j}'(y, h) \right)^2 , \\
\frac{1}{\gamma_\tau(y) - \frac{\tau}{2}} &= y\kappa(y) - \int_1^y dz \kappa(z) .
\end{aligned} \tag{A11}$$

Using these equations it is possible to derive the marginal stability condition also in the soft sphere case. We can derive the equation for $\kappa(y)$ in terms of \widehat{P} with respect to y to get

$$\left(\frac{\gamma_\tau(y)}{\gamma_\tau(y) - \tau/2} \right)^2 = \frac{\widehat{\varphi}}{2} \int_{-\infty}^\infty dh e^h \widehat{P}(y, h) \widetilde{f}''(y, h)^2 , \tag{A12}$$

where $\widetilde{f}(y, h) = \gamma_\tau(y) \widehat{f}(y, h)$. Note that again, this equation holds only if there is a domain where $\gamma_\tau(y)$ is not piecewise constant, namely where a fullRSB solution is present. By deriving again this equation with respect to y we get

$$-\tau \frac{\gamma_\tau^2(y)}{(\gamma_\tau(y) - \frac{\tau}{2})^3} = \frac{\widehat{\varphi}}{2} \int dh e^h \widehat{P}(y, h) \left[2 \left(\widetilde{f}''(y, h)^2 + \widetilde{f}'''(y, h)^3 \right) - \frac{\gamma_\tau(y)}{y} \widetilde{f}'''(y, h)^2 \right] , \tag{A13}$$

that can be rewritten as

$$y = \frac{1}{2} \gamma_\tau(y) \frac{\int dh e^h \widehat{P}(y, h) \widetilde{f}'''(y, h)^2}{\frac{\tau}{\widehat{\varphi}} \frac{\gamma_\tau^2(y)}{(\gamma_\tau(y) - \frac{\tau}{2})^3} + \int dh e^h \widehat{P}(y, h) \widetilde{f}''(y, h)^2 \left[1 + \widetilde{f}''(y, h) \right]} . \tag{A14}$$

The above equation can be seen as an equation for the breaking points of the fullRSB profile of $\gamma_\tau(y)$.

It is interesting to compute the effective potential (A3) in the limit $m \rightarrow 0$. Using Eq. (A6), and with similar manipulations, we obtain

$$e^{-\phi_{\text{eff}}(h)} = \begin{cases} e^{-\frac{1}{m\tau} h^2} \int_{-\infty}^\infty dz \frac{e^{-\frac{(h-z+m\widehat{\gamma}_k)^2}{2m\widehat{\gamma}_k} + \frac{1}{m} \frac{z^2}{2\widehat{\gamma}_k + \tau}}}{\sqrt{2\pi m \tau \widehat{\gamma}_k / (\tau + 2\widehat{\gamma}_k)}} \widehat{P}(y_k, z) \sim \left(1 + \frac{2\widehat{\gamma}_k}{\tau} \right) e^{\frac{2\widehat{\gamma}_k}{\tau} h} \widehat{P} \left[y_k, h \left(1 + \frac{2\widehat{\gamma}_k}{\tau} \right) \right] & \text{for } h < 0 \\ \int_{-\infty}^\infty dz \frac{e^{-\frac{(h-z+m\widehat{\gamma}_k)^2}{2m\widehat{\gamma}_k}}}{\sqrt{2\pi m \widehat{\gamma}_k}} \widehat{P}(y_k, z) \sim \widehat{P}(y_k, h) & \text{for } h > 0 \end{cases} \tag{A15}$$

From this result, we can compute the number of contacts using Eq. (213). For soft spheres, all particles with $h < 0$ are in contact, and we have

$$z = d\widehat{\varphi} \int_{-\infty}^0 dh e^h e^{-\phi_{\text{eff}}(h)} = d\widehat{\varphi} \left(1 + \frac{2\widehat{\gamma}_k}{\tau} \right) \int_{-\infty}^0 dh e^{\left(1 + \frac{2\widehat{\gamma}_k}{\tau} \right) h} \widehat{P} \left[y_k, h \left(1 + \frac{2\widehat{\gamma}_k}{\tau} \right) \right] = d\widehat{\varphi} \int_0^\infty dt e^{-t} \widehat{P} [y_k, -t] . \tag{A16}$$

2. The jamming limit and the force distribution

It is natural to expect that away from jamming (a small) τ acts as a cutoff for the scalings of Sec. IX, like m for hard spheres. We assume therefore that all the scalings of Sec. IX hold, but with a cutoff at $y_{\max}(\tau)$. In the limit $\tau \rightarrow 0$, the cutoff must diverge to recover the jamming physics.

For soft spheres, the inter-particle force is $f = 2\frac{\epsilon}{D}(1 - |r|/D) = -\frac{2\epsilon}{dD}h$ for $h < 0$. Let us rescale the forces by a factor $\frac{dD}{2\epsilon}$ in such a way that $f = -h$ exactly. In any case we are not interested in the prefactors in the overall scaling of forces. Then the probability distribution of forces is, following [27] and recalling that $f \geq 0$:

$$P(f) = \frac{e^{-f - \phi_{\text{eff}}(-f)}}{\int_0^\infty df' e^{-f' - \phi_{\text{eff}}(-f')}} . \quad (\text{A17})$$

Using Eq. (A15), we then obtain

$$P(f) \propto e^{-f\left(1 + \frac{2\hat{\gamma}_k}{\tau}\right)} \hat{P}\left[y_k, -f\left(1 + \frac{2\hat{\gamma}_k}{\tau}\right)\right] . \quad (\text{A18})$$

In the jamming limit $\tau \rightarrow 0$, we expect that $\hat{\gamma}_k \sim \gamma_\infty y_{\max}^{-c}$ and $\hat{P}(y_k, h) \propto y_{\max}^c p_0(h y_{\max}^c)$. Note that we also have

$$\Delta_{\text{EA}} = \hat{\Delta}_k = m\hat{\gamma}_k = \frac{T}{\tau} \gamma_\infty y_{\max}^{-c} . \quad (\text{A19})$$

We also must assume that $\hat{\gamma}_k/\tau \sim \gamma_\infty y_{\max}(\tau)^{-c}/\tau$ diverges for $\tau \rightarrow 0$, because Δ_{EA}/T must diverge on approaching jamming to match with the hard sphere regime. Therefore

$$P(f) \propto e^{-f\frac{2\hat{\gamma}_k}{\tau}} \hat{P}\left[y_k, -f\frac{2\hat{\gamma}_k}{\tau}\right] \propto e^{-f\frac{2\gamma_\infty y_{\max}^{-c}}{\tau}} p_0\left(-f\frac{2\gamma_\infty y_{\max}^{-c}}{\tau} y_{\max}^c\right) = e^{-f\frac{2\gamma_\infty y_{\max}^{-c}}{\tau}} p_0\left(-f\frac{2\gamma_\infty}{\tau}\right) \sim p_0\left(-f\frac{2\gamma_\infty}{\tau}\right) \quad (\text{A20})$$

where the exponential factor can be neglected in the last step because the natural scale of forces is $f \sim \tau$. This is correct because the pressure scales as τ [14].

It is customary in the literature to scale the forces in such a way that the average force is 1. We have for the average force in the limit $\tau \rightarrow 0$

$$\bar{f} = \frac{\int_0^\infty df f p_0\left(-f\frac{2\gamma_\infty}{\tau}\right)}{\int_0^\infty df p_0\left(-f\frac{2\gamma_\infty}{\tau}\right)} = \frac{\tau \int_0^\infty dt t p_0(-t)}{2\gamma_\infty \int_0^\infty dt p_0(-t)} = \frac{\tau}{2\gamma_\infty} \bar{t} \quad (\text{A21})$$

Defining therefore a scaled force $\hat{f} = f\frac{2\gamma_\infty}{\tau}$, we have for the scaled distribution

$$P(\hat{f}) = \frac{p_0(-\hat{f}\bar{t})}{\int_0^\infty d\hat{f} p_0(-\hat{f}\bar{t})} = \frac{p_0(-\hat{f}\bar{t})}{\int_0^\infty d\hat{f} \hat{f} p_0(-\hat{f}\bar{t})} , \quad (\text{A22})$$

which confirms the validity of Eqs. (209) and (210). Note that from Eq. (A16) we find that also jammed soft spheres are isostatic. In fact, for $\tau \rightarrow 0$,

$$z = d\hat{\varphi} \int_0^\infty dt e^{-t} \hat{P}[y_k, -t] \sim d\hat{\varphi} \int_0^\infty dt e^{-t} y_{\max}^{-c} p_0(-t y_{\max}^{-c}) \sim d\hat{\varphi} \int_0^\infty dt p_0(-t) = 2d . \quad (\text{A23})$$

Actually, using Eq. (193) and Eq. (198), we can also compute the scaling of the corrections to this result:

$$\begin{aligned} \frac{z}{2d} &= \frac{\hat{\varphi}}{2} \int_0^\infty dt e^{-t} \hat{P}[y_k, -t] = \frac{\hat{\varphi}}{2} \int_{-\infty}^\infty dh e^h \hat{P}[y_k, h] [\theta(-h) + \tilde{f}''(y_k, h)^2 - \tilde{f}'(y_k, h)^2] \\ &= 1 + \frac{\hat{\varphi}}{2} \int_{-\infty}^\infty dh e^h \hat{P}[y_k, h] [\theta(-h) - \tilde{f}''(y_k, h)^2] = 1 + \frac{\hat{\varphi}}{2} \int_{-\infty}^\infty dh e^h \hat{P}[y_k, h] \left[-\frac{c^2}{4} J''(hy_k^b)^2 - cJ''(hy_k^b)\theta(-h)\right] \\ &= 1 + \frac{\hat{\varphi}}{2} \int_{-\infty}^\infty dh e^h y_k^a p_1(hy_k^b) \left[-\frac{c^2}{4} J''(hy_k^b)^2 - cJ''(hy_k^b)\theta(-h)\right] = 1 + y_k^{a-b} \frac{\hat{\varphi}}{2} \int_{-\infty}^\infty dt p_1(t) \left[-\frac{c^2}{4} J''(t)^2 - cJ''(t)\theta(-t)\right] . \end{aligned} \quad (\text{A24})$$

Therefore, we conclude that $\delta z = z - 2d \propto y_{\max}^{a-b} = y_{\max}^{-c}$, using the relations $b = (1+c)/2$ and $a = 1 - b = (1-c)/2$.

From this analysis we conclude that the pressure $P \propto \tau$, that the cutoff is such that $y_{\max}^{-c} \propto \delta z$, and that

$$\Delta_{\text{EA}} \propto \frac{T}{P} \delta z. \quad (\text{A25})$$

Note that we expect that pressure scales linearly in $\delta\hat{\varphi} = \hat{\varphi} - \hat{\varphi}_j$, hence also $\tau \propto P \propto \delta\hat{\varphi}$. The scaling of $y_{\max}(\tau)$ remains however undetermined from this analysis. If we assume that $y_{\max} \sim \tau^{-\nu} \sim \delta\hat{\varphi}^{-\nu}$, then we have $\delta z = \delta\hat{\varphi}^{c\nu}$ and $\Delta_{\text{EA}} \sim T\delta\hat{\varphi}^{-1+c\nu}$. We note that the choice $\nu c = 1/2$ allows us to recover the scaling of [43], i.e. $\delta z = \delta\hat{\varphi}^{1/2}$ and $\Delta_{\text{EA}} \sim T\delta\hat{\varphi}^{-1/2}$.

-
- [1] J. Kurchan, G. Parisi, and F. Zamponi, *Journal of Statistical Mechanics: Theory and Experiment* **2012**, P10012 (2012).
- [2] J. Kurchan, G. Parisi, P. Urbani, and F. Zamponi, *J. Phys. Chem. B* **117**, 12979 (2013).
- [3] T. R. Kirkpatrick and P. G. Wolynes, *Phys. Rev. B* **36**, 8552 (1987).
- [4] T. R. Kirkpatrick and D. Thirumalai, *Phys. Rev. A* **37**, 4439 (1988).
- [5] T. R. Kirkpatrick, D. Thirumalai, and P. G. Wolynes, *Phys. Rev. A* **40**, 1045 (1989).
- [6] P. Wolynes and V. Lubchenko, eds., *Structural Glasses and Supercooled Liquids: Theory, Experiment, and Applications* (Wiley, 2012).
- [7] T. R. Kirkpatrick and D. Thirumalai, *Journal of Physics A: Mathematical and General* **22**, L149 (1989).
- [8] R. Monasson, *Phys. Rev. Lett.* **75**, 2847 (1995).
- [9] M. Mézard and G. Parisi, *The Journal of Chemical Physics* **111**, 1076 (1999).
- [10] M. Mezard and G. Parisi, in *Structural Glasses and Supercooled Liquids: Theory, Experiment and Applications*, edited by P. G. Wolynes and V. Lubchenko (Wiley & Sons, 2012), [arXiv:0910.2838](https://arxiv.org/abs/0910.2838).
- [11] G. Parisi and F. Zamponi, *Rev. Mod. Phys.* **82**, 789 (2010).
- [12] P. Charbonneau, A. Ikeda, G. Parisi, and F. Zamponi, *Phys. Rev. Lett.* **107**, 185702 (2011).
- [13] P. Charbonneau, A. Ikeda, G. Parisi, and F. Zamponi, *Proceedings of the National Academy of Sciences* **109**, 13939 (2012).
- [14] L. Berthier, H. Jacquin, and F. Zamponi, *Phys. Rev. E* **84**, 051103 (2011).
- [15] C. F. Moukarzel, *Phys. Rev. Lett.* **81**, 1634 (1998).
- [16] A. V. Tkachenko and T. A. Witten, *Phys. Rev. E* **60**, 687 (1999).
- [17] J.-N. Roux, *Phys. Rev. E* **61**, 6802 (2000).
- [18] C. S. O'Hern, S. A. Langer, A. J. Liu, and S. R. Nagel, *Phys. Rev. Lett.* **88**, 075507 (2002).
- [19] C. S. O'Hern, L. E. Silbert, A. J. Liu, and S. R. Nagel, *Phys. Rev. E* **68**, 011306 (2003).
- [20] M. Wyart, L. Silbert, S. Nagel, and T. Witten, *Physical Review E* **72**, 051306 (2005).
- [21] C. Brito and M. Wyart, *Europhysics Letters (EPL)* **76**, 149 (2006).
- [22] C. Brito and M. Wyart, *Journal of Statistical Mechanics: Theory and Experiment* **2007**, L08003 (2007).
- [23] C. Brito and M. Wyart, *The Journal of Chemical Physics* **131**, 024504 (2009).
- [24] A. Liu, S. Nagel, W. Van Saarloos, and M. Wyart, in *Dynamical Heterogeneities and Glasses*, edited by L. Berthier, G. Biroli, J.-P. Bouchaud, L. Cipelletti, and W. van Saarloos (Oxford University Press, 2011), [arXiv:1006.2365](https://arxiv.org/abs/1006.2365).
- [25] M. Wyart, *Phys. Rev. Lett.* **109**, 125502 (2012).
- [26] A. Ikeda, L. Berthier, and G. Biroli, *J. Chem. Phys.* **138**, 12A507 (2013).
- [27] P. Charbonneau, E. I. Corwin, G. Parisi, and F. Zamponi, *Phys. Rev. Lett.* **109**, 205501 (2012).
- [28] E. Lerner, G. During, and M. Wyart, *Soft Matter* **9**, 8252 (2013).
- [29] A. J. Bray and M. A. Moore, *Journal of Physics C: Solid State Physics* **12**, L441 (1979).
- [30] M. Mézard, G. Parisi, and M. A. Virasoro, *Spin glass theory and beyond* (World Scientific, Singapore, 1987).
- [31] A. Montanari and F. Ricci-Tersenghi, *The European Physical Journal B-Condensed Matter and Complex Systems* **33**, 339 (2003).
- [32] A. Montanari and F. Ricci-Tersenghi, *Phys. Rev. B* **70**, 134406 (2004).
- [33] T. Rizzo, *Phys. Rev. E* **88**, 032135 (2013).
- [34] F. Krzakala and L. Zdeborová, *Journal of Physics: Conference Series* **473**, 12022 (2013).
- [35] E. Gardner, *Nuclear Physics B* **257**, 747 (1985).
- [36] D. J. Gross, I. Kanter, and H. Sompolinsky, *Phys. Rev. Lett.* **55**, 304 (1985).
- [37] C. J. Fullerton and M. Moore, [arXiv:1304.4420](https://arxiv.org/abs/1304.4420) (2013).
- [38] T. R. Kirkpatrick and P. G. Wolynes, *Phys. Rev. A* **35**, 3072 (1987).
- [39] D. J. Thouless, J. R. L. de Almeida, and J. M. Kosterlitz, *Journal of Physics C: Solid State Physics* **13**, 3271 (1980).
- [40] C. De Dominicis and I. Kondor, *Physical Review B* **27**, 606 (1983).
- [41] A. V. Goltsev, *Journal of Physics A: Mathematical and General* **16**, 1337 (1983).
- [42] I. Kondor and C. de Dominicis, *EPL (Europhysics Letters)* **2**, 617 (1986).
- [43] E. DeGiuli, E. Lerner, C. Brito, and M. Wyart, [arXiv:1402.3834](https://arxiv.org/abs/1402.3834) (2014).
- [44] A. Donev, S. Torquato, and F. H. Stillinger, *Physical Review E (Statistical, Nonlinear, and Soft Matter Physics)* **71**, 011105 (pages 14) (2005).
- [45] L. E. Silbert, A. J. Liu, and S. R. Nagel, *Physical Review E (Statistical, Nonlinear, and Soft Matter Physics)* **73**, 041304 (pages 8) (2006).

- [46] S. Torquato and F. H. Stillinger, *Rev. Mod. Phys.* **82**, 2633 (2010).
- [47] H. Yoshino and M. Mézard, *Phys. Rev. Lett.* **105**, 015504 (2010).
- [48] H. Yoshino, *The Journal of Chemical Physics* **136**, 214108 (2012).
- [49] H. Yoshino, *AIP Conference Proceedings* **1518**, 244 (2013), [arXiv:1210.6826](#).
- [50] P. Le Doussal, M. Müller, and K. J. Wiese, *EPL (Europhysics Letters)* **91**, 57004 (2010).
- [51] T. Castellani and A. Cavagna, *Journal of Statistical Mechanics: Theory and Experiment* **2005**, P05012 (2005).
- [52] P. Charbonneau, J. Kurchan, G. Parisi, P. Urbani, and F. Zamponi, *Nature Communications* **5**, 3725 (2014).
- [53] T. R. Kirkpatrick and D. Thirumalai, *Phys. Rev. B* **36**, 5388 (1987).
- [54] S. Franz and G. Parisi, *Journal de Physique I* **5**, 1401 (1995).
- [55] S. Franz and G. Parisi, *Phys. Rev. Lett.* **79**, 2486 (1997).
- [56] M. Cardenas, S. Franz, and G. Parisi, *The Journal of Chemical Physics* **110**, 1726 (1999).
- [57] F. Krzakala and L. Zdeborová, *EPL (Europhysics Letters)* **90**, 66002 (2010).
- [58] L. F. Cugliandolo and J. Kurchan, *Phys. Rev. Lett.* **71**, 173 (1993).
- [59] M. Mézard, *Physica A* **265**, 352 (1999).
- [60] M. Mézard and G. Parisi, *Journal of Physics: Condensed Matter* **12**, 6655 (2000).
- [61] M. Mézard and G. Parisi, *Journal de Physique I* **1**, 809 (1991).
- [62] B. Duplantier, *Journal of Physics A: Mathematical and General* **14**, 283 (1981).
- [63] H.-J. Sommers and W. Dupont, *Journal of Physics C: Solid State Physics* **17**, 5785 (1984).
- [64] H. L. Frisch and J. K. Percus, *Phys. Rev. E* **60**, 2942 (1999).
- [65] F. Caltagirone, U. Ferrari, L. Leuzzi, G. Parisi, and T. Rizzo, *Phys. Rev. B* **83**, 104202 (2011).
- [66] T. Temesvári, C. De Dominicis, and I. Pimentel, *The European Physical Journal B-Condensed Matter and Complex Systems* **25**, 361 (2002).
- [67] G. Parisi and G. Toulouse, *Journal de Physique Lettres* **41**, 361 (1980).
- [68] S. Pankov, *Physical review letters* **96**, 197204 (2006).
- [69] A. Crisanti and C. De Dominicis, *Philosophical Magazine* **92**, 280 (2012).
- [70] J.-P. Hansen and I. R. McDonald, *Theory of simple liquids* (Academic Press, London, 1986).
- [71] M. Müller and S. Pankov, *Phys. Rev. B* **75**, 144201 (2007).
- [72] M. Van Hecke, *Journal of Physics: Condensed Matter* **22**, 033101 (2010).
- [73] M. Skoge, A. Donev, F. H. Stillinger, and S. Torquato, *Physical Review E (Statistical, Nonlinear, and Soft Matter Physics)* **74**, 041127 (pages 11) (2006).
- [74] S. Atkinson, F. H. Stillinger, and S. Torquato, *Physical Review E* **88**, 062208 (2013).
- [75] Y. Kallus, E. Marcotte, and S. Torquato, *Phys. Rev. E* **88**, 062151 (2013).
- [76] A. Barrat, S. Franz, and G. Parisi, *Journal of Physics A: Mathematical and General* **30**, 5593 (1997).
- [77] P. Olsson and S. Teitel, *Physical Review Letters* **99**, 178001 (2007).
- [78] S. Okamura and H. Yoshino, [arXiv:1306.2777](#) (2013).
- [79] M. Castellana, A. Decelle, S. Franz, M. Mézard, and G. Parisi, *Phys. Rev. Lett.* **104**, 127206 (2010).
- [80] C. Cammarota, G. Biroli, M. Tarzia, and G. Tarjus, *Phys. Rev. Lett.* **106**, 115705 (2011).
- [81] J. Yeo and M. A. Moore, *Phys. Rev. E* **86**, 052501 (2012).